Next-to-Soft Radiative Corrections in QCD and Quantum Gravity.

Miss Stacey Elizabeth Melville

Submitted in fulfilment of the requirements for the Degree of Doctor of Philosophy

School of Physics and Astronomy

College of Science and Engineering

University of Glasgow

October 2016

Abstract

The origin of divergent logarithmic contributions to gauge theory cross sections arising from soft and collinear radiation is explored and a general prescription for tackling next-to-soft logarithms is presented. The NNLO Abelian-like contributions to the Drell-Yan K-factor are reproduced using this generalised prescription. The soft limit of gravity is explored where the interplay between the eikonal phase and Reggeization of the graviton is explained using Wilson line techniques. The Wilson line technique is then implemented to treat the set of next-to-soft contributions arising from dressing external partons with a next-to-soft Wilson line.

Contents

List of Figures

Acknowledgement

I'd like to give special thanks to my primary supervisor Dr. Chris White for his constant help, not just in re-reading this thesis many times through, but also for his teaching and guiding me to this point. I'd also like to acknowledge my friend Liam Moore who has provided me with immense amounts of support both in learning the intricacies of particle physics and in coping with the stresses that have arisen during the course of the PhD.

My thanks also go to my fellow PhD students, members of academia, my friends and family who have supported me and made what at times appeared as an overwhelming challenge, an enjoyable and motivating experience.

Declaration

I declare that the work within this thesis is my own work except where explicit reference is made to the contribution of others. This thesis has not been submitted for another degree at the University of Glasgow or any other institution.

The work presented in chapters 2 and 5 of this thesis has been published in the papers:

- D. Bonocore et al. "A factorization approach to next-to-leading-power threshold logarithms". In: *JHEP 1506 (2015) 008* (2015). arXiv: `1503.05156 [hep-ph]`,
- S. Melville et al. "Wilson line approach to gravity in the high energy limit". In: *Phys.Rev. D89 (2014) no.2, 025009* (2014). arXiv: `1306.6019 [hep-th]`,

The work of chapter 6 is part of a paper in preparation

- A. Luna et al. *Next-to-soft corrections to high energy scattering in QCD and gravity.* Pre Print November 2016

(*Miss Stacey E. Melville*)

Notations and Conventions

- Throughout the thesis natural units of $c = \hbar = 1$ have been used.
- Unless stated otherwise the metric signature will be $\{+, -, -, ..., -\}$
- It should be noted that log is to the natural basis.
- We use the Feynman slash notation $\not{p} = \gamma^{\mu} p_{\mu}$

Chapter 1

Introduction

Gauge quantum field theories are the current mathematical frameworks with which we can explain the fundamental forces of nature. To each of the fundamental forces detectable to us there exists a gauge field theory describing it. The quantum field theory treatment of fundamental particle interactions began with quantum electrodynamics (QED) which describes the interactions of photons with matter. The great success of this theory is what has inspired us to proceed with applying this gauge field theoretic knowledge to the other fundamental forces. QED is outstanding in the level of theoretical precision it has allowed us, one of the most remarkable accomplishments being the calculation of the anomalous magnetic moment of the electron where its predicted value matching the measured value of $g/2 = 1.00115965218073(28)$ is viewed as the pinnacle of scientific precision.

Currently the Large Hadron Collider (LHC) is the highest energy particle accelerator created by man and its aim is to search and explore for new physics at an untested energy regime. By colliding together bunches of protons which are composed of quarks and gluons, particles currently treated theoretically in the framework of quantum chromodynamics (QCD), and observing the results we can detect new physics such as the recent indication of a Higgs boson like particle signature. Increasing the theoretical precision of calculations made in QCD will enable a more accurate ability to examine and discover new physics at the LHC. The role of this thesis is to develop techniques that will increase the accuracy of such calculations as well as to develop our theoretical understanding.

The standard model of particle physics has the gauge group $SU(3) \times SU(2) \times U(1)$. However this theory is incomplete: it does not include gravity, and it is an effective field theory valid at current collider energy levels. Being an incomplete theory causes mathematical infinities to arise in quantum field theory calculations. The most familiar of these are UV divergences. UV divergences are caused by very high energy modes

being included in calculations. Modes that have energy of this scale are outside the range of applicability of the standard model. As such they can be safely decoupled from the low energy modes that are describable. We tackle the problem of UV divergences through renormalisation. Renormalisation allows us to absorb the divergent nature of these modes into the Lagrangian parameters of the theory. The values of these constants are no longer treated as being fixed values but to be dependent upon the energy they are being measured at. How these quantities depend on the energy is governed by the renormalisation group equations. Through the work of regularising and then renormalising these UV divergences are manageable.

There are other sources of divergence that appear in our theories besides the high energy UV ones. Divergences associated with low energy (or long distance) modes are correspondingly referred to as IR divergences. Once again we know these infinities must be non-physical and we must find a way to manage them in our theory for theoretical predictability. UV divergences are much studied, the focus of this thesis will be towards IR divergences most importantly those arising when one includes soft radiative enhancements to amplitudes.

1.1 IR Divergences in Quantum Field Theory

In this section we shall explain where the IR divergences originate from and how they can arise from considerations of Feynman rules in scattering amplitudes.

1.1.1 Soft radiation

Soft radiation is radiation whose four momentum $k^\mu \to 0$ with respect to the other scales in the process. How emissions of bosons with such low momentum can lead to divergences is best explained through a heuristic example. Consider a scattering event where a single soft boson is emitted from an external leg of a scattering process, diagrammatically represented in figure (1.1). In the strictly soft limit $k^\mu \to 0$ we can view this emitted particle as having an infinite Compton wavelength and as such it is unable to probe the hard interaction, it is therefore insensitive to the details of it, which leads to a factorisation between hard and soft physics. Interactions between the soft region and hard region enter at higher orders in the soft expansion which will be the focus of later sections in this thesis. The emitted particle could be real in which it will appear in the final state. However, its soft momentum will make it indiscernible to the detector. An alternative interaction would be for this boson to be re-absorbed by one of the external legs making it a virtual boson. Once again the zero momentum of the particle will make this indistinguishable to the bare interaction and the real one

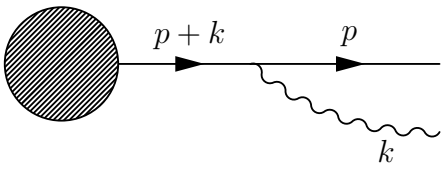

Figure 1.1: A Feynman diagram showing the emission of a soft photon with momentum $k \to 0$ from an external leg of a scattering process with final state momentum p. The factorisation of the soft radiation from the hard radiation makes knowledge of the details of the hard interaction unnecessary when concerned with the infra-red contributions to the amplitude.

mentioned above. This will be true for any number of such emissions. The same argument can be extended to consider collinear emissions also needing to be considered for the full cross section. It is therefore clear that if one wishes to calculate the scattering cross section for this interaction detected in collider experiments one must calculate the superposition of all (infinity) such degenerate soft and or collinear enhancements to the bare cross section. The integrations performed to obtain scattering amplitudes will become IR divergent, but there exist theorems demonstrating that these divergences cancel when amplitudes are summed. This idea was first demonstrated by Bloch and Nordsieck [4] when considering infra-red divergences in electron scattering that related to massless particles. They showed that if one combines the bremsstrahlung contribution with the radiative correction to the elastic process the IR divergence cancels. The general form of this theorem was presented by Kinoshita-Lee-Nauenberg [5–7] which states that the fully inclusive cross section including all degenerate energy states in both the initial and final states leads to an infra-red divergence free cross section. The divergences arising from loop level graphs can be shown to cancel with those coming from real emissions (phase space integrals) for all of the standard model.

1.1.2 Soft divergences at 1 loop

Soft divergences appear at orders beyond tree level in perturbation theory, the added emission necessitating added factor(s) of the coupling constant. Consider the tree level diagram of a fermion anti-fermion pair producing an off-shell photon shown in figure (1.2). Using the Feynman rules derived from the lagrangian, the associated amplitude contribution for this graph in momentum space is

$$\mathcal{M}_{tree} = ie\bar{u}(p)\gamma^{\mu}\nu(\bar{p}). \tag{1.1}$$

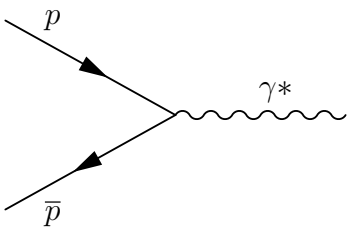

Figure 1.2: Feynman diagram for an off shell photon being produced from a fermion anti-fermion pair.

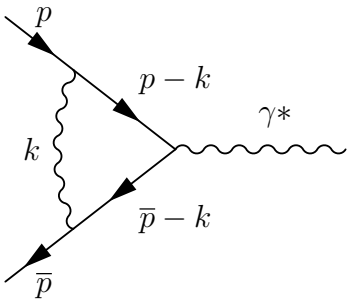

Figure 1.3: Feynman diagram showing the vertex correction to figure (1.2) where a virtual photon is exchanged between the fermion anti-fermion pair.

The photon will then go on to decay further but for the purposes of this demonstration the details are not important. In order to achieve greater precision, as is required for phenomenology one must also include contributions from graphs that arise at higher orders in the perturbation series expansion w.r.t. to the coupling constant e.g. loop graphs. Strictly speaking, the renormalised coupling constant is a measure of whether these higher order graphs are required. At current collider energies, the couplings are small such that higher order contributions are relatively suppressed, but still numerically important. As a simple example consider the emission and re-absorption of a virtual photon between the two fermions shown in figure (1.3). The associated amplitude for this graph is

$$\mathcal{M}_{virtual} = e^3\mu^{2\epsilon}\bar{u}(p)\gamma^\nu \int \frac{d^dk}{(2\pi)^d}\frac{1}{k^2}\frac{(\not{p}-\not{k})}{(p-k)^2}\gamma^\mu\frac{(\not{\bar{p}}-\not{k})}{(\bar{p}-k)^2}\gamma_\nu\nu(\bar{p}), \tag{1.2}$$

where we are working in the Feynman gauge for the photon propagator and using dimensional regularisation to regulate the infra-red divergences, $d = 4 - 2\epsilon$. The scale μ is inserted to keep the coupling constant dimensionless. The Feynman $i\varepsilon$ prescription is implied for the propagators. The fermions are on-shell and massless such that they obey $p^2 = \bar{p}^2 = 0$, allowing us to write the amplitude as

$$\mathcal{M}_{virtual} = e^3\mu^{2\epsilon}\bar{u}(p)\gamma^\nu \int \frac{d^dk}{(2\pi)^d}\frac{1}{k^2}\frac{(\not{p}-\not{k})}{k^2-2p\cdot k}\gamma^\mu\frac{(\not{\bar{p}}-\not{k})}{k^2-2\bar{p}\cdot k}\gamma_\nu\nu(\bar{p}), \tag{1.3}$$

this would also be the result for on-shell massive fermions. The origins of soft divergences can now be observed, they arise due to the integral over the virtual particle momentum including the region where $k \to 0$. If we work in the limit of very small virtual momenta i.e. $k^\mu \to 0$ we can expand the denominators in the integrand about small k

$$\begin{aligned}(k^2 + 2p \cdot k)^{-1} &= (2p \cdot k)^{-1} \left(1 + \frac{k^2}{2p \cdot k}\right)^{-1} \\ &= (2p \cdot k)^{-1} \left[1 + \sum_{n=1}^{\infty} (-1)^n \left(\frac{k^2}{2p \cdot k}\right)^n\right]. \end{aligned} \tag{1.4}$$

For vanishing virtual momentum the leading order contribution to the amplitude is

$$\mathcal{M}_{virtual} = e^3 \mu^{2\epsilon} \bar{u}(p) \gamma^\nu \int \frac{d^d k}{(2\pi)^d} \frac{1}{k^2} \frac{\not{p}}{2p \cdot k} \gamma^\mu \frac{\not{\bar{p}}}{2\bar{p} \cdot k} \gamma_\nu \nu(\bar{p}). \tag{1.5}$$

In this "soft limit" it can be observed that the integral is logarithmically divergent in four dimensions. Introducing the added dimensionality through the ϵ parameter allows us to regulate this divergence. Also apparent from this amplitude is the origin of another form of divergence, one relating to either $p \cdot k = 0$ or $\bar{p} \cdot k = 0$. This could be the consequence of the momentum being soft or due to the virtual boson having momentum such that it travels parallel to either of the external legs. These are known as collinear divergences. Collinear divergences require the boson and its emitter to be massless, it can be seen that if a mass term were present in the Feynman rule it would regulate these divergences. In the example used it may appear unnatural to use massless emitting fermions because none exist in the standard model however the masses of the lightest quarks will be small enough with respect to the other scales in the scattering process that they can be considered massless.

1.1.3 Eikonal Feynman rules

It has already been demonstrated that in the soft limit (also known as the *eikonal approximation* for the emitting particles) the amplitudes for diagrams become simplified. The leading order terms of the expanded full Feynman rules can be interpreted as a set of effective eikonal Feynman rules that can be used to obtain the leading order soft amplitude. Using eikonal Feynman rules will allow for much simpler calculations. Also they have uses for making manifest the factorisation of soft effects from the hard amplitude, and for deriving resummation properties of eikonal logarithms.

If we recall from before the amplitude in the soft limit for our massless QED process was given in equation (1.5). We can go further in our treatment and anticommute

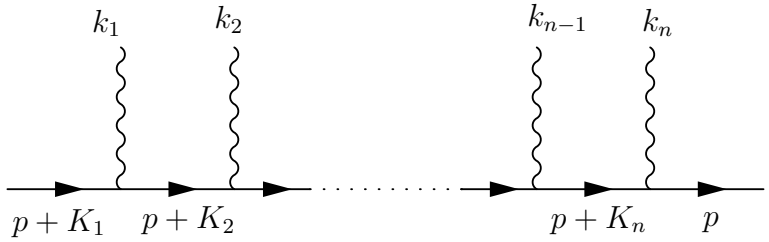

Figure 1.4: Section of the Feynman diagram for an external fermion of final momentum p emitting n-soft photons of momentum k_i.

through the Dirac matrices in the numerator utilising their Clifford algebra $\{\gamma_\mu, \gamma_\nu\} = 2\eta_{\mu\nu}$ to obtain

$$\mathcal{M}_{virtual} = e^3 \mu^{2\epsilon} \bar{u}(p)\gamma^\mu \nu(\bar{p}) \int \frac{d^d k}{(2\pi)^d} \frac{1}{k^2} \frac{p \cdot \bar{p}}{(p \cdot k)(\bar{p} \cdot k)}. \tag{1.6}$$

We can see that the hard amplitude has factorised, demonstrating the factorisability of long and short distance effects in the soft limit. The soft enhancement to the diagram has taken the form of multiplying the tree level graph by a divergent integral over the eikonal Feynman rules. We can identify the vertex with the soft photon as being

$$e\frac{p^\mu}{p \cdot k}. \tag{1.7}$$

The soft radiation is insensitive to the spin of the emitting particle so this rule will apply for dressing scalar amplitudes too. We can use the effective Feynman rules to construct all possible graphs at a given order in perturbation theory to gain the leading soft contribution to the amplitude at that order.

It is worth demonstrating that for numerous real emissions from a single external line in the eikonal limit we can dress the external line with an eikonal Feynman rule for each emission. Consider a fermion with n soft gluon emissions, represented in figure (1.4). The amplitude for this process takes the form of

$$\mathcal{M}_{multiple} = \mathcal{M}_{Hard}(p) \frac{\not{p} + \not{K}_1}{(p + K_1)^2} \gamma^{\mu_1} ... \frac{\not{p} + \not{K}_n}{(p + K_n)^2} \gamma^{\mu_n} \bar{u}(p), \tag{1.8}$$

where $K_i = \sum_{m=i}^{n} k_m$ is a sum over soft gluon momenta. In the eikonal limit we drop the factors of K from the numerator and keep only leading order denominators:

$$\mathcal{M}_{multiple} = \mathcal{M}_{Hard}(p) \frac{\not{p}}{2p \cdot K_1} \gamma^{\mu_1} ... \frac{\not{p}}{2p \cdot K_n} \gamma^{\mu_n} \bar{u}(p). \tag{1.9}$$

We consider the external particle to be on the mass shell such that $\not{p}^2 = 0$ and using

the Clifford algebra the numerator reduces to

$$\mathcal{M}_{multiple} = \mathcal{M}_{Hard}(p)\frac{p^{\mu_1}}{p\cdot K_1}...\frac{p^{\mu_n}}{p\cdot K_n}\bar{u}(p). \tag{1.10}$$

Next we can go on to impose Bose symmetry and sum over all the permutations of orders in which the soft gluon is emitted to obtain the full eikonal factor for this amplitude

$$E^{\mu_1...\mu_n}(p,k_i) = \frac{1}{n!}\sum_{\pi}\frac{p^{\mu_1}}{p\cdot K_{\pi_1}}...\frac{p^{\mu_n}}{p\cdot K_{\pi_n}}. \tag{1.11}$$

The summation is over all the permutations, π, of emissions. This eikonal factor can then be simplified by use of the eikonal identity

$$\sum_{\pi}\frac{p^{\mu_1}}{p\cdot K_{\pi_1}}...\frac{p^{\mu_n}}{p\cdot K_{\pi_n}} = \prod_i \frac{p^{\mu_i}}{p\cdot k_i}. \tag{1.12}$$

We therefore see that the leading soft amplitude can be obtained by replacing the full Feynman rules for a given diagram with eikonal Feynman rules for each soft boson emission, either real or virtual. As will be demonstrated, at next-to-soft level there are more contributions to amplitudes, that require more work than only linearising the denominators of the propagators.

This analysis has considered abelian-like gauge theories only. For non-abelian gauge theories one must tackle the added combinatoric complications that arise with the non-commutativity of the charge matrices. It can be demonstrated that for such theories one must utilise special Feynman diagrams called "webs" defined for two-line processes in [8–10] and for processes involving more than two lines in [11–20] (see e.g. [21] for a review).

1.2 Threshold Logarithms

For fully inclusive processes the KLN theorem states that the IR poles will cancel between real and virtual emission diagrams. After this cancellation there will still remain residual factors left to contribute to physical cross sections that take the form of logarithms of ratios of variables, that become divergent as one approaches the soft or collinear limit. These logarithmic enhancements become the dominant contributions to cross sections that are computed beyond leading order in the soft energy limit. When the logarithms diverge faster than the coupling constant suppresses them these logarithms must be resummed to all orders in perturbation theory. In the following section we shall indicate how the differential cross section for a hadronic process depends on such logarithms and make clear the importance of being able to manage these effects

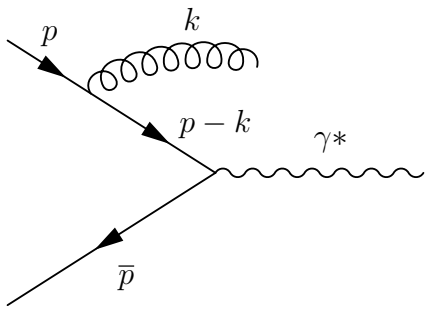

Figure 1.5: Feynman diagram showing the real emission of a gluon from an external fermion

to leading order and beyond.

1.2.1 Threshold expansion

For different hadronic cross sections there exist different parametrisations by which one can measure the deviation from the soft limit. Consider the scattering event shown in figure (1.5). This is the Feynman diagram representation of $q\bar{q} \to g + \gamma^*$ which is a radiative correction to Drell-Yan scattering. The total squared partonic initial state energy is given by $s = (p + \bar{p})^2$ and the outgoing virtual photon carries total energy q^2. It is then possible to construct the ratio of these two values to find the fraction of the total energy carried by the emitted virtual boson: $z = \frac{q^2}{s}$. The limit in which the gluon becomes soft is $z \to 1$. We can create a threshold parameter $\xi = 1 - z$, such that as the momentum of this gluon becomes soft, the threshold parameter tends to zero. We can expand the perturbative cross-section in this threshold parameter and it will take the following form:

$$\frac{d\sigma}{d\xi} = \sum_{n=0}^{\infty} \left(\frac{\alpha_s}{\pi}\right)^n \sum_{m=0}^{2n-1} \left[c_{nm}^{(-1)} \left(\frac{\log^m \xi}{\xi} \right)_+ + c_{nm}^{(\delta)} \delta\left(1 - \xi\right) + c_{nm}^{(0)} \log^m \xi + ... \right], \quad (1.13)$$

where the + indicates a plus distribution defined in appendix A.2.5 and the ellipsis indicates terms further suppressed by the threshold parameter. Although we are discussing Drell-Yan scattering, this formula is generally applicable to any process, where the constant factors c_{nm} are process dependent. The first terms in this expansion, characterised by the coefficients $c_{nm}^{(-1)}$, are the leading power (LP) threshold logarithms which are reproduced by using the eikonal approximation. The terms characterised by $c_{nm}^{(0)}$ are next-to-leading power (NLP) threshold logarithms, the prescription for computing which are the basis for the following sections of the thesis.

1.3 Soft-Collinear Amplitude factorisation

IR divergences are known to factorise from the infra-red safe, process dependent part of scattering amplitudes as demonstrated in [22, 23]. It is then possible to write a scattering amplitude in the following form:

$$\mathcal{A}\left(\frac{Q^2}{\mu^2},\alpha_s(\mu^2),\epsilon\right)=\mathcal{H}\left(\{p_i\},\{n_i\},\alpha_s(\mu^2),\epsilon\right)\times\mathcal{S}\left(\{\beta_i\},\alpha_s(\mu^2),\epsilon\right)\times\prod_{i=1}^{n}\left[\frac{J_i(p_i,n_i,\alpha_s(\mu^2),\epsilon)}{\mathcal{J}_i(\beta_i,n_i,\alpha_s(\mu^2),\epsilon)}\right], \tag{1.14}$$

where p_i (β_i) is the momentum (four-velocity) of the i^{th} particle and Q is the hard process energy scale, the product runs over all n external lines in the scattering process. $\mathcal{H}$ is the process-dependent hard function that is IR divergence free. $\mathcal{S}$ is the soft function, which collects all IR divergent terms relating to soft radiation from external particles. The soft function is independent of the spin of the emitting particles. J_i is the jet function which contains all IR divergences relating to the emitted radiation being collinear to the external leg i. The product then includes a jet function for each of the external particles, and such divergences each depend upon the spin and charge quantum numbers of a single emitting particle. $\mathcal{J}_i$ is the eikonal jet function which includes divergences that are both soft and collinear in origin and removes those terms that have been double counted in both the soft and jet functions. The factorisation of the amplitude leads to the possibility of resummming the infra-red divergences to all orders in perturbation theory, for which at leading soft order a multitude of methods exist [24–34].

We will now formally define the above quantities for use in the coming chapters dealing with next-to-soft effects. The definition of the jet function for a leg of momentum p is [23]

$$J\left(p,n,\alpha_s(\mu^2)\right)u(p)=\langle 0|\Phi_n(\infty,0)\psi(0)|p\rangle. \tag{1.15}$$

Here the incoming parton of momentum p is absorbed by the quantum field $\psi(x)$ at the spacetime point $x=0$. The function $\Phi_n(\infty,0)$ is a Wilson line extending from the spacetime point $x=0$ to infinity in the direction of the auxiliary gauge link given by n^μ. The Wilson line is defined to be

$$\Phi_n(\lambda_2,\lambda_1)=\mathcal{P}\exp\left[ig_s\int_{\lambda_1}^{\lambda_2}d\lambda n\cdot A(\lambda n)\right], \tag{1.16}$$

where $\mathcal{P}$ denotes path ordering over the gauge fields A^μ in the exponent necessary for

non-abelian field theories. Wilson lines are inherently gauge covariant. Similarly, the eikonal jet is defined to be

$$\mathcal{J}(\beta, n, \alpha_s(\mu^2), \epsilon) = \langle 0|\Phi_n(\infty, 0)\Phi_\beta(0, -\infty)|0\rangle, \tag{1.17}$$

where the external leg of momentum p is replaced with a Wilson line of four-velocity β. It was the work of [27, 28] that first demonstrated that soft divergences come from treating external legs as Wilson lines.

The auxiliary four-vector n_i^μ that has been used throughout this section is a factorisation vector that cannot appear in the final amplitude. The dependence on the vector n_i^μ must therefore cancel between the jet and hard functions. We are therefore free to pick any value for the vector n_i^μ. It is useful for our purposes of considering massless quarks to define two dimensionless light-like vectors $\hat{n}_i$ to be in directions anti-collinear to the p_i such that

$$\hat{n}_i^2 = 0, \qquad \hat{n}_i \cdot p_i = Q. \tag{1.18}$$

We can then define the dimensionful vectors to be:

$$n_i = \frac{Q}{2}\hat{n}_i, \qquad n_i \cdot p_i = \frac{Q^2}{2}. \tag{1.19}$$

Note for the two parton process we are considering p_1 is anticollinear to p_2 and vice-versa. We can therefore make the replacements

$$n_1 = p_2, \qquad n_2 = p_1. \tag{1.20}$$

The soft function for the two parton amplitude is defined as [23]

$$\mathcal{S}(\beta_1 \cdot \beta_2, \alpha_s(\mu^2), \epsilon) = \langle 0|\Phi_{\beta_2}(\infty, 0)\Phi_{\beta_1}(0, -\infty)|0\rangle. \tag{1.21}$$

this differs from the eikonal jet of equation 1.17 in that the Wilson lines are following the path of the external particles via their four-velocities β_1 and β_2 and are not dependent upon the auxiliary vector. It will be useful for the following analysis to keep soft and collinear divergences treated separately. For this purpose we can define the reduced soft function

$$\bar{S}\left(\frac{\beta_1 \cdot \beta_2}{\beta_1 \cdot n_1 \beta_2 \cdot n_2}, \alpha_s(\mu^2), \epsilon\right) = \frac{S(\beta_1 \cdot \beta_2, \alpha_s(\mu^2), \epsilon)}{\prod_i \mathcal{J}_i(\beta_i \cdot n_i, \alpha_s(\mu^2), \epsilon)}. \tag{1.22}$$

Here we have removed the soft-collinear divergences from the soft function so it is collinear divergence free and all collinear divergences will be treated by the jet functions. The ratio in the argument of the reduced soft function is invariant under re-scalings of

$\beta_i \to \lambda_i \beta_i$ as discussed in [23, 35, 36]. The soft function and eikonal jet functions alone are not invariant under this rescaling for light-like β_i due to the presence of collinear singularities in both factors. The construction of the reduced soft function restores this symmetry.

It has been demonstrated how the factorisation structure of a gauge theory amplitude is carried out and we can write it in a schematic form as

$$\mathcal{A} = \mathcal{H} \times \bar{\mathcal{S}} \times \prod_{i=1}^{2} J_i. \tag{1.23}$$

where all collinear singularities are contained in the jet functions and the reduced soft function is collinear divergence free. We can therefore define a collinear divergence free factor as first constructed in [37]

$$H \equiv \mathcal{H} \times \bar{\mathcal{S}}, \tag{1.24}$$

which will be useful in what follows.

1.4 Next-to-soft contributions

We saw earlier how soft radiative corrections produce the LP threshold logarithms in the scattering cross section. NLP threshold logarithms arise from next-to-soft radiative corrections to amplitudes. Next-to-soft terms can be understood by first considering rescaling the soft momentum by a soft parameter i.e. $k_i^\mu \to \eta k_i^\mu$. The eikonal amplitude for n soft emissions was order η^{-n}, and thus the next-to-eikonal (NE) terms will be of order η^{n-1}.

NLP contributions are still singular in the limit of $\xi \to 0$ but integrably so. However they still give large contributions to amplitude calculations. The current level of precision required by collider phenomenology makes the investigation of such effects important for enhancing our theoretical predictions. It is expected that NLP effects will give large corrections to scattering cross sections and a large body of work into the significance of these effects when considering Higgs production exists [38–43].

There are two types of contributions to the NLP threshold logarithms that we call internal and external emissions. We have described previously how eikonal emissions dress external partons to give us soft amplitudes. If we consider the leading soft amplitude we can consider replacing one of the soft (eikonal) Feynman rules for a next-to-soft (next-to-eikonal) one. At next-to-soft level there may be numerous such next-to-soft Feynman rules that we can insert in place of each eikonal rule. All of these will be considered and will build up the so-called external emission contributions.

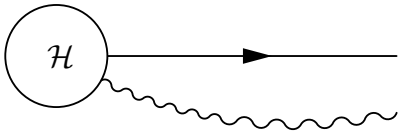

Figure 1.6: This figure shows the schematic diagram for the internal emission of a boson that would contribute at next-to-soft level. $\mathcal{H}$ represents the hard interaction process

At next-to-soft level we can no longer consider the emissions to have an infinite Compton wavelength so they can probe the hard interaction details. Consequently the spin of the emitter will be resolvable by the emissions and we will see in what follows how this appears in the Feynman rules and the amplitude.

Internal emissions are soft bosonic emissions from within the hard interaction. For the reason mentioned above such terms have no analogue in the soft limit and will produce extra diagrams not present in the soft case. The way in which we manage such effects is via the Low-Burnett-Kroll-Del Duca theorem [37, 44, 45] which will be discussed in the next section.

1.5 The Low-Burnett-Kroll-Del Duca (LBKDD) theorem

Important for the tackling of next-to-soft effects is the Low-Burnett-Kroll [44, 45] theorem and its extension to a greater regime of applicability for massless particles by Del-Duca [37]. At next-to-soft level one must consider added contributions to amplitudes arising from the soft bosons being emitted from within the hard interaction. Such occurrences shown schematically in figure (1.6) are named internal emission contributions. The theory manages internal emission contributions to amplitudes by relating them to derivatives of the non-radiative amplitude.

The initial work of Low in the field of quantum electrodynamics utilised the Ward identity of QED to relate the amplitude for a general bremsstrahlung process to that of the non-radiative amplitude. The leading and next-to-leading behaviour of the amplitude on the photon energy was shown to be reproduced by this method. The work was initially performed in a regime such that the photon energy was the smallest scale in the amplitude, this has uses for soft radiation emission but is no longer valid with the case of massless emitting particles at next-to-leading order due to jet contributions. It is the work of Del Duca that extended the regime of applicability to $m^2/Q \leq \omega_k \leq m$

where m is the mass of the emitting particle, Q is the hard process scale where $Q \to \infty$ with respect to the other scales and ω_k is the emitted photon's energy. Low's work was also restricted to scalar emitting particles, and the magnetic moment one has to consider when the emitter has spin can also enter at next-to-leading order. The intermediate work of Burnett and Kroll extended Low's theorem to consider fermions in unpolarised cross sections. Further work was carried out to finally extend the theory to cover processes with arbitrary spin and polarisation. We shall follow the work of Del-Duca [37] in this section to indicate how the theory utilises the Ward identity to relate the internal emission contributions to amplitudes, to the non-radiative amplitude.

We write an amplitude with an additional gluon emission as

$$\mathcal{A}_\mu \epsilon^\mu(k) = \mathcal{A}^J_\mu \epsilon^\mu(k) + \mathcal{A}^H_\mu \epsilon^\mu(k), \tag{1.25}$$

where ϵ^μ is the polarisation vector of the emitted gluon and $\mathcal{A}^J_\mu(\mathcal{A}^H_\mu)$ represent amplitudes relating to the emission being from within the jet and collinear-free functions respectively. We can write the jet emission amplitude as

$$\mathcal{A}^J_\mu = \sum_{i=1}^{2} H(p_i - k; p_j, n_j) J_\mu(p_i, k, n_i) \prod_{j \neq i} J(p_j, n_j) \equiv \sum_{i=1}^{2} \mathcal{A}^{J_i}_\mu. \tag{1.26}$$

The semi-colon is to separate out the momentum factor that will be affected by the emission. Here we have introduced the radiative jet function first defined in [37]

$$J_\mu(p, n, k, \alpha_s(\mu^2), \epsilon) u(p) = \int d^d y \exp(-i(p-k)\cdot y) \langle 0 | \Phi_n(y, \infty) \psi(y) j_\mu(0) | p \rangle, \tag{1.27}$$

where $j_\mu(0)$ is the chromo-electric current that enables the emission of a soft gluon of momentum k. This jet is an incoming quark of momentum p which gets absorbed by the field at spacetime point y and whose gauge phase factor is transported to ∞ by the Wilson line factor. This function represents the emission of a gluon from inside of the jet function, this has not previously been calculated. The calculation of it will be performed in the following chapter.

Provided the chromo-electric current used in the definition of the jet function is conserved the radiative jet function obeys the Ward identity [37]

$$k^\mu J_\mu(p, n, k, \alpha_s(\mu^2), \epsilon) = q J(p, n, \alpha_s(\mu^2), \epsilon), \tag{1.28}$$

where q is the charge of the external line and will be positive or negative if p is incoming or outgoing respectively. The Ward identity for the radiative jet function is none-zero

however the Ward identity for the entire amplitude is

$$k^\mu \mathcal{A}_\mu = 0. \tag{1.29}$$

From the definition for the total amplitude this implies

$$k^\mu \mathcal{A}^H_\mu = -k^\mu \mathcal{A}^J_\mu. \tag{1.30}$$

This Ward identity makes clear the interplay between the collinear-free function H and the jets. Using equation (1.26) the right-hand-side takes the form of

$$k^\mu \mathcal{A}^J_\mu(p_i, k) = \sum_{i=1}^{2} q_i H(p_i - k; p_j, n_j) \prod_{j=1}^{2} J(p_j, n_j), \tag{1.31}$$

we can then Taylor expand the hard function about the soft momentum to next-to-soft level

$$H(p_i - k; p_j, n_j) = \left(1 - k^\mu \left(\frac{\partial}{\partial p_i^\mu}\right)\right) H(p_i; p_j, n_j). \tag{1.32}$$

Inserting this back into equation (1.31) one obtains:

$$k^\mu \mathcal{A}^J_\mu(p_i, k) = \sum_{i=1}^{2} q_i \left[H(p_i; p_j, n_j) - k^\mu \frac{\partial}{\partial p_i^\mu} H(p_i; p_j, n_j)\right] \prod_{j=1}^{2} J(p_j, n_j). \tag{1.33}$$

The first term can be seen to vanish due to charge conservation (color conservation in QCD). The Ward identity of equation (1.30) can then be used to obtain

$$k^\mu \mathcal{A}^H_\mu = k^\mu \sum_{i=1}^{2} q_i \frac{\partial}{\partial p_i^\mu} H(p_i; p_j, n_j) \prod_{j=1}^{2} J(p_j, n_j). \tag{1.34}$$

It is convenient to decompose the polarisation into a sum over polarisation tensors as performed in references [37, 46] to consider emissions of G/K polarised photons individually.

$$\eta^{\mu\nu} = G^{\mu\nu} + K^{\mu\nu}, \tag{1.35}$$

where

$$K^{\mu\nu}(p; k) = \frac{(2p - k)^\nu}{2p \cdot k - k^2} k^\mu. \tag{1.36}$$

From equations (1.35) and (1.36) $G^{\mu\nu}$ must therefore satisfy:

$$p^\mu G_{\mu\nu} = \mathcal{O}(k), \qquad G_{\mu\nu} k^\nu = 0. \tag{1.37}$$

This decomposition allows us to write the expression for the emission of a K-gluon from the jet function

$$\begin{aligned}\mathcal{A}_\nu^{J_i} K_i^{\nu\mu} &= q_i \frac{(2p_i - k)^\mu}{2p_i \cdot k - k^2} H(p_i - k; p_j, n_j) \prod_{j=1}^{2} J(p_j, n_j) \\ &= q_i \left[\frac{(2p_i - k)^\mu}{2p_i \cdot k - k^2} \mathcal{A} - \left(K_i^{\nu\mu} \frac{\partial}{\partial p_i^\nu} H(p_i; p_j, n_j) \right) \prod_{j=1}^{2} J(p_j, n_j) \right], \end{aligned} \tag{1.38}$$

where $K_i^{\nu\mu}$ is the K-tensor for the i-th jet, $\mathcal{A}$ is the non-radiative amplitude and the hard process has been Taylor expanded in the second line. Next we can consider the emission of a G-gluon from a jet

$$\mathcal{A}_\nu^{J_i} G_i^{\nu\mu} = G_i^{\nu\mu} H(p_i - k; p_j, n_j) J_\nu(p_i, k, n_i) \prod_{j \neq i} J(p_j, n_j). \tag{1.39}$$

The G tensor ensures this term enters at next-to-soft order therefore we only need to keep the leading term in the Taylor expansion of the hard function. All of these ingredients together for the full amplitude for a two jet process

$$\mathcal{A}^\mu = \mathcal{A}^{H,\mu} + \sum_{i=1}^{2} \left(\mathcal{A}_\nu^{J_i} K_i^{\nu\mu} + \mathcal{A}_\nu^{J_i} G_i^{\nu\mu} \right), \tag{1.40}$$

The result is

$$\begin{aligned}\mathcal{A}^\mu(p_j, k) = \sum_{i=1}^{2} \Bigg[& q_i \left(\frac{(2p_i - k)^\mu}{2p_i \cdot k - k^2} + G_i^{\nu\mu} \frac{\partial}{\partial p_i^\nu} \right) \mathcal{A}(p_i; p_j) + \\ & + \mathcal{H}(p_j, n_j) \bar{\mathcal{S}}(\beta_j, n_j) G_i^{\nu\mu} \left(J_\nu(p_i, k, n_i) - q_i \frac{\partial}{\partial p_i^\nu} J(p_i, n_i) \right) \prod_{j \neq i} J(p_j, n_j) \Bigg], \end{aligned} \tag{1.41}$$

where the hard amplitude has been replaced using the leading order factorisation formula. Doing so has caused derivatives formerly acting on the hard function to now act upon the full amplitude and jet functions. The internal emission contributions are now described through the derivative of the non radiative amplitude, the process independent jet function and the radiative jet function for emissions in the collinear region. The derivatives are with respect to the hard momenta of the emitting particles, and the sum ensures we get contributions from all places such an emission can occur. The only parts of this amplitude that are process dependent are the hard function $\mathcal{H}$ and the non-radiative amplitude $\mathcal{A}$.

We can construct the NNLO annihilation cross section from the amplitude formula

in equation (1.41) by contracting it with the tree-level 1-real emission matrix element and integrating over the real gluon phase space. Doing so will compute the NLP logarithms we are trying to reproduce. It is worth mentioning that the factorisation of the leading order phase space is well understood and will be needed for these NLP matrix elements. There will also be contributions at NLP order from LP matrix elements being integrated over the NLP corrected phase space which are discussed in reference [47].

Chapter 2

NLP corrections in Drell-Yan scattering

The previous chapter has explained the origins of all NLP contributions to amplitudes and demonstrated that all of these effects are captured in the factorised form of equation (1.41). The formalism constructed is applicable to any process. As a non-general check of this we shall attempt to recreate all abelian-like NLP threshold logarithms contributing to the NNLO Drell-Yan K-factor. The Drell-Yan process is ubiquitous in the background of current proton-proton colliders. It is the process of a quark anti-quark pair colliding to form a virtual electro-weak boson that decays into a lepton anti-lepton pair. By considering the graphs that have 1 real and 1 virtual emission of soft gluons we have a non-trivial check of the formalism as in such a process poles of both collinear and soft origin will be present. By restricting the investigation to abelian like logarithms the combinatorics required for the color matrices can be avoided for an initial test of the formalism. The Drell-Yan process has been selected for its simplicity in that it only involves two color charge carrying particles at leading order and it will not involve final state jets. For uses in current phenomenology it would be the aim to extend this work for application to Higgs production via gluon fusion where work exists detailing NLP logs up to N^3LO [43, 48].

The previous section outlined the LBKDD theorem and left us with a way of relating a radiative amplitude to its non-radiative counterpart. It shall be the work of the initial sections of this chapter to give detail into how to calculate the components on the right hand side of equation (1.41) for a general process, before looking at the specific amplitude for Drell-Yan scattering.

2.1 Radiative Jet Function

We introduced the radiative jet function previously in equation (1.27). It was mentioned that $j_\mu(0)$ is the chromo-electric current that enables the emission of a soft gluon of momentum k. For constructing the abelian-like logarithms it is sufficient to use the current

$$j_a^\mu(x) = \bar{\psi}(x)\gamma^\mu T_a \psi(x), \tag{2.1}$$

which is the QED-like current for QCD. We will now go on to compute the radiative jet function for this QED-like current. We will be concerned with generating the abelian-like logarithms and so we wish for the terms proportional to C_F^n at $\mathcal{O}(\alpha_s^n)$ i.e. discard terms that arise from Feynman diagrams with multi-gluon vertices. To this end we can disregard terms proportional to $C_F C_A$ where C_F and C_A are the quadratic Casimir operators in the fundamental and adjoint representations of the group respectively.

2.2 Jet functions for light-like reference vector

The jet function is parameterised by the reference vector n^μ. It is normal to keep the reference vector off the light cone. This allows one to manage and remove spurious collinear singularities relating to the n^μ Wilson line and it allows a check of the final amplitude by seeing if it is n^μ independent. For these reasons the non-radiative jet function J and the eikonal jet function $\mathcal{J}$ have been computed at one-loop order for non-null n as discussed in [23, 24].

For our purposes it will be computationally simpler to work with a light-like reference vector, i.e. one that satisfies $n^2 = 0$. This will also lead to simplifications to the total amplitude that we are needing to compute to be discussed later in this chapter.

2.2.1 Tree level radiative jet function

We shall now go on to compute the radiative jet function. For our purposes we only need to compute terms up to next-to-leading order where we define perturbative coefficients via

$$J^\nu(p, n, k; \alpha_s, \epsilon) = g_s \sum_{n=0}^{\infty} J^{\nu(n)}(p, n, k; \epsilon) \left(\frac{\alpha_s}{4\pi}\right)^n. \tag{2.2}$$

The Feynman diagram for the tree level radiative jet function is shown in figure (2.1) and has the associated expression of

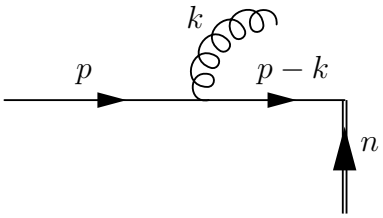

Figure 2.1: Feynman diagram of the tree level radiative jet function. The double line represents the jet leg.

$$J^{\nu(0)}(p,n,k) = \frac{(\not{p}-\not{k})}{-2p\cdot k}\gamma^{\mu}u(p) = \left(\frac{\not{k}\gamma^{\nu}}{2p\cdot k} - \frac{p^{\nu}}{p\cdot k}\right)u(p). \tag{2.3}$$

The radiative jet function is spin dependent and so the amplitude can be split into its spin dependent and spin independent parts:

$$J^{\nu(0)}(p,n,k) = \left(-\frac{p^{\nu}}{p\cdot k} + \frac{k^{\nu}}{2p\cdot k} - \frac{ik_{\alpha}\Sigma^{\alpha\nu}}{p\cdot k}\right)u(p), \tag{2.4}$$

where we have used the Lorentz generators for spin 1/2

$$\Sigma^{\alpha\mu} = \frac{i}{4}\left[\gamma^{\alpha},\gamma^{\mu}\right]. \tag{2.5}$$

To generalise the expression to an emitter of different spin one would need to replace the Lorentz generator with the appropriate one.

2.2.2 LBKDD continued

The LBKDD theorem was used to create an expression for the radiative amplitude given in equation (1.41). We wish for all terms in this equation to multiply the non-radiative amplitude, we can accomplish this by multiplying and dividing through by the non-radiative jet function

$$\mathcal{A}^{\mu}(p_j,k) = \sum_{i=1}^{2}\left[q_i\left(\frac{(2p_i-k)^{\mu}}{2p_i\cdot k - k^2} + G_i^{\nu\mu}\frac{\partial}{\partial p_i^{\nu}}\right) + G_i^{\nu\mu}\left(\frac{J_{\nu}(p_i,k,n_i)}{J(p_i,n_i)} - q_i\frac{\partial}{\partial p_i^{\nu}}\left(\ln J(p_i,n_i)\right)\right)\right]\mathcal{A}(p_i;p_j). \tag{2.6}$$

The L.H.S. of the amplitude is renormalisation group invariant as it is a physical amplitude. One may therefore choose to work with bare or renormalised quantities on the R.H.S. .The eikoinal Feynman rules are invariant under the rescaling $n^{\mu} \to \lambda n^{\mu}$

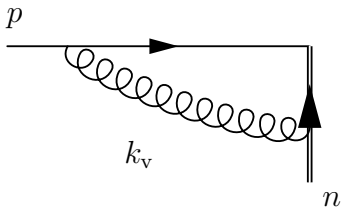

Figure 2.2: The one-loop correction to the non-radiative Jet function vertex.

thus effectively ruling out the Jet functions dependence on $(n\cdot p)$ by rescaling invariance arguments. The scale invariant dimensionless quantity that could survive is $\frac{(p\cdot n)^2}{n^2\mu^2}$ but the choice of $n^2=0$ rules this out implying the loop corrections to the non-radiative jet function should be scaleless and manifestly zero. However it is worth calculating the non-radiative jet function to make clear why bare-quantities are preferable. If we consider the one loop vertex correction to the non-radiative jet function given in figure (2.2) its expression is

$$\begin{aligned} J_{\rm V}^{(1)}(p,n;\epsilon) &= 2i\mu^{2\epsilon}g_s^2\int\frac{d^dk}{(2\pi)^d}\frac{(\not p-\not k)\not n}{k^2 2n\cdot k(p-k)^2} \\ &= 2i\mu^{2\epsilon}g_s^2\int\frac{d^dk}{(2\pi)^d}\int_0^1 dx\int_0^1 dy\frac{2y(\not p-\not k)\not n}{\left[yk^2-2xyk\cdot p+2(1-y)n\cdot k\right]^3} \\ &= \frac{\alpha_s}{2\pi}(4\pi\mu^2)^\epsilon\Gamma(1+\epsilon)(-2p\cdot n)^{-\epsilon}\frac{1}{\epsilon(\epsilon-1)}\int_0^1 dy y^{-1+\epsilon}(1-y)^{-1-\epsilon}. \end{aligned} \tag{2.7}$$

The result is dependent upon the scale $(n\cdot p)$ this is the result of the hard collinear divergence breaking rescaling invariance. If one were to work with renormalised quantities then the UV pole can be removed however this result is badly behaved for all values of ϵ It is therefore sensible to work with bare quantities and take the y-integral in equation (2.7) to be zero. We therefore see that for the choice of $n^2=0$, all loop corrections to the bare non-radiative jet function can be taken to be manifestly zero in dimensional regularisation allowing one to set

$$J(p_i;n_i)=1. \tag{2.8}$$

This leaves us with the final expression for the radiative amplitude in this renormalisation scheme choice of

$$\mathcal{A}^\mu(p_j,k)=\sum_{i=1}^{2}\left[q_i\left(\frac{(2p_i-k)^\mu}{2p_i\cdot k-k^2}+G_i^{\nu\mu}\frac{\partial}{\partial p_i^\nu}\right)+G_i^{\nu\mu}J_\nu(p_i;k)\right]\mathcal{A}(p_i;p_j). \tag{2.9}$$

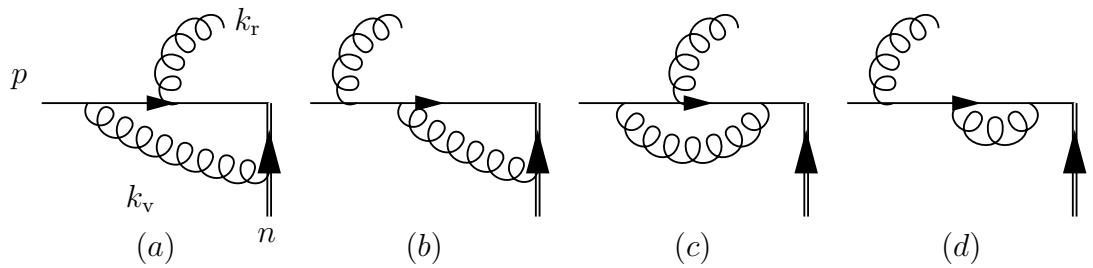

Figure 2.3: Graphs contributing to the one-loop radiative jet function. The labelling convention used for diagram (a) is used for all graphs but has been supressed for clarity.

This form will be used for the Drell-Yan analysis. It shall now be our goal to compute each component of the amplitude in equation (2.9).

2.3 Radiative jet function at 1-loop

The four Feynman diagrams that will contribute to the one real one virtual radiative jet function at NNLO are shown in figure (2.3). The virtual boson in diagrams (a) and (b) connects the Wilson line and external parton legs and so they will be dependent upon the reference vector n^μ. Diagrams (c) and (d) involve the virtual gluon being emitted and reabsorbed by the external parton leg and will therefore be n^μ independent.

2.3.1 Vertex correction

The diagram (b) from the one loop diagrams in figure (2.3) has the amplitude

$$J^\mu_{(b)} = 2i\mu^{2\epsilon} g_s^3 T^a \int \frac{d^d k_v}{(2\pi)^d} \frac{(\not{p} - \not{k}_v - \not{k}_r)\not{n}(\not{p} - \not{k}_r)\gamma^\mu u(p)}{k_v^2 (p - k_v - k_r)^2 (p - k_r)^2 2n \cdot k_v}. \tag{2.10}$$

In order to begin computing this we first introduce Feynman parameters to re-write the integral as

$$J^\mu_{(b)} = \frac{2i\mu^{2\epsilon} g_s^3 T^a}{(-2p \cdot k_r)} \int_0^1 dx \int_0^1 dy \int \frac{d^d k_v}{(2\pi)^d} 2(1-y)\mathcal{N} D^{-3}, \tag{2.11}$$

where we have defined:

$$\begin{aligned} D =& (1-y)k_v^2 + y2n \cdot k_v + (1-y)x(-2p \cdot k_v - 2p \cdot k_r + 2k \cdot k_r), \\ \mathcal{N} =& (\not{p} - \not{k}_v - \not{k}_r)\not{n}(\not{p} - \not{k}_r)\gamma^\mu u(p). \end{aligned} \tag{2.12}$$

The Feynman parameters have been implemented using

$$\frac{1}{AB} = \int_0^1 dx \frac{1}{[xA + (1-x)B]^2}, \tag{2.13}$$

in such a way that the two terms quadratic in $k_{\rm v}$ are grouped together with the first parameter and the term linear in $k_{\rm v}$ is grouped in with the second parameter. This choice of grouping will make the integrals over the Feynman parameters simpler and more recognisable. Next complete the square in the denominator and shift the integration parameter defining

$$\frac{D}{(1-y)} = k'^2 - M^2, \tag{2.14}$$

where

$$\begin{aligned} k' &= k_{\rm v} + \frac{yn}{(1-y)} - xp + xk_r \\ M^2 &= x2p\cdot k_r + \frac{xy}{(1-y)}(-2n\cdot p) + \frac{xy}{(1-y)}(2n\cdot k_r) + x^2(-2p\cdot k_r). \end{aligned} \tag{2.15}$$

Shifting the loop momentum and utilising the Clifford algebra of the gamma matrices the numerator factor can be written as

$$\mathcal{N} = (1-x)[2n\cdot p(2p^\mu - \not{k}_r\gamma^\mu) + 2p\cdot k_r \not{n}\gamma^\mu - 2p^\mu 2n\cdot k_r]u(p). \tag{2.16}$$

Terms have been neglected whose numerators are linear in the shifted loop momentum as these will be zero on integration and $\not{n}^2 = 0$ has been used. Performing the integration over the loop momentum we are left with

$$J^\mu_{(b)} = \frac{2\mu^{2\epsilon} g_s^3 T^a}{(-2p\cdot k_r)} \frac{\Gamma(1+\epsilon)}{(4\pi)^{2-\epsilon}} [2n\cdot p(2p^\mu - \not{k}_r\gamma^\mu) + 2p\cdot k_r \not{n}\gamma^\mu - 2p^\mu 2n\cdot k_r]u(p) I_b, \tag{2.17}$$

where we have defined

$$\begin{aligned} I_{(b)} = \int_0^1 dx \int_0^1 dy (1-x)(1-y)^{-2} \\ \times \left[x(1-x)(2p\cdot k_r) + \frac{xy}{(1-y)}(-2n\cdot p) + \frac{xy}{(1-y)}(2n\cdot k_r)\right]^{d/2-3}. \end{aligned} \tag{2.18}$$

We can perform the y integral first

$$I_{(b)} = \frac{(2p\cdot k_r)^{-\epsilon}}{\epsilon(2n\cdot k_r - 2p\cdot n)} \int_0^1 dx x^{-1-\epsilon}(1-x)^{1-\epsilon}. \tag{2.19}$$

The x integral is recognisable as the definition of the beta function

$$I_{(b)} = \frac{(2p\cdot k_r)^{-\epsilon}}{\epsilon(2n\cdot k_r - 2p\cdot n)} \frac{\Gamma(-\epsilon)\Gamma(2-\epsilon)}{\Gamma(2-2\epsilon)}. \tag{2.20}$$

The result for the diagram is now

$$J^{\mu}_{(b)} = \frac{-2\mu^{2\epsilon} g_s^3 T^a}{(4\pi)^{2-\epsilon}} [2n\cdot p(2p^\mu - \not{k}_r\gamma^\mu) + 2p\cdot k_r \not{n}\gamma^\mu - 2p^\mu 2n\cdot k_r] u(p) \times \\ \times \frac{(2p\cdot k_r)^{-1-\epsilon}}{(2n\cdot k_r - 2p\cdot n)} \frac{\Gamma(1+\epsilon)\Gamma(-\epsilon)\Gamma(2-\epsilon)}{\epsilon\Gamma(2-2\epsilon)}. \tag{2.21}$$

This result can be expanded to linear order in the real emission momentum k_r and we can make use of the definition of

$$\Gamma_{(b)} = \frac{\Gamma(1+\epsilon)\Gamma(1-\epsilon)\Gamma(2-\epsilon)}{\Gamma(2-2\epsilon)}, \tag{2.22}$$

to write the result as

$$J^{\mu}_{(b)} = \frac{2\mu^{2\epsilon} g_s^3 T^a}{(4\pi)^{2-\epsilon}} (2p\cdot k_r)^{-1-\epsilon}\Gamma_b \left[-2p^\mu + \not{k}_r\gamma^\mu + \frac{2p\cdot k_r}{-2p\cdot n}(2n^\mu - \gamma^\mu \not{n})\right] u(p). \tag{2.23}$$

2.3.2 Diagram (a), Box diagram

The next diagram to tackle is diagram (a) where the real gluon is emitted from within the virtual emission loop. This leads to a virtual momentum dependent propagator factor in the integral. Calculating this integral is more difficult and such diagrams are referred to as "box diagrams". The diagram's integral takes the form

$$J^{\mu}_{(a)} = 2i\mu^{2\epsilon} g_s^3 T^a \int \frac{d^d k_{\rm v}}{(2\pi)^d} \frac{(\not{p} - \not{k}_{\rm v} - \not{k}_r)\gamma^\mu(\not{p} - \not{k}_{\rm v})\not{n}}{k_{\rm v}^2 (p-k_{\rm v}-k_r)^2 (p-k_{\rm v})^2 2n\cdot k_{\rm v}} u(p). \tag{2.24}$$

The first step as for diagram (b) is to introduce Feynman parameters to write the integral in the form of

$$J^{\mu}_{(a)} = 2i\mu^{2\epsilon} g_s^3 T^a \int \frac{d^d k_{\rm v}}{(2\pi)^d} \int_0^1 dx \int_0^1 dy \int_0^1 dz \Gamma(4) z(1-z) \mathcal{N}^\mu D^{-4}, \tag{2.25}$$

where we have defined:

$$D = z\left[x k_{\rm v}^2 + (1-x) 2n\cdot k_{\rm v}\right] + (1-z)\left[y(p-k_{\rm v}-k_r)^2 + (1-y)(p-k_{\rm v})^2\right], \\ \mathcal{N}^\mu = (\not{p} - \not{k}_{\rm v} - \not{k}_r)\gamma^\mu(\not{p} - \not{k}_{\rm v})\not{n} u(p). \tag{2.26}$$

The next step is to complete the square in the denominator

$$\frac{D}{[zx + (1-z)]} = k_{\rm v}'^{\,2} - M^2, \tag{2.27}$$

where we have defined:

$$k_{\rm v}{}' = k_{\rm v} + \frac{(1-z)y}{[zx+(1-z)]}(k_r) + \frac{(1-z)}{[zx+(1-z)]}(-p) + \frac{z(1-x)}{[zx+(1-z)]}n$$
$$M^2 = \frac{[-zx(1-z)y(-2p\cdot k_r) + (1-z)z(1-x)y(2n\cdot k_r) + (1-z)z(1-x)(-2p\cdot n)]}{[zx+(1-z)]^2}. \tag{2.28}$$

Inserting the shifted momentum parameter into the numerator one obtains:

$$\begin{aligned}
\mathcal{N}^\mu =& \{(zx\ \not{p} + [(1-z)(1-y)+zx](-\not{k}_r) + z(1-x)\ \not{n})\,\gamma^\mu\,(zx\ \not{p} + (1-z)y(\not{k}_r)) \\
&+\not{k}_{\rm v}\gamma^\mu\not{k}_{\rm v}\}\ \not{n}u(p)\,[zx+(1-z)]^{-2}\,, \\
=& \big\{(zx)^2\ \not{p}\gamma^\mu\ \not{p} + zx(1-z)y\,[2p^\mu\ \not{k}_r - 2p\cdot k_r\gamma^\mu + (2k_r{}^\mu - \not{k}_r\gamma^\mu)\ \not{p}] + \\
&\quad + zx\,[-zx-(1-z)(1-y)]\ \not{k}_r\gamma^\mu\ \not{p} + \\
&\quad + z(1-x)zx\ \not{n}\gamma^\mu\ \not{p} + z(1-x)(1-z)y\ \not{n}\gamma^\mu\ \not{k}_r + \\
&\quad + [zx+(1-z)]^2\,\not{k}_{\rm v}\gamma^\mu\not{k}_{\rm v}\big\}\ \not{n}u(p), \\
=& \overline{\mathcal{N}}^\mu + [zx+(1-z)]^2\,\not{k}_{\rm v}\gamma^\mu\not{k}_{\rm v}\ \not{n}u(p),
\end{aligned} \tag{2.29}$$

where terms linear in the shifted momentum and those proportional to $\not{n}^2$ have been discarded, along the term quadratic in k_r since it will not contribute at NLP order. We can compute the integral proportional to the non-quadratic term $\overline{\mathcal{N}}^\mu$ first:

$$J^\mu_{(a)}\Big|_{non-quad} = \frac{2\mu^{2\epsilon}g_s^3\Gamma(2+\epsilon)}{(4\pi)^{2-\epsilon}}\int_0^1 dx\int_0^1 dy\int_0^1 dz z(1-z)[zx+(1-z)]^{-6}\overline{\mathcal{N}}^\mu[M^2]^{-2-\epsilon}. \tag{2.30}$$

Each term corresponds to a separate integration to be performed. Rather than compute each term individually it would be more ideal to come up with a general integral that we can compute, from which the solution for each term can be obtained. We name such an integral a master integral, and define for our present purposes

$$\begin{aligned}
I_{(a)}(n_a,n_b,n_c,n_d) =& \frac{\Gamma(2+\epsilon)}{(4\pi)^{2-\epsilon}}\int_0^1 dx\int_0^1 dy x^{n_a}(1-x)^{n_b}y^{n_d}(1-y)^{n_c} \\
&\times[(1-x)(-2p\cdot n) + (1-x)y(2n\cdot k_r) - xy(-2p\cdot k_r)]^{-2-\epsilon} \\
&\times\int_0^1 dz(1-z)^{-1-\epsilon+n_c+n_d}z^{-1-\epsilon+n_a+n_b}\,[1-z(1-x)]^{2\epsilon-2}\,,
\end{aligned} \tag{2.31}$$

where n_a,n_b,n_c and n_d correspond to the Feynman parameter combinations of zx,$z(1-x)$,$(1-y)(1-z)$ and $y(1-z)$ respectively. The full result for the amplitude in terms

of the master integral is

$$\begin{aligned} J^{\mu}_{(a)}\Big|_{non-quad} = 2\mu^{2\epsilon} g_s^3 T^a \, [&2p^\mu 2p\cdot n I_a(2,0,0,0) \\ &+ (2p^\mu \not{k}_r \not{n} - 2p\cdot k_r \gamma^\mu \not{n} + 2k_r^\mu 2p\cdot n)\, I_a(1,0,0,1) - \\ &- \not{k}_r \gamma^\mu 2p\cdot n (I_a(2,0,0,0) + I_a(1,0,1,0) + I_a(1,0,0,1)) \\ &- \not{k}_r \gamma^\mu \not{k}_r \not{n} (I_a(0,0,1,1) + I_a(1,0,0,1)) \\ &+ (2n^\mu - \gamma^\mu \not{n}) 2p\cdot n I_a(1,1,0,0) \\ &+ (2n^\mu \not{k}_r \not{n} - 2n\cdot k_r \gamma^\mu \not{n}) I_a(0,1,0,1)]\, u(p), \end{aligned} \tag{2.32}$$

where anti-commutation of Dirac matrices has been used on the numerator factors. After performing the integrations over the z parameter, the master integral becomes

$$\begin{aligned} I_{(a)}(n_a,n_b,n_c,n_d) =& \frac{\Gamma(2+\epsilon)}{(4\pi)^{2-\epsilon}} \frac{\Gamma(-\epsilon+n_a+n_b)\Gamma(-\epsilon+n_c+n_d)}{\Gamma(2-2\epsilon)} \\ &\times \int_0^1 dx (1-x)^{n_b} x^{\epsilon-n_b} \int_0^1 dy y^{n_d} (1-y)^{n_c} \\ &\times [(1-x)(-2p\cdot n) + (1-x)y(2n\cdot k_r) - xy(-2p\cdot k_r)]^{-2-\epsilon}. \end{aligned} \tag{2.33}$$

Next perform the x integration:

$$\begin{aligned} I_{(a)}(n_a,n_b,n_c,n_d) =& (2p\cdot k_r)^{n_b-1-\epsilon} \frac{\Gamma(1+\epsilon-n_b)}{(4\pi)^{2-\epsilon}} \frac{\Gamma(-\epsilon+n_a+n_b)\Gamma(-\epsilon+n_c+n_d)}{\Gamma(2-2\epsilon)} \\ &\times \int_0^1 dy y^{n_d+n_b-1-\epsilon} (1-y)^{n_c} (-2p\cdot n + 2n\cdot k_r y)^{-1-n_b}. \end{aligned} \tag{2.34}$$

Finally the y integral can be recognised as a hypergeometric function

$$\begin{aligned} I_{(a)}(n_a,n_b,n_c,n_d) =& (2p\cdot k_r)^{n_b-1-\epsilon} (-2p\cdot n)^{-1-n_b} \frac{\Gamma(1+\epsilon-n_b)}{(4\pi)^{2-\epsilon}} \frac{\Gamma(1+n_c)}{\Gamma(2-2\epsilon)} \\ &\times \frac{\Gamma(-\epsilon+n_a+n_b)\Gamma(-\epsilon+n_c+n_d)\Gamma(n_d+n_b-\epsilon)}{\Gamma(n_d+n_b-\epsilon+1+n_c)} \\ &\times {}_2F_1\left(n_d+n_b-\epsilon, 1+n_b, n_d+n_b-\epsilon+1+n_c, \frac{2n\cdot k_r}{2p\cdot n}\right). \end{aligned} \tag{2.35}$$

Next to compute is the term that has the numerator factor quadratic in $k_{\rm v}$. We can use

$$\int d^d k_{\rm v} \frac{k_{\rm v}^\mu k_{\rm v}^\nu}{(k_{\rm v}^2 - M^2)^4} = \frac{\eta^{\mu\nu}}{6} \int d^d k_{\rm v} \frac{1}{(k_{\rm v}^2 - M^2)^3}, \tag{2.36}$$

the derivation of which can be found in appendix A.2.4, to write the term in a form that is more familiar to compute. Using this the momentum integral can be performed

and the amplitude contribution is:

$$\begin{aligned}
J^{\mu}_{(a)}\Big|_{\text{quad}} =& -\frac{\mu^{2\epsilon} g_s^3 T^a \Gamma(1+\epsilon)}{(4\pi)^{2-\epsilon}} (2\epsilon)\gamma^{\mu} \not{n} u(p) \\
& \times \int_0^1 dx \int_0^1 dy \int_0^1 dz (1-z) z [zx + (1-z)]^{-4} [M^2]^{-1-\epsilon}, \\
=& -\frac{\mu^{2\epsilon} g_s^3 T^a \Gamma(1+\epsilon)}{(4\pi)^{2-\epsilon}} (2\epsilon)\gamma^{\mu} \not{n} u(p) \\
& \times \int_0^1 dx \int_0^1 dy \int_0^1 dz [(1-z)z]^{-\epsilon} [zx + (1-z)]^{2\epsilon-2} \\
& \times [-xy(-2p\cdot k_r) + (1-x)y(2n\cdot k_r) + (1-x)(-2p\cdot n)]^{-1-\epsilon}. \qquad (2.37)
\end{aligned}$$

Following the integration steps for the master integral the result for this term is

$$\begin{aligned}
J^{\mu}_{(a)}\Big|_{\text{quad.}} =& -\frac{\mu^{2\epsilon} g_s^3 T^a \Gamma(1+\epsilon)}{(4\pi)^{2-\epsilon}} (2\epsilon)\gamma^{\mu} \not{n} u(p) \\
& \times \int_0^1 dx \int_0^1 dy \int_0^1 dz [(1-z)z]^{-\epsilon} [zx + (1-z)]^{2\epsilon-2} \\
& \times [-xy(-2p\cdot k_r) + (1-x)y(2n\cdot k_r) + (1-x)(-2p\cdot n)]^{-1-\epsilon}, \\
=& \frac{-2\mu^{2\epsilon} g_s^3 T^a \Gamma(1+\epsilon)}{(4\pi)^{2-\epsilon}} \frac{(2p\cdot k_r)^{-\epsilon}}{-2p\cdot n} \gamma^{\mu} \not{n} u(p) \\
& \times \frac{\Gamma(2-\epsilon)\Gamma(1-\epsilon)}{\Gamma(2-2\epsilon)} {}_2F_1\left(1, 1-\epsilon, 2-\epsilon, \frac{2n\cdot k_r}{2p\cdot n}\right). \qquad (2.38)
\end{aligned}$$

2.3.3 n-independent diagrams

In this sub-section the two n-independent diagrams will be computed. The expressions we need to compute are

$$J^{\nu}_{(c)} = i\mu^{2\epsilon} C_F g_s^3 T^a \int \frac{d^d k_{\text{v}}}{(2\pi)^d} \frac{(\not{p} - \not{k}_r)\gamma^{\mu}(\not{p} - \not{k}_r - \not{k}_{\text{v}})\gamma^{\nu}(\not{p} - \not{k}_{\text{v}})\gamma_{\mu} u(p)}{k_{\text{v}}^2 (p-k_r)^2 (p-k_{\text{v}}-k_r)^2 (p-k_{\text{v}})^2}, \qquad (2.39)$$

and

$$J^{\nu}_{(d)} = i\mu^{2\epsilon} C_F g_s^3 T^a \int \frac{d^d k_{\text{v}}}{(2\pi)^d} \frac{(\not{p} - \not{k}_r)\gamma^{\mu}(\not{p} - \not{k}_r - \not{k}_{\text{v}})\gamma_{\mu}(\not{p} - \not{k}_r)\gamma^{\nu} u(p)}{k_{\text{v}}^2 (p-k_r)^2 (p-k_{\text{v}}-k_r)^2 (p-k_r)^2}. \qquad (2.40)$$

The integrals one needs to compute are therefore

$$\begin{aligned}
I_{(d)} &= \int \frac{d^d k_{\text{v}}}{(2\pi)^d} \frac{(\not{p} - \not{k}_r - \not{k}_{\text{v}})}{k_{\text{v}}^2 (p-k_{\text{v}}-k_r)^2}, \\
I_{(c)} &= \int \frac{d^d k_{\text{v}}}{(2\pi)^d} \frac{(\not{p} - \not{k}_r - \not{k}_{\text{v}})\gamma^{\nu}(\not{p} - \not{k}_{\text{v}})}{k_{\text{v}}^2 (p-k_{\text{v}}-k_r)^2 (p-k_{\text{v}})^2}. \qquad (2.41)
\end{aligned}$$

Firstly we shall solve the simpler integral corresponding to graph (d):

$$\begin{aligned} I_{(d)} =& \int \frac{d^d k_{\rm v}}{(2\pi)^d} \frac{(\not{p} - \not{k}_r - \not{k}_{\rm v})}{k_{\rm v}^2 (p - k_{\rm v} - k_r)^2}, \\ =& \int_0^1 dx \int \frac{d^d k'_{\rm v}}{(2\pi)^d} (1-x)(\not{p} - \not{k}_r)[{k'_{\rm v}}^2 - (1-x)x(2p\cdot k_r)]^{-2}, \\ =& \frac{i\Gamma(2-d/2)}{(4\pi)^{d/2}} \int_0^1 dx (1-x)(\not{p} - \not{k}_r)[x(1-x)(2p\cdot k_r)]^{d/2-2}, \\ =& \frac{i\Gamma(\epsilon)}{(4\pi)^{2-\epsilon}} (2p\cdot k_r)^{-\epsilon} (\not{p} - \not{k}_r) \left[\frac{\Gamma(1-\epsilon)\Gamma(2-\epsilon)}{\Gamma(3-2\epsilon)}\right]. \end{aligned} \tag{2.42}$$

The numerator for diagram (d) is:

$$\begin{aligned} \mathcal{N}_{(d)} =& (\not{p} - \not{k}_r)\gamma^\mu (\not{p} - \not{k}_r)\gamma_\mu (\not{p} - \not{k}_r)\gamma^\nu u(p), \\ =& (2-d)(\not{p} - \not{k}_r)(\not{p} - \not{k}_r)(\not{p} - \not{k}_r)\gamma^\nu u(p), \\ =& (2-d)(\not{k}_r \not{p} \not{k}_r - \not{p}\not{k}_r \not{p})\gamma^\nu u(p), \\ =& (-2+2\epsilon)(2p\cdot k_r \not{k}_r \gamma^\nu - 2p^\nu 2p\cdot k_r) u(p). \end{aligned} \tag{2.43}$$

This gives the contribution from graph (d) of

$$J^\nu_{(d)} = (2-2\epsilon) 2\mu^{2\epsilon} C_F g_s^3 T^a \frac{\Gamma(\epsilon)}{(4\pi)^{2-\epsilon}} (2p\cdot k_r)^{-1-\epsilon} (\not{k}_r \gamma^\nu - 2p^\nu) u(p) \left[\frac{\Gamma(2-\epsilon)\Gamma(1-\epsilon)}{\Gamma(3-2\epsilon)}\right]. \tag{2.44}$$

We will now compute graph (c) where the real emission occurs from within the virtual emission loop. Firstly consider the scalar integral

$$I_{\rm s} = \int \frac{d^d k_{\rm v}}{(2\pi)^d} \frac{1}{k_{\rm v}^2 (p - k_{\rm v} - k_r)^2 (p - k_{\rm v})^2}. \tag{2.45}$$

Introducing Feynman parameters the integral can be written in the form

$$\begin{aligned} I_{\rm s} =& \int \frac{d^d k_{\rm v}}{(2\pi)^d} \int_0^1 dx \int_0^1 dy 2(1-y) \\ & \times \left[k_{\rm v}^2 - (1-y)2p\cdot k_{\rm v} + (1-y)x 2k_{\rm v}\cdot k_r - (1-y)x 2p\cdot k_r\right]^{-3}. \end{aligned} \tag{2.46}$$

Next shift the loop momentum

$$k'_{\rm v} = k_{\rm v} - (1-y)p + (1-y)x k_r. \tag{2.47}$$

Performing the integration over the loop momentum we have

$$I_{\rm s} = \frac{-i\Gamma(1+\epsilon)}{(4\pi)^{2-\epsilon}} \int_0^1 dx \int_0^1 dy (1-y)^{-\epsilon} y^{-1-\epsilon} x^{-1-\epsilon} (2p\cdot k_r)^{-1-\epsilon}. \tag{2.48}$$

We can use this integral form in what follows. The next thing to consider is the numerator algebra. Firstly we can insert the shifted momentum variable. Neglecting terms linear in $k'_{\rm v}$, the numerator becomes

$$\begin{aligned}\mathcal{N}_{(c)} =&(\not{p} - \not{k}_r)\gamma^\mu \left[(y\not{p} + [(1-y)x-1]\not{k}_r)\gamma^\nu (y\not{p} + (1-y)x\not{k}_r) + \not{k}'_{\rm v}\gamma^\nu \not{k}'_{\rm v}\right]\gamma_\mu u(p),\\ =&\overline{\mathcal{N}}_{(c)} + (\not{p} - \not{k}_r)\gamma^\mu \not{k}'_{\rm v}\gamma^\nu \not{k}'_{\rm v}\gamma_\mu u(p).\end{aligned} \tag{2.49}$$

The anti-commutation of the gamma matrices can be performed using

$$\begin{aligned}\not{a}\gamma^\mu \not{b}\gamma^\nu \not{c}\gamma_\mu =&2\not{a}\not{c}\not{b}\gamma^\nu - \not{a}\gamma^\mu \not{b}\gamma^\nu \gamma_\mu \not{c},\\ =&2\not{a}\not{c}\not{b}\gamma^\nu - 2\not{a}\gamma^\nu \not{b}\not{c} + \not{a}\gamma^\mu \not{b}\gamma_\mu \gamma^\nu \not{c},\\ =&2\not{a}\not{c}\not{b}\gamma^\nu - 2\not{a}\gamma^\nu \not{b}\not{c} + (2-d)\not{a}\not{b}\gamma^\nu \not{c},\\ =&2(2-d)c^\nu \not{a}\not{b} - (2-d)\not{a}\not{b}\not{c}\gamma^\nu + 2\not{a}\not{c}\not{b}\gamma^\nu - 4\not{a}\not{c}b^\nu + 2\not{a}\not{b}\gamma^\nu \not{c},\\ =&2(4-d)c^\nu \not{a}\not{b} - (4-d)\not{a}\not{b}\not{c}\gamma^\nu - 4b^\nu \not{a}\not{c} + 2\not{a}\not{c}\not{b}\gamma^\nu.\end{aligned} \tag{2.50}$$

We shall firstly solve for the case of the non-quadratic numerator terms in $\overline{\mathcal{N}}_{(c)}$. Utilising the Clifford algebra and $\not{p}u(p) = p^2 = k_r^2 = 0$ we reduce this numerator factor to

$$\overline{\mathcal{N}}_{(c)} = 2p\cdot k_r \left\{k_r^\nu 4(\epsilon-1)(1-y)x[(1-y)x-1] + 2\not{k}_r\gamma^\nu[(\epsilon-1)y(1-y)x + y]\right\}. \tag{2.51}$$

Using the above ingredients we can get the integral contribution to the amplitude for the non-quadratic term

$$\begin{aligned}I|_{(c),\rm non-quad} =&\frac{-i\Gamma(1+\epsilon)}{(4\pi)^{d/2}} \int_0^1 dx \int_0^1 dy (1-y)^{-\epsilon} y^{-1-\epsilon} x^{-1-\epsilon} (2p\cdot k_r)^{-\epsilon}\\ &\times \left\{k_r^\nu 4(\epsilon-1)(1-y)x[(1-y)x-1] + 2\not{k}_r\gamma^\nu[(\epsilon-1)y(1-y)x+y]\right\},\\ =&-i\frac{\Gamma(1+\epsilon)}{(4\pi)^{2-\epsilon}}(2p\cdot k_r)^{-\epsilon}\left\{4(\epsilon-1)k_r^\nu\left[\frac{\Gamma(3-\epsilon)\Gamma(-\epsilon)}{\Gamma(3-2\epsilon)}\frac{1}{2-\epsilon} - \frac{\Gamma(2-\epsilon)\Gamma(-\epsilon)}{\Gamma(2-2\epsilon)}\frac{1}{1-\epsilon}\right]\right.\\ &\left.+2\not{k}_r\gamma^\nu\left[(\epsilon-1)\frac{\Gamma(1-\epsilon)\Gamma(2-\epsilon)}{\Gamma(3-2\epsilon)}\frac{1}{1-\epsilon} + \frac{\Gamma(1-\epsilon)\Gamma(1-\epsilon)}{\Gamma(2-2\epsilon)}\frac{1}{-\epsilon}\right]\right\},\\ =&-i\frac{\Gamma(1+\epsilon)}{(4\pi)^{2-\epsilon}}(2p\cdot k_r)^{-\epsilon}\left\{2k_r^\nu\frac{\Gamma(2-\epsilon)\Gamma(-\epsilon)}{\Gamma(2-2\epsilon)} +\right.\end{aligned}$$

$$+2\not{k}_r\gamma^\nu\left[\frac{-\Gamma(2-\epsilon)\Gamma(1-\epsilon)}{\Gamma(3-2\epsilon)}+\frac{\Gamma(1-\epsilon)\Gamma(-\epsilon)}{\Gamma(2-2\epsilon)}\right]\Bigg\}. \tag{2.52}$$

The result for the non-quadratic contribution of diagram (c) is

$$\begin{aligned}J|_{(c),\text{non-quad}} =& -\mu^{2\epsilon}C_F g_s^3 T^a\frac{\Gamma(1+\epsilon)}{(4\pi)^{2-\epsilon}}(2p\cdot k_r)^{-1-\epsilon}\Bigg\{2k_r^\nu\frac{\Gamma(2-\epsilon)\Gamma(-\epsilon)}{\Gamma(2-2\epsilon)}\\ &+2\not{k}_r\gamma^\nu\left[\frac{-\Gamma(2-\epsilon)\Gamma(1-\epsilon)}{\Gamma(3-2\epsilon)}+\frac{\Gamma(1-\epsilon)\Gamma(-\epsilon)}{\Gamma(2-2\epsilon)}\right]\Bigg\}\end{aligned} \tag{2.53}$$

The quadratic term left to compute is

$$I|_{(c),\text{quad}} = \int_0^1 dx\int_0^1 dy\int\frac{d^dk'_{\rm v}}{(2\pi)^d}\not{k}'_{\rm v}\gamma^\nu\not{k}'_{\rm v}2(1-x)[{k'_{\rm v}}^2-x(1-x)y(2p\cdot k_r)]^{-3}$$
$$. \tag{2.54}$$

We can make use of the identity

$$\int d^dk'_{\rm v}\frac{k'^{\mu}_{\rm v}k'^{\nu}_{\rm v}}{[{k'_{\rm v}}^2-M^2]^3}=\frac{\eta^{\mu\nu}}{4}\int d^dk_{\rm v}{}'\frac{1}{[{k'_{\rm v}}^2-M^2]^2}, \tag{2.55}$$

so that the integral is now

$$\begin{aligned}I|_{(c),\text{quad}} =&\frac{-\eta^{\alpha\beta}}{2}\gamma_\alpha\gamma^\nu\gamma_\beta\int_0^1 dx\int_0^1 dy\int_0^\infty d\nu(1-x)\nu\exp(-i\nu M^2)\int\frac{d^dk'_{\rm v}}{(2\pi)^d}\exp(i\nu k'^2_{\rm v}),\\ =&\frac{i\Gamma(\epsilon)}{(4\pi)^{2-\epsilon}}\frac{-2+2\epsilon}{2}\gamma^\nu\int_0^1 dx\int_0^1 dy(1-x)[x(1-x)y(2p\cdot k_r)]^{-\epsilon},\\ =&\frac{i\Gamma(\epsilon)(\epsilon-1)}{(4\pi)^{2-\epsilon}}\gamma^\nu(2p\cdot k_r)^{-\epsilon}\frac{\Gamma(2-\epsilon)\Gamma(1-\epsilon)}{\Gamma(3-2\epsilon)}\frac{1}{1-\epsilon}.\end{aligned} \tag{2.56}$$

The quadratic contribution to the diagram is therefore

$$J|_{(c),\text{quad}} =(-2+2\epsilon)2\mu^{2\epsilon}C_F g_s^3 T^a\frac{\Gamma(\epsilon)}{(4\pi)^{2-\epsilon}}(2p\cdot k_r)^{-1-\epsilon}(\not{k}_r\gamma^\nu-2p^\nu)u(p)\frac{\Gamma(2-\epsilon)\Gamma(1-\epsilon)}{\Gamma(3-2\epsilon)}. \tag{2.57}$$

This term exactly cancels the contribution we calculated earlier from graph (d) in equation (2.44).

2.3.4 Combined result

The combined radiative jet is obtained by summing over all four of these graphs. Firstly we can sum together the two graphs that depend upon the jet leg. The result in the form of the master integrals, neglecting ϵ and k_r independent pre-factors (and the factor of $\mu^{2\epsilon}(4\pi)^{\epsilon}\Gamma(1+\epsilon)$), is

$$\begin{aligned}J^{\nu}_{(a)+(b)}(p,n,k;\epsilon) = (2p\cdot k_2)^{-\epsilon}\Big\{&\left[2\Gamma_b + 2(-2p\cdot n)I_a(2,0,0,0)\right]p^{\nu} + 2I_a(1,0,0,1)p^{\nu}\not{k}\not{n}\\ &- \left[\left(1+\frac{2n\cdot k}{2p\cdot n}\right)\Gamma_b - (2p\cdot n)\left(I_a(2,0,0,0)+I_a(1,0,1,0)+I_a(1,0,0,1)\right)\right]\not{k}\gamma^{\nu}\\ &- \left[\frac{2(2p\cdot k)}{(-2p\cdot n)}\Gamma_b + (4p\cdot n)I_a(1,1,0,0)\right]n^{\nu} + (4p\cdot n)I_a(1,0,0,1)k^{\nu}\\ &+ \left[\frac{2p\cdot k}{-2p\cdot n}\Gamma_b + 2p\cdot k_2 I_a(1,0,0,1) - (2p\cdot n)I_a(1,1,0,0) + I_q\right]\gamma^{\nu}\not{n}.\Big\}, \end{aligned} \tag{2.58}$$

where $k = k_r$ and I_q is the contribution from the quadratic term. Expanding the result in both the soft momentum and regularisation parameter, one obtains

$$\begin{aligned}J^{\nu}_{(a)+(b)}(p,n,k;\epsilon) =&(2p\cdot k)^{-\epsilon}\left[\left(\frac{2}{\epsilon}+4+8\epsilon\right)\left(\frac{n\cdot k}{p\cdot k}\frac{p^{\nu}}{p\cdot n} - \frac{\not{k}\gamma^{\nu}}{2p\cdot k} - \frac{n^{\nu}}{p\cdot n}\right) + \right.\\ &\left. +(1+3\epsilon)\left(-\frac{2k^{\nu}}{p\cdot k} + \frac{\gamma^{\nu}\not{n}}{p\cdot n} - \frac{p^{\nu}\not{k}\not{n}}{p\cdot k p\cdot n}\right)\right]. \end{aligned} \tag{2.59}$$

Once combined the double pole cancels between the two n dependent graphs. As demonstrated earlier the quadratic term of graph (c) cancelled graph (d). Therefore the combined diagram contribution is just the expanded non-quadratic part of graph (c)

$$\begin{aligned}J^{\nu}_{(c)+(d)}(p,n,k;\epsilon) =&(2p\cdot k)^{-\epsilon}\left[\frac{1}{\epsilon}\left(\frac{\not{k}\gamma^{\nu}}{p\cdot k} + \frac{k^{\nu}}{p\cdot k}\right)\right.\\ &\left. +\frac{5}{2}\frac{\not{k}\gamma^{\nu}}{p\cdot k} + \frac{k^{\nu}}{p\cdot k} + \epsilon\left(5\frac{\not{k}\gamma^{\nu}}{p\cdot k} + 2\frac{k^{\nu}}{p\cdot k}\right)\right]. \end{aligned} \tag{2.60}$$

The total radiative jet contribution is therefore

$$\begin{aligned}J^{\nu}(p,n,k;\epsilon) =&(2p\cdot k)^{-\epsilon}\left[\left(\frac{2}{\epsilon}+4+8\epsilon\right)\left(\frac{n\cdot k}{p\cdot k}\frac{p^{\nu}}{p\cdot n} - \frac{n^{\nu}}{p\cdot n}\right) - (1+2\epsilon)\frac{ik_{\alpha}\Sigma^{\alpha\nu}}{p\cdot k} + \right.\\ &\left. +\left(\frac{1}{\epsilon}-\frac{1}{2}-3\epsilon\right)\frac{k^{\nu}}{p\cdot k} + (1+3\epsilon)\left(\frac{\gamma^{\nu}\not{n}}{p\cdot n} - \frac{p^{\nu}\not{k}\not{n}}{p\cdot k p\cdot n}\right)\right]. \end{aligned} \tag{2.61}$$

Now that we have computed all the necessary ingredients for computing the radiative corrections to the amplitude using the LBKDD theorem we can apply this formalism to Drell-Yan scattering to test if it correctly reproduces the NLP logarithms.

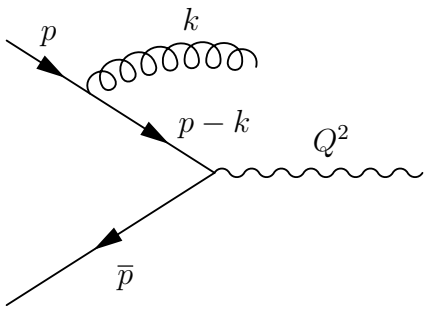

Figure 2.4: Feynman diagram for the inital part of Drell-Yan scattering where the virtual photon will go on to decay into a lepton anti-lepton pair.

2.4 Application to Drell-Yan scattering

We shall now turn our attention to constructing the amplitude of equation (2.9) for application to Drell-Yan scattering. The amplitude will be required in the construction of the K-factor. The K-factor is the ratio of a higher order cross section prediction over leading order encapturing some of the higher order effects. It is a function of the renormalisation and factorisation scales as well as the parton distribution functions and is useful in collider physics to add on some information from higher orders for specified regions of phase space to leading order results. The K-factor at a fixed order in perturbation theory is defined as

$$K^{(n)}(z) = \frac{1}{\sigma^{(0)}} \frac{d\sigma^{(n)}(z)}{dz}, \tag{2.62}$$

where $\sigma^{(n)}$ is the n-loop Drell-Yan cross section and z is the dimensionless threshold variable

$$z = \frac{Q^2}{s}, \tag{2.63}$$

representing the fraction of the total energy carried by the final state photon, where the threshold limit is $z \to 1$. Here we have used the center of mass energy s, and can define the Mandelstam invariants as:

$$s = (p + \overline{p})^2, \qquad t = -2k \cdot p, \qquad u = -2k \cdot \overline{p}. \tag{2.64}$$

These variable definitions can be obtained from considering the Feynman diagram of figure (2.4). Following the work of [49] we can parameterise these variables as:

$$t = -2s(1 - y)(1 - z), \qquad u = -2sy(1 - z), \tag{2.65}$$

where $0 < y < 1$. We can use these to write the real-virtual contribution to the NNLO K-factor as

$$K_{rv}^{(2)}(z) = \frac{1}{16\pi^2}\frac{(4\pi)^\epsilon}{\Gamma(2-\epsilon)} z^\epsilon (1-z)^{1-2\epsilon} \int_0^1 dy [y(1-y)]^{-\epsilon} \left[\mathcal{A}_{rv}^\dagger \mathcal{A}_r + \mathcal{A}_r^\dagger \mathcal{A}_{rv}\right], \quad (2.66)$$

where $\mathcal{A}_r$ is the leading order real emission amplitude and $\mathcal{A}_{rv}$ the next-to-leading order real emission amplitude and we have set the renormalisation scale to $\mu^2 = Q^2$.

The full Drell-Yan K-factor at NNLO has been calculated in [49]. For the purposes of examining the real-virtual contributions this result was recalculated and the result is

$$\begin{aligned} K_{rv}^{(2)}(z) = \left(\frac{\alpha_s}{4\pi}C_F\right)^2 \Bigg\{ & \frac{32}{\epsilon^3}\left[\mathcal{D}_0(z) - 1\right] + \frac{16}{\epsilon^2}\left[-4\mathcal{D}_1(z) + 3\mathcal{D}_0(z) + 4L(z) - 6\right] \\ & + \frac{4}{\epsilon}\left[16\mathcal{D}_2(z) - 24\mathcal{D}_1(z) + 32\mathcal{D}_0(z) - 16L^2(z) + 52L(z) - 49\right] \\ & - \frac{128}{3}\mathcal{D}_3(z) + 96\mathcal{D}_2(z) - 256\mathcal{D}_1(z) + 256\mathcal{D}_0(z) \\ & + \frac{128}{3}L^3(z) - 232L^2(z) + 412L(z) - 408 \Bigg\}, \end{aligned} \quad (2.67)$$

where

$$\mathcal{D}_n(z) = \left(\frac{\log^n(1-z)}{(1-z)}\right)_+, \qquad L(z) = \log(1-z), \quad (2.68)$$

and the $_+$ indicates a plus distribution see appendix A.2.5. Terms proportional to transcendental constants have not been included as they will not exhibit new information and neither have we included the Dirac delta functions due to their mixing with virtual corrections irrelevant for our purposes.

2.5 NLP phase space corrections

From equation (2.66) we can see that there are two threshold variable dependent components. Firstly there is the amplitude factor

$$\begin{aligned} \mathcal{P} &= \left[\mathcal{A}_{rv}^\dagger \mathcal{A}_r + \mathcal{A}_r^\dagger \mathcal{A}_{rv}\right] \\ &= \mathcal{P}_{LP} + \mathcal{P}_{NLP} + ..., \end{aligned} \quad (2.69)$$

where the terms in the second line represent the leading power and next-to-leading power in the threshold expansion contributions to the amplitude respectively. The

second component is the phase space pre-factor arising from the real gluon phase space

$$z^{\epsilon}(1-z)^{(1-2\epsilon)} = (1-z)^{(1-2\epsilon)}\left[1-\epsilon(1-z)+\mathcal{O}\left((1-z)^2\right)\right]. \tag{2.70}$$

One can schematically write the differential cross section to NLP in $(1-z)$ as

$$d\sigma = d\Phi_{3,LP}(\mathcal{P}_{LP}+\mathcal{P}_{NLP}) + d\Phi_{3,NLP}\mathcal{P}_{LP}, \tag{2.71}$$

where $\Phi_{3,LP}$ is the 3 particle phase space at leading power. It is clear that in computing the NLP contribution we need to consider the full squared amplitude (up to next-to-leading order) contracted with the eikonal phase space, and the leading order contribution to the squared amplitude contracted with the NLO phase space. Appendix B of [47] contains a discussion on obtaining the multi-gluon phase space at NE order. For our purposes of one gluon emission we only need to use the two-body phase space which can be written in differential form as

$$dPS(p+\overline{p}\to q+k) = \frac{1}{8\pi}\frac{(4\pi)^{\epsilon}}{\Gamma(1-\epsilon)}s^{-1+\epsilon}(tu-Q^2s)^{1/2-\epsilon}d\phi, \tag{2.72}$$

where we have introduced ϕ via the parameterisation of the Mandelstam invariants

$$\begin{aligned} t =& -2k\cdot p = -\sqrt{s}(\sqrt{|\vec{q}|^2+Q^2}-|\vec{q}|\cos\phi), \\ u =& -2k\cdot\overline{p} = -\sqrt{s}(\sqrt{|\vec{q}|^2+Q^2}+|\vec{q}|\cos\phi). \end{aligned} \tag{2.73}$$

2.6 Amplitude calculation

The next step is to compute all contributions to the amplitude given in equation (2.9). It will be necessary to first expand this result as

$$\begin{aligned} \mathcal{A}^{\mu}(p_j,k) = \sum_{i=1}^{2}\Bigg\{\left[q_i\left(\frac{(2p_i-k)^{\mu}}{2p_i\cdot k-k^2}+G_i^{\nu\mu}\frac{\partial}{\partial p_i^{\nu}}\right)+G_i^{\nu\mu}J_{\nu}^{(0)}(p_i;k)\right]\mathcal{A}^{(1)}(p_i;p_j)+ \\ +G_i^{\nu\mu}J_{\nu}^{(1)}(p_i,k)\mathcal{A}^{(0)}(p_i;p_j)\Big\}, \end{aligned} \tag{2.74}$$

where the superscripts (0) and (1) indicate tree level and one loop level respectively. The tree level jet function is given in equation (2.4). The result of acting upon this with the $G^{\nu\mu}$ tensor is

$$G_i^{\nu\mu}J_{\nu}^{(0)}(p,n,k) = -\frac{ik_{\alpha}\Sigma^{\alpha\mu}}{p\cdot k}J^{(0)}(p,n). \tag{2.75}$$

We can again set $J^{(0)}(p,n)=1$.

2.6.1 Dressed Amplitude contribution

The first and third terms on the right hand side of equation (2.74) we shall refer to as the dressed non-radiative amplitude contribution. The first term in the brackets in equation (2.74) acts to dress the non-radiative amplitude with the spin-independent part of an external gluon emission, as can be seen by comparison with equation (2.4). The expression for the one-loop non-radiative amplitude can be obtained from the quark form factor at one loop (see reference [23]) and is

$$\mathcal{A}^{(1)}(z) = -\frac{\alpha_s}{4\pi} z^{\epsilon} \frac{\Gamma^2(1-\epsilon)\Gamma(1+\epsilon)}{\Gamma(1-2\epsilon)} \left(\frac{2}{\epsilon^2} + \frac{3}{\epsilon} + 8 + 16\epsilon + \mathcal{O}(\epsilon^2) \right), \tag{2.76}$$

where the renormalisation scale has been fixed to $\mu^2 = Q^2$ and working in the $\overline{\text{MS}}$ scheme factors of $\ln(4\pi)$ and γ_E have been reabsorbed into the renormalisation scale. This term will contribute at NLP by dressing the tree-level radiative amplitude. At leading power in the threshold expansion the squared matrix element contribution reviewed in [47] is

$$|\mathcal{A}_{r,LP}|^2 = 16(1-\epsilon) g_s^2 \frac{s^2}{ut}, \tag{2.77}$$

The next-to-leading power matrix element is given by

$$\mathcal{A}^{\dagger}_{r,NLP}\mathcal{A}_{r,LP} + \mathcal{A}^{\dagger}_{r,LP}\mathcal{A}_{r,NLP} = 8(1-\epsilon) g_s^2 \left(\frac{s}{t} + \frac{s}{u} \right). \tag{2.78}$$

In order to find the contribution of these terms to the K-factor of equation (2.66) they need to be summed and then multiplied by the one-loop non-radiative amplitude of equation (2.76). The result one obtains is

$$\begin{aligned} K^{(2)}_{dB}(z) = \left(\frac{\alpha_s}{4\pi} C_F \right)^2 \Bigg\{ & \frac{32}{\epsilon^3} \left[\mathcal{D}_0(z) - 1 \right] + \frac{16}{\epsilon^2} \left[-4\mathcal{D}_1(z) + 3\mathcal{D}_0(z) + 4L(z) - 7 \right] + \\ & + \frac{4}{\epsilon} \left[16\mathcal{D}_2(z) - 24\mathcal{D}_1(z) + 32\mathcal{D}_0(z) - 16L^2(z) + 56L(z) - 56 \right] - \\ & - \frac{128}{3}\mathcal{D}_3(z) + 96\mathcal{D}_2(z) - 256\mathcal{D}_1(z) + 256\mathcal{D}_0(z) + \\ & + \frac{128}{3}L^3(z) - 224L^2(z) + 448L(z) - 512 \Bigg\}. \end{aligned} \tag{2.79}$$

The dressed Born amplitude is responsible for all of the plus distribution functions in equation (2.67). This is to be expected as the contributions from the derivative and radiative jet functions are expected to be strictly NLP in origin.

2.6.2 Derivative term

The next term to compute is that involving the derivative of the non-radiative amplitude with respect to each of the external momenta, consider first the derivative with respect to p

$$G^{\nu\mu}(p,k)\frac{\partial\mathcal{A}^{(1)}}{\partial p^{\nu}} = \left[-\frac{\epsilon}{p\cdot\bar{p}}\left(-p^{\mu}+\frac{\bar{p}\cdot k}{p\cdot k}\bar{p}^{\mu}\right)\right]\mathcal{A}^{(1)}. \tag{2.80}$$

There will be another such contribution for the term with the derivative with respect to $\bar{p}$. These terms are then contracted with the the radiative tree-level amplitude and plugged into equation (2.66) to obtain, after phase space integration, the K-factor contribution of

$$K^{(2)}_{\partial\mathcal{A}}(z) = \left(\frac{\alpha_s}{4\pi}C_F\right)^2\left\{\frac{32}{\epsilon^2}+\frac{16}{\epsilon}\left[-4L(z)+3\right]+64L^2(z)-96L(z)+128\right\}. \tag{2.81}$$

2.6.3 Radiative Jet term

The final ingredient is the contribution from the term involving the one loop radiative jet. The n-dependence in the entire amplitude should cancel out however we have made the choice of $n^2=0$ causing certain terms required to cancel n-dependent poles to be absent.

The radiative jet function manages collinear singularities, to disentangle soft and collinear singularities we make the choice that the four momentum n^{μ} must be anti-collinear to the momentum of the parton it is interacting with following the method of regions approach of [50]. For example if we work in the frame such that the momentum of the parton is $p_i^{\mu}=(1,0,0,1)$ then the vector parameterising the jet by definition must be $n^{\mu}=(1,0,0,-1)$. In the example we have considered there are only two scattering partons. To conserve momentum this causes the n^{μ} vector to be the momentum of the other parton such that we can make the substitution:

$$n=\bar{p}, \qquad\qquad \bar{n}=p. \tag{2.82}$$

Performing this substitution into the previously calculated radiative jet result, equation (2.61) and contracting it with the NLO tree-level amplitude, including complex conjugate diagrams, we can insert it into the K-factor equation (2.66) and integrate over the phase space to obtain the collinear contribution

$$K^{(2)}_{collinear}(z) = \left(\frac{\alpha_s}{4\pi}C_F\right)^2\left\{-\frac{16}{\epsilon^2}+\frac{4}{\epsilon}\left[12L(z)-5\right]-72L^2(z)+60L(z)-24\right\}. \tag{2.83}$$

2.6.4 Combined K-factor

The combination of the three components detailed above gives the total K-factor including the constant terms obtained from the full perturbative result given in equation (2.67):

$$K^{(2)}_{rv}(z) = K^{(2)}_{dB}(z) + K^{(2)}_{\partial\mathcal{A}}(z) + K^{(2)}_{collinear}(z). \tag{2.84}$$

This result demonstrates the effectiveness of our formalism for correctly reproducing all the abelian-like NLP logarithms.

It has therefore been demonstrated that the generalised formalism constructed building off of the work of [37] can reproduce all of the NLP logarithms one obtains from the full perturbative treatment of the NNLO Drell-Yan cross section for one-real one-virtual gluon emission, where the final-state gluon is forced to be next-to-soft. This non-trivial check of the formalism has helped to clarify the interplay of collinear effects with those arising just from next-to-soft considerations. This generalised approach should pave the way to develop resummation techniques to fully treat NLP threhsold logarithms arising in g theoretical scattering cross section calculations.

Chapter 3

A regularisation prescription for next-to-soft integrals

Virtual external emission contributions at the next-to-soft level necessitate the use of higher order terms in the eikonal expansion. Although these contributions were not necessary for computing in the case of chapter 2 which only required real external emissions, they will appear in the gravity study of chapter 6. The integrals for external emissions necessitate a novel regularisation prescription due to an unusual spurious cancellation of poles introduced from linearising denominators of propagators. In this chapter we shall detail this method and explain and demonstrate the matching of terms produced in the eikonal expansion to those of the full result.

The eikonal expansion is created by Taylor expanding the Feynman rules of our integrals in the soft momentum. By truncating the Taylor series due to soft momentum considerations we introduce a spurious ultra-violet (UV) divergence into our result. We know that the total amplitude must be UV finite therefore we must introduce a UV counterterm which will cancel off the spurious divergence. This will leave the infra-red (IR) divergent term that we derive from the full result.

Divergences throughout this thesis have been regulated through dimensional regularisation. The advantage to using dimensional regularisation over other methods is that it is manifestly gauge and Lorentz invariant and also able to regulate both the IR and UV singularities. Consequently we see an exact cancellation between the UV and IR poles in loop integrations constructed from eikonalised Feynman rules without the need for converting between regularisation methods.

3.1 Regularisation and removal of UV divergences

When considering integrals computed in the eikonal approximation we arrive at the result being zero. This is due to them being scaleless integrals which vanish in dimensional regularisation, and the cause of this can be interpreted as an exact cancellation between UV and IR poles. We implement UV renormalisation via the $\overline{MS}$ formalism to cancel off the UV pole regulated with the dimensional regularisation parameter by introducing counterterms. As will become more clear in the next-to-eikonal graphs and beyond the use of the eikonal expansion introduces an added spurious cancellation of UV and IR poles. One must develop a new method to remove these divergences from the integrals that arise at higher orders in the eikonal expansion. A similar method given the name power divergent subtraction in the work of [51] has been implemented to remove spurious divergences in the field of nuclear physics, and we will make contact with this in what follows. If we consider the vertex correction Feynman diagram depicted in figure (1.3) the loop integral with an eikonal numerator and full denominators is

$$I_{full,E} = \int \frac{d^dk}{(2\pi)^d} \frac{p\cdot\bar{p}}{k^2(p-k)^2(\bar{p}+k)^2}. \tag{3.1}$$

After introducing Feynman parameters we arrive at the result

$$\begin{aligned} I_{full,E} =& \frac{-i\Gamma(1+\epsilon)}{(4\pi)^{2-\epsilon}} p\cdot\bar{p}(-2p\cdot\bar{p})^{-1-\epsilon} \\ &\times \int_0^1 dx \int_0^1 dy (1-y)x^{-1-\epsilon}(1-x)^{-1-\epsilon}(1-y)^{-2-2\epsilon}. \end{aligned} \tag{3.2}$$

Recognising the integrals as beta functions one obtains

$$I_{full,E} = \frac{i\Gamma(1+\epsilon)}{2(4\pi)^{2-\epsilon}}(-2p\cdot\bar{p})^{-\epsilon}\frac{\Gamma^2(-\epsilon)}{\Gamma(-2\epsilon)}\frac{\Gamma(-2\epsilon)}{\Gamma(1-2\epsilon)}. \tag{3.3}$$

The leading order in ϵ contribution is

$$I_{full,E} = \frac{i\Gamma(1+\epsilon)}{2(4\pi)^{2-\epsilon}}(-2p\cdot\bar{p})^{-\epsilon}\frac{1}{\epsilon^2}. \tag{3.4}$$

Now if we implement the eikonal approximation in equation (3.1) we expect to reproduce this leading order in ϵ result. The integral of equation (3.1) to leading order in the eikonal expansion is

$$I_E = \int \frac{d^dk}{(2\pi)^d} \frac{p\cdot\bar{p}}{k^2(-2p\cdot k)(2\bar{p}\cdot k)}. \tag{3.5}$$

As before we introduce Feynman parameters to compute the integration over the momentum parameter to obtain the result:

$$\begin{aligned} I_E =& \frac{-i\Gamma(1+\epsilon)}{(4\pi)^{2-\epsilon}} p\cdot\overline{p}(-2p\cdot\overline{p})^{-1-\epsilon} \\ & \times \int_0^1 dx \int_0^1 dy (1-y)^{-2\epsilon-1} y^{2\epsilon-1} x^{-\epsilon-1}(1-x)^{-\epsilon-1}, \\ =& \frac{-i\Gamma(1+\epsilon)}{(4\pi)^{2-\epsilon}} p\cdot\overline{p}(-2p\cdot\overline{p})^{-1-\epsilon} \frac{\Gamma(-2\epsilon)\Gamma(2\epsilon)\Gamma^2(-\epsilon)}{\Gamma(0)\Gamma(-2\epsilon)} \end{aligned} \tag{3.6}$$

This result appears to be zero as made manifest in the division by $\Gamma(0) = \infty$. The reason for this is the spurious cancellation of the UV and IR poles introduced through performing the eikonal expansion and keeping the leading order result. As mentioned it is our aim to remove this spurious UV divergence to leave the IR divergent result we expect from the full integral.

3.1.1 Interpreting the UV and IR pole

In order to understand where in the integration the cancellation occurs it is useful to assess the initial linearised integral after Feynman parameters have been introduced, but before the momentum integration has been performed. The denominator is of the form of

$$\int_0^1 dx \int_0^1 dy \left[yk^2 + (1-y)k\cdot a(x,p,\bar{p}) \right]^{-3}, \tag{3.7}$$

The Feynman parameter y here is the final one introduced into the calculation. The first parameter is managing the two terms linear in k, whereas the y parameter separates the terms that are squared and linear in the loop momentum. Consider $d = 4$ and examine the integrand as it approaches the limits of the y integration; as $y \to 0$ the denominator becomes of $\mathcal{O}(k^{-3})$, so that after the loop momentum integration is performed it will be $\mathcal{O}(k)$, and thus divergent for $k \to \infty$. We can therefore interpret this as being the source of the UV divergence. Conversely as $y \to 1$ the integrand is of $\mathcal{O}(k^{-2})$ after the loop momentum integration and is divergent for $k \to 0$. We can therefore recognise the $y \to 0$ limit as isolating the UV divergent part.

The division by ∞ in the eikonal integral of equation (3.6) arises from the integration over the y Feynman parameter as expected from the above discussion. It is therefore possible to make the cancellation manifest as being between two terms by multiplying the integrand by $1 = y + (1-y)$. The integral to be performed is now

$$I_E = \frac{-i\Gamma(1+\epsilon)}{(4\pi)^{2-\epsilon}} p\cdot\overline{p}(-2p\cdot\overline{p})^{-1-\epsilon} \times \int_0^1 dx \int_0^1 dy (1-y)^{-2\epsilon-1} y^{2\epsilon-1} x^{-\epsilon-1}(1-x)^{-\epsilon-1}(y+(1-y)). \tag{3.8}$$

Giving the result in terms of Euler-Gamma functions

$$I_E = \frac{i\Gamma(1+\epsilon)}{2(4\pi)^{2-\epsilon}}(-2p\cdot\overline{p})^{-\epsilon}\frac{\Gamma^2(-\epsilon)}{\Gamma(-2\epsilon)}[\Gamma(1-2\epsilon)\Gamma(2\epsilon)+\Gamma(-2\epsilon)\Gamma(1+2\epsilon)]. \tag{3.9}$$

The two terms differ by a minus sign at leading order as $\epsilon \to 0$, and to correctly isolate the IR pole one must consider the previous analysis. We indicated that as $y \to 1$ the integrand would be IR divergent, in this limit the term multiplied by $(1-y)$ would be discarded leaving us with the IR limit contribution of

$$I_E = \frac{i\Gamma(1+\epsilon)}{2(4\pi)^{2-\epsilon}}(-2p\cdot\overline{p})^{-\epsilon}\frac{\Gamma^2(-\epsilon)}{\Gamma(-2\epsilon)}\Gamma(1+2\epsilon)\Gamma(-2\epsilon). \tag{3.10}$$

The leading order in ϵ contribution is

$$I_E = \frac{i\Gamma(1+\epsilon)}{2(4\pi)^{2-\epsilon}}(-2p\cdot\overline{p})^{-\epsilon}\frac{1}{\epsilon^2}. \tag{3.11}$$

This matches the leading order contribution obtained from the full denominator approach in equation (3.4). As has been demonstrated this method works for extracting the poles from eikonal integrals and has been used for decades (see e.g. [52]). This argument works for the eikonal case but for the coming next-to-eikonal and higher order integrals a more rigorous method is necessary. For this we return to the previous integral of equation (3.9) defined in the form of

$$\begin{aligned} I_E &= \frac{i\Gamma(1+\epsilon)}{2(4\pi)^{2-\epsilon}}(-2p\cdot\overline{p})^{-\epsilon}\frac{\Gamma^2(-\epsilon)}{\Gamma(-2\epsilon)}[\Gamma(1-2\epsilon)\Gamma(2\epsilon)+\Gamma(-2\epsilon)\Gamma(1+2\epsilon)], \\ &= \tilde{I}_E[\Gamma(1-2\epsilon)\Gamma(2\epsilon)+\Gamma(-2\epsilon)\Gamma(1+2\epsilon)] \end{aligned} \tag{3.12}$$

We wish to subtract off the UV divergence so we isolate the UV divergent term, calculate the residue of the divergent integral at $\epsilon \to 0$ and subtract it from the main result using

$$\Gamma(1-2\epsilon)\Gamma(2\epsilon)+\Gamma(-2\epsilon)\Gamma(1+2\epsilon) - \frac{1}{(\epsilon)} Res(\Gamma(1-2\epsilon)\Gamma(2\epsilon), \epsilon=0) = \frac{1}{-2\epsilon}, \tag{3.13}$$

which can be read as the UV pole being subtracted from the full result. Reinserting

this into the integral we have

$$\begin{aligned} I_E|_{\text{IR}} &= \frac{i\Gamma(1+\epsilon)}{2(4\pi)^{2-\epsilon}}(-2p\cdot\bar{p})^{-\epsilon}\frac{\Gamma^2(-\epsilon)}{\Gamma(-2\epsilon)}\frac{1}{-2\epsilon}, \\ &= \frac{i\Gamma(1+\epsilon)}{2(4\pi)^{2-\epsilon}}(-2p\cdot\bar{p})^{-\epsilon}\frac{\Gamma^2(-\epsilon)}{\Gamma(-2\epsilon)}\frac{\Gamma(-2\epsilon)}{\Gamma(1-2\epsilon)} \end{aligned} \tag{3.14}$$

We see that this reproduces the double pole of equation (3.1) where the denominators aren't linearised.

3.2 Next-to-Eikonal behaviour

We can now consider how to extend this analysis for tackling next-to-eikonal integrals. Firstly let's consider the result for the integral with a next-to-eikonal numerator but with full denominators

$$I^{\mu}_{full,NE} = \int \frac{d^dk}{(2\pi)^d}\frac{k^{\mu}}{k^2(p-k)^2(\bar{p}+k)^2}. \tag{3.15}$$

After introducing Feynman parameters and performing the momentum integration we arrive at the integral to be computed of

$$\begin{aligned} I^{\mu}_{full,NE} =& \frac{-i\Gamma(1+\epsilon)}{(4\pi)^{2-\epsilon}}(-2p\cdot\bar{p})^{-1-\epsilon} \\ &\times\int_0^1 dx\,[(1-x)\bar{p^{\mu}}-xp^{\mu}]\,x^{-\epsilon-1}(1-x)^{-\epsilon-1}\int_0^1 dy(1-y)^{-2\epsilon}, \\ =& \tilde{I}^{\mu}_{NE}\int_0^1 dy(1-y)^{-2\epsilon}, \\ =& \tilde{I}^{\mu}_{NE}\frac{1}{1-2\epsilon}. \end{aligned} \tag{3.16}$$

In terms of Euler-Gamma functions the full result is

$$I^{\mu}_{full,NE} = \frac{-i\Gamma(1+\epsilon)}{(4\pi)^{2-\epsilon}}(-2p\cdot\bar{p})^{-1-\epsilon}\,[\bar{p^{\mu}}-p^{\mu}]\,\frac{\Gamma(-\epsilon)\Gamma(1-\epsilon)}{\Gamma(1-2\epsilon)}\frac{\Gamma(1-2\epsilon)}{\Gamma(2-2\epsilon)}. \tag{3.17}$$

The leading order in ϵ result is

$$I^{\mu}_{full,NE} = \frac{i\Gamma(1+\epsilon)}{(4\pi)^{2-\epsilon}}(-2p\cdot\bar{p})^{-1-\epsilon}\,[\bar{p^{\mu}}-p^{\mu}]\,\frac{1}{\epsilon}. \tag{3.18}$$

One may now compare this result to the next-to-eikonal integral where the denominators are linearised:

$$\begin{aligned}
I^{\mu}_{NE} =& \int \frac{d^dk}{(2\pi)^d}\frac{k^\mu}{k^2(-2p\cdot k)(2\bar{p}\cdot k)}\\
=&\frac{-i\Gamma(1+\epsilon)}{(4\pi)^{2-\epsilon}}(-2p\cdot\bar{p})^{-1-\epsilon}\\
&\times\int_0^1 dx\left[(1-x)\bar{p^\mu}-xp^\mu\right]x^{-\epsilon-1}(1-x)^{-\epsilon-1}\int_0^1 dy(1-y)^{-2\epsilon}y^{2\epsilon-2},\\
=&\frac{-i\Gamma(1+\epsilon)}{(4\pi)^{2-\epsilon}}(-2p\cdot\bar{p})^{-1-\epsilon}\left[\bar{p^\mu}-p^\mu\right]\frac{\Gamma(-\epsilon)\Gamma(1-\epsilon)}{\Gamma(1-2\epsilon)}\int_0^1 dy(1-y)^{-2\epsilon}y^{2\epsilon-2},\\
=&\tilde{I}^{\mu}_{NE}\int_0^1 dy(1-y)^{-2\epsilon}y^{2\epsilon-2}.
\end{aligned}\tag{3.19}$$

We can again introduce multiplication by $y+(1-y)$ and write the y-integral in terms of Euler-gamma functions

$$\begin{aligned}
I_{y,NE} &= \int_0^1 dy(1-y)^{-2\epsilon}y^{2\epsilon-2}(y+(1-y)),\\
&= \Gamma(2-2\epsilon)\Gamma(2\epsilon-1)+\Gamma(1-2\epsilon)\Gamma(2\epsilon).
\end{aligned}\tag{3.20}$$

Similarly to before we subtract the residue of the UV pole. However as made manifest in the Euler gamma functions the integral now has the exact cancellation of UV and IR poles due to a spurious divergence at $d=3$ rather than $d=4$. This is due to the NE Feynman rule keeping an extra factor of k in the integrand. Therefore we perform the previous analysis but instead subtract the pole at $\epsilon=1/2$:

$$\begin{aligned}
I_{y,NE}|_{IR} &= I_{y,NE}-\frac{1}{\epsilon-1/2}Res\left(\Gamma(2-2\epsilon)\Gamma(2\epsilon-1),\epsilon=1/2\right),\\
&= I_{y,NE}-\frac{1}{2\epsilon-1},\\
&= \frac{1}{1-2\epsilon}.
\end{aligned}\tag{3.21}$$

The NE result is now

$$\begin{aligned}
I^{\mu}_{NE}|_{IR} &= \tilde{I}^{\mu}_{NE}\ I_{y,NE}|_{IR},\\
&= \frac{-i\Gamma(1+\epsilon)}{(4\pi)^{2-\epsilon}}(-2p\cdot\bar{p})^{-1-\epsilon}\left[\bar{p^\mu}-p^\mu\right]\frac{\Gamma(-\epsilon)\Gamma(1-\epsilon)}{\Gamma(1-2\epsilon)}\frac{1}{1-2\epsilon},\\
&= I^{\mu}_{full,NE}.
\end{aligned}\tag{3.22}$$

3.3 Denominator corrections

The previous example demonstrated how one tackles the numerator corrections to the eikonal expansion that arise at NE order. There are also terms to consider that will arise from expansion of the denominators to higher orders in their Taylor expansions from equation (1.4). It is clear that the leading order result reproduces the familiar eikonal linearised term. It can also be seen that when one is trying to obtain the full contribution at $\mathrm{N}^L\mathrm{E}$ order for any diagram divergent integral contributions arise from combining numerator factors of $\mathcal{O}(k^m)$ with the $(L-m)$'th term in the series expansion of the denominator. The terms arising from the denominator corrections will have integrals of the form

$$I_{\mathcal{D}} = \int \frac{d^dk}{(2\pi)^d} \frac{1}{(k^2+i\varepsilon)(2\overline{p}\cdot k+i\varepsilon)} \frac{(-k^2)^n}{(-2p\cdot k+i\varepsilon)^{n+1}}. \tag{3.23}$$

The terms can be grouped using Feynman parameters as usual

$$\begin{aligned} I_{\mathcal{D}} = &\int_0^1 dy \int_0^1 dx \int \frac{d^dk}{(2\pi)^d} (n+1)(n+2)(1-y)^{n+1}(1-x)^n(-k^2)^n \\ &\times \left[(yk^2+(1-y)x2\overline{p}\cdot k+(1-y)(1-x)(-2p\cdot k)+i\varepsilon)\right]^{-n-3}. \end{aligned} \tag{3.24}$$

For the sake of clarity here on we shall discard the Feynman $i\varepsilon$ term. We can perform a change of variable of the form

$$\begin{aligned} \mu =& \frac{y}{(1-y)}, \\ d\mu =& dy \frac{1}{(1-y)^2}, \end{aligned} \tag{3.25}$$

such that the integral is now in the form

$$I_{\mathcal{D}} = \int_0^\infty d\mu \int_0^1 dx \int \frac{d^dk}{(2\pi)^d} \frac{(n+1)(n+2)(1-x)^n(-k^2)^n}{(\mu k^2+x2\overline{p}\cdot k+(1-x)(-2p\cdot k))^{n+3}}. \tag{3.26}$$

To make the integration over the loop momentum simpler it is possible to recognise that differentiating the denominator with respect to the parameter μ will extract factors of k^2 giving us the relation of

$$(k^2)^n \left[\mu k^2+...\right]^{m-n} = (-1)^n \frac{\Gamma(-m)}{\Gamma(n-m)} \frac{\partial^n}{\partial\mu^n} \left[\mu k^2+...\right]^m, \tag{3.27}$$

where the ellipsis denotes μ independent terms. Using this we can write the integral in the form

$$I_{\mathcal{D}} = \int_0^\infty d\mu \int_0^1 dx \int \frac{d^d k}{(2\pi)^d} \frac{2}{\Gamma(n+1)} (1-x)^n \times \frac{\partial^n}{\partial \mu^n} \left[\mu k^2 + x 2\overline{p} \cdot k + (1-x)(-2p \cdot k) \right]^{-3}. \tag{3.28}$$

We can now complete the square in the integral and perform the integration over the loop momentum

$$I_{\mathcal{D}} = \frac{i\Gamma(3-d/2)}{(4\pi)^{d/2}\Gamma(n+1)} \times \int_0^1 dx (1-x)^n \int_0^\infty d\mu \frac{\partial^n}{\partial \mu^n} \mu^{-3} \left(\frac{x(1-x)}{\mu^2} (-2p \cdot \overline{p}) \right)^{d/2-3}. \tag{3.29}$$

Performing the x integration and the differentiation with respect to μ we obtain

$$I_{\mathcal{D}} = \frac{i\Gamma(3-d/2)}{(4\pi)^{d/2}\Gamma(n+1)} (-2p \cdot \overline{p})^{d/2-3} \frac{\Gamma(d/2-2)\Gamma(d/2-2+n)}{\Gamma(d-4+n)} I_\mu. \tag{3.30}$$

Once again we must remove the spurious UV divergence at $d = 4-n$ from the μ integral

$$I_\mu = \frac{\Gamma(4-d)}{\Gamma(4-d-n)} \int_0^\infty d\mu \mu^{3-d-n}. \tag{3.31}$$

For the sake of investigating the pole cancellation it is useful to convert the μ parameter back to being in terms of y

$$I_\mu = \frac{\Gamma(4-d)}{\Gamma(4-d-n)} \int_0^1 dy y^{3-d-n} (1-y)^{d+n-5}. \tag{3.32}$$

Next multiply by $y+(1-y)$ and write the integral in the form of Euler-gamma functions

$$I_\mu = \frac{\Gamma(4-d)}{\Gamma(4-d-n)} \left[\Gamma(5-d-n)\Gamma(d+n-4) + \Gamma(4-d-n)\Gamma(d+n-3) \right]. \tag{3.33}$$

Once again we subtract the spurious UV pole that now arises at $d = 4-n$

$$\begin{aligned} I_{\mu,UV\,free} = & \frac{\Gamma(4-d)}{\Gamma(4-d-n)} \left[\Gamma(5-d-n)\Gamma(d+n-4) + \Gamma(4-d-n)\Gamma(d+n-3) \right] - \\ & - \frac{1}{d-4+n} Res \left(\frac{\Gamma(4-d)}{\Gamma(4-d-n)} \Gamma(4-d-n)\Gamma(d+n-3), d = 4-n \right), \\ & = 0. \end{aligned} \tag{3.34}$$

Therefore it can be seen that the denominator corrections are exactly zero as we expect from the numerator corrections reproducing the leading order in ϵ full next-to-soft result. This method has utilised Feynman parameters and dimensional regularisation

to remove spuriously introduced power like divergences from integrals. After developing this method the work of [51] was made aware to me which uses a similar prescription (minimal subtraction of poles in $(d = 3)$) in effective field theories for use in nuclear physics. The formulation developed here is more suited to tackling integrals that arise in studies of next-to-soft radiation in scattering amplitudes for soft virtual corrections. It is a useful result drawing together the necessary considerations needed to isolate the UV pole. I have also proven here the interesting and useful result that corrections to the denominators in the eikonal expansion do not contribute at any sub-leading order in the soft expansion. This means that linearising denominators as in the eikonal Feynman rules is sufficient for capturing all order in soft expansion effects. Therefore additional Feynman diagrams built from insertions of the expanded denominator contributions at order $\mathrm{N}^n\mathrm{E}$ can be discarded reducing necessary work for future studies.

Chapter 4

Path integral approach to (next-to) soft physics

So far we have worked in the field of QCD but the general prescription for dealing with next-to-soft contributions will be applicable to any theory exhibiting factorisation. The theory that we shall be interested in for the final section of this thesis will be the high energy regime of quantum gravity (QG). The eikonal limit of QCD is well studied for its use in phenomenology and consequently there exist many tools and techniques to examine it. As will be demonstrated there are many calculational similarities between QCD and QG scattering amplitude calculations. This similarity is due to a correspondence between their charges, color and kinematics respectively that becomes clearly manifest when one calculates amplitudes using the same techniques. A recent example of this is the double copy [53, 54] relating amplitudes in gauge theories and gravity once an initial symmetry known as BCJ duality [55] has been made manifest in the gauge theory. Recently there has been a flurry of interest into next-to-soft effects in quantum gravity when considering real soft graviton emissions from scattering amplitudes, detailed in the works of [56–77]. It should be the case that my work towards formulating a full next-to-soft treatment of amplitudes in quantum gravity will provide a testing ground for these next-to-soft results.

In this thesis we have investigated soft radiative corrections to gauge theory amplitudes, and their next-to-soft extensions. Contributions to amplitudes in the soft limit are IR divergent. One of the most difficult problems facing a quantisation of general relativity is that it is not UV renormalisable in four dimensions. When we examine quantum gravity in the eikonal (IR) limit the lack of UV renormalisability will not effect the infra-red singular parts of the amplitude that we will be investigating through use of the soft limit techniques.

Fully generalised next-to-soft treatments for quantum gravity have not yet been

performed in such a clearly formulated and general way as the approach we have outlined for gauge theories in the previous chapters. It will be the aim of the coming chapter to apply this formalism to quantum gravity for arbitrary masses of the scattering matter particles. Quantum gravity affords a simplification over standard model gauge field theories when one is considering the IR structure as it is free of collinear singularities [78]. In terms of the generalised LBKDD theorem of equation (2.9) this allows us to neglect the radiative jet contribution.

4.1 Quantised General Relativity

We shall be using quantised general relativity and for comparison to other works supersymmetric extensions of this theory. It shall therefore be instructive to outline the fundamentals of general relativity starting from the Einstein-Hilbert action and then showing it in its quantised form. The Einstein-Hilbert action describing classical general relativity in d dimensions is:

$$S_{grav} = \kappa \int \sqrt{g} R d^d x, \tag{4.1}$$

where $\kappa = \frac{1}{16\pi G}$, R is the Ricci scalar and g is the determinant of the metric tensor. This action will describe the curvature of space time. One must introduce matter particles into our theory by the addition of their Lagrangians to induce curvature. The combined action will take the form:

$$S_{grav} = \int \left(\kappa R + \mathcal{L}_M\right) \sqrt{g} d^d x. \tag{4.2}$$

From equation (4.2) one can derive the classical Einstein field equations describing the propagation of matter through curved space-time and how matter causes curvature in space-time. The simplest matter Lagrangian one can use and that will be useful for this example is that of a scalar field:

$$\mathcal{L}_M = -g^{\mu\nu} \partial_\mu \phi^* \partial_\nu \phi - m^2 \left|\phi\right|^2. \tag{4.3}$$

In order to quantise the theory we expand the metric about a Minkowski background

$$g^{\mu\nu} = \eta^{\mu\nu} + \kappa h^{\mu\nu}. \tag{4.4}$$

The introduced perturbed metric field $h^{\mu\nu}$ will be our gauge field that we recognise as the "graviton".

(4.5)

4.2 Path Integral Method

So far we have looked at the linearised forms of the momentum space Feynman rules applicable in the Eikonal limit working in momentum space. We can also consider things in position space. In the eikonal limit the hard emitting particle follows a straight line trajectory. We can replace the QCD scattering process involving soft emission with a first-quantised path integral over this classical trajectory. In position space it is intuitive to think of the emission occurring at any point along the classical trajectory, and the sum over all possible points of this emission is described by the path integral. When we go on to consider the next-to-eikonal radiation emission processes i.e. emissions with non-zero momentum we will have to consider small perturbations from this classical trajectory. The sum over all possible small perturbations to the classical trajectory that will occur will naturally be treated as a Feynman path integral. We can therefore expand about the classical trajectory to get all next-to-eikonal results and sum over all possible insertions to obtain the full next-to-eikonal result using a path integral formulation. In the next section it shall be demonstrated how to associate the propagator for an external particle with a first quantised path integral in quantum mechanics following the work of [34] which was built upon the works of [79–81]. We shall also outline how to treat all the soft and next-to-soft gluon physics in the language of path integrals.

4.2.1 Scalar propagator as a Path Integral

As a simple first example it shall be shown how to reproduce the quantum field theory propagator for a free scalar particle between spacetime points x and y. The propagator is given by the Green's function of the Klein-Gordon equation

$$\begin{aligned} &i(S - i\epsilon)\Delta_F(x,y) = \delta^{(d)}(x,y), \\ &S = (-\Box_x + m^2). \end{aligned} \tag{4.6}$$

We can schematically write the solution to this as

$$\begin{aligned} \Delta_F(x,y) &= [i(S(x,y) - i\epsilon)]^{-1}, \\ &= \frac{1}{2}\int_0^\infty dT e^{-i\frac{1}{2}(S-i\epsilon)T}, \end{aligned} \tag{4.7}$$

where we have introduced a Schwinger parameter in the second line. We can then write this integrand as a single function $U(T) = e^{-i\frac{1}{2}ST}$, which can be promoted to an operator acting on states in a Hilbert space. This operator is recognisable as an evolution operator; it is both unitary and satisfies the Schrödinger equation

$$i\frac{d}{dT}U(T) = \hat{H}U(T), \tag{4.8}$$

where we can recognise $\hat{H} = \frac{1}{2}S$ as the Hamiltonian of this system.

We wish to use this evolution equation to calculate the expectation value for this system between a state of known position at $t = 0$ and a state of known momentum at $t = T$. This mixed position-momentum space description will be useful in the Wilson line approach used in the thesis. We introduce states into our Hilbert space on which the Hamiltonian acts and rewrite the Hamiltonian as

$$\hat{H}(\hat{x}, \hat{p}) = \sum_{n=0}^{\infty} \hat{p}_{\mu_1}...\hat{p}_{\mu_n} H^{\mu_1...\mu_n}_{\nu_1...\nu_n} \hat{x}^{\nu_1}...\hat{x}^{\nu_n}, \tag{4.9}$$

where $\hat{x}$ and $\hat{p}$ are operators acting on the Hilbert space and this has been written in Weyl ordered form. We can now compute expectation values of the evolution operator. Let us consider this for an infinitesimal time separation Δt:

$$\langle p|e^{-i\hat{H}\Delta t}|x\rangle = e^{-iH(p,x)\Delta t + \mathcal{O}[(\Delta t)^2]}\langle p|x\rangle, \tag{4.10}$$

where H is the c-number obtained by acting with the position and momentum operators on the Hilbert space states. We can use this result to consider the evolution for a non infinitesimal time period T. The time T can be split into N intervals of width Δt, and a complete set of position and momentum states can then be inserted at each slice

$$\int dx_1...dx_N \int dp_0...dp_{N-1} \exp\left[-i\sum_{k=0}^{N-1} H(p_k, x_k)\Delta t\right] \prod_{k=0}^{N} \langle p_k|x_k\rangle \prod_{k=0}^{N-1} \langle x_{k+1}|p_k\rangle. \tag{4.11}$$

The basis states are normalised such that $\langle x|p\rangle = \frac{e^{ixp}}{(2\pi)^d}$. The continuum limit of this expectation value is

$$\langle p_f|U(T)|x_i\rangle = \int_{x(0)=x_i}^{p(T)=p_f} \mathcal{D}p\mathcal{D}x \exp\left[-ip(T)x(T) + i\int_0^T dt(p\dot{x} - H(p,x))\right]. \tag{4.12}$$

We have now arrived at the path integral for the system's evolution operator between known initial position and final momentum states. The second term in the exponent is familiar as the term for the evolution between two known position states, and the

first term arises due to the mixed position-momentum space description.

The momentum space Hamiltonian for the free massive scalar is given by

$$H(p) = \frac{1}{2}(p^2 + m^2). \tag{4.13}$$

We can write the momentum and position paths as expansions about the classical trajectory:

$$\begin{aligned} p(t) &= p_f + p'(t), \\ x(t) &= x_i + p_f t + x'(t), \end{aligned} \tag{4.14}$$

where $p'(T) = 0$ and $x'(0) = 0$. The expectation value is now

$$\langle p_f|U(T)|x_i\rangle = e^{-ip_f x_i - i\frac{1}{2}(p_f^2+m^2)T} \int_{x(0)=0}^{p(T)=0} \mathcal{D}p\mathcal{D}x \exp\left[i\int_0^T dt(p\dot{x} - \frac{1}{2}p^2)\right], \tag{4.15}$$

where the primed notation has been dropped from the time dependent variables. The path integral in p is a Gaussian integral and the result of performing it will leave a Gaussian integral for x. The integration measure is defined such that the result after integration is one. This leaves us with the expectation value for the evolution operator as

$$\langle p_f|U(T)|x_i\rangle = \exp\left[-ip_f x_i - \frac{1}{2}i(p_f^2 + m^2)T\right]. \tag{4.16}$$

As a check on equation (4.7) we can perform the integration to compute the propagator

$$\Delta_F(p_f^2) = \frac{1}{2}\int_0^\infty dT \frac{\langle p_f|U(T)|x_i\rangle}{\langle p_f|x_i\rangle} = \frac{-i}{p_f^2 + m^2 - i\epsilon}, \tag{4.17}$$

which correctly reproduces the momentum space propagator for a free particle.

4.2.2 Gauge coupled particle

In the previous example we dealt with the free massive scalar particle. For the purposes of studying soft radiation we must allow for interactions with a gauge field. As is normal in quantum field theory we introduce a covariant derivative to introduce coupling between the kinematics and the gauge field, such that the Lagrangian for a charged scalar field becomes

$$\begin{aligned} \mathcal{L} &= -\phi^* D_\mu D^\mu \phi + m^2\phi^2, \\ D_\mu &= \partial_\mu - igA_\mu. \end{aligned} \tag{4.18}$$

We know that $-i\partial_\mu = p_\mu$ which allows us to write the Lagrangian as

$$\hat{\mathcal{L}} = (m^2 + p_\mu p^\mu) + A_\mu A^\mu - i(\partial_\mu A^\mu) - 2p_\mu A^\mu, \tag{4.19}$$

where we have re-ordered such that momentum operators appear to the left i.e. $A \cdot p = p \cdot A + i(\partial_\mu A^\mu)$ and defined $\mathcal{L} = \phi^* \hat{\mathcal{L}} \phi$. We can replace the Hamiltonian of the previous example with the one constructed from this Lagrangian, and obtain the first quantised path integral representation for the expectation value of the evolution operator between the known initial position and final momentum states:

$$\langle p_f|U(T)|x_i\rangle = \int_{x(0)=x_i}^{p(T)=p_f} \mathcal{D}p\mathcal{D}x \exp\left[-ip(T)x(T) + i\int_0^T dt \left(p\dot{x} - \frac{1}{2}(m^2+p^2) - \right.\right.$$
$$\left.\left. -\frac{1}{2}A_\mu A^\mu + \frac{i}{2}(\partial_\mu A^\mu) + p_\mu A^\mu\right)\right]. \tag{4.20}$$

This is the result for a scalar. If the emitting particle were a fermion then one would have another term dependent upon the spin and the resulting expectation value would be

$$\langle p_f|U(T)|x_i\rangle = \int_{x(0)=x_i}^{p(T)=p_f} \mathcal{D}p\mathcal{D}x \exp\left[-ip(T)x(T) + i\int_0^T dt \left(p\dot{x} - \frac{1}{2}(m^2+p^2) - \right.\right.$$
$$\left.\left. -\frac{1}{2}A_\mu A^\mu + \frac{i}{2}(\partial_\mu A^\mu) + p_\mu A^\mu\right) + \frac{1}{2}\sigma^{\mu\nu}F_{\mu\nu}\right], \tag{4.21}$$

where $\sigma^{\mu\nu} = -\frac{i}{4}[\gamma^\mu, \gamma^\nu]$ are the Lorentz group generators. The added term will lead to seagull vertices which will not concern us for the external emission contributions of this thesis.

4.2.3 Eikonal approximation

The Green's function we are looking to compute is for a scattering event where there are n external particles emitted from the hard interaction. Writing this in eikonally factorised form we have

$$G(p_1, ..., p_n) = \int \mathcal{D}A_s^\mu H(x_1, ..., x_n) \left\langle p_1|(S - i\varepsilon)^{-1}|x_1\right\rangle ... \left\langle p_n|(S - i\varepsilon)^{-1}|x_n\right\rangle, \tag{4.22}$$

where ε is the Feynman prescription parameter, S is defined as in equation (4.6) and $H(x_1, ..., x_n)$ is the hard function. We have also split the gauge field into hard and soft

modes. By matching to the full Green's function we find

$$H(x_1,...,x_n) = \int \mathcal{D}A_h^\mu \mathcal{D}\phi\mathcal{D}\phi^* \frac{1}{i^n}\frac{\delta}{\delta J(y_1)}...\frac{\delta}{\delta J(y_n)} \langle y_1|S-i\varepsilon|x_1\rangle ... \langle y_n|S-i\varepsilon|x_n\rangle$$
$$\exp\left\{ i\int d^dx \mathcal{L}\left[\phi,\phi^*,A^\mu\right] + i\int d^dx \left[J(x)\phi^*(x)+J(x)\phi^*(x)\right]\right\}, \quad (4.23)$$

where ϕ is the matter field and $J(x)$ the source terms with the associated functional derivatives.

We see from equation (4.22) that all of the information for the soft part of the Green's function is obtained by integrating the external leg propagators over the soft gauge field. Therefore our development of the propagators as first-quantised path integrals following the classical trajectory of the hard particle in the soft limit can be substituted in to develop the soft function. For our development of the soft function it is therefore possible to use the paths $p(t)$ and $x(t)$ from (4.14), substituting these into the integral we obtain:

$$\langle p_f|U(T)|x_i\rangle = \exp\left[-ip_fx_i - i\frac{1}{2}(p_f^2+m^2)T\right] f(T), \quad (4.24)$$

where for a scalar:

$$f(T) = \int_{x(0)=0}^{p(T)=0} \mathcal{D}p\mathcal{D}x \exp\left[i\int_0^T dt(p\dot{x} - \frac{1}{2}p^2 + (p_f+p)\cdot A(x_i+p_ft+x)\right.$$
$$\left. +\frac{i}{2}\partial\cdot A(x_i+p_ft+x) - \frac{1}{2}A^2(x_i+p_ft+x)\right]. \quad (4.25)$$

We can now perform the path integral in the momentum by recognising it as a Gaussian integral such that

$$f(T) = \int_{x(0)=0} \mathcal{D}x \exp\left[i\int_0^T dt\left(\frac{1}{2}\dot{x}^2 + (p_f+\dot{x})\cdot A(x_i+p_ft+x)\right.\right.$$
$$\left.\left. +\frac{i}{2}\partial\cdot A(x_i+p_ft+x)\right)\right]. \quad (4.26)$$

To get scattering amplitude contributions from this Green's function one must truncate each external leg propagator according to the LSZ prescription, this requires multiplying leg i by $p_i^2+m^2$. The external line contributions we are looking to compute are therefore:

$$i(p_f^2+m^2)\langle p_f| - i(S-i\varepsilon)^{-1}|x_i\rangle = i(p_f^2+m^2)\frac{1}{2}e^{-ip_fx_i}\int_0^\infty dT e^{-i\frac{1}{2}(p_f^2+m^2-i\varepsilon)T} f(T)$$

$$
\begin{aligned}
&= -e^{-ip_f x_i} \int_0^\infty dT \left[\frac{d}{dT} e^{-i\frac{1}{2}(p_f^2+m^2)T}\right] \left[e^{-\frac{1}{2}\varepsilon T} f(T)\right] \\
&= -e^{-ip_f x_i} \left\{-f(0) - \int_0^\infty dT e^{-i\frac{1}{2}(p_f^2+m^2)T} \left[\frac{d}{dT} e^{-\frac{1}{2}\varepsilon T} f(T)\right]\right\} \\
&= -e^{-ip_f x_i} \left\{-f(0) - \int_0^\infty dT e^{-i\frac{1}{2}(p_f^2+m^2)T} \left[\frac{d}{dT} f(T)\right]\right\},
\end{aligned}
\tag{4.27}
$$

where $\varepsilon \to 0$ in the last line. Considering the limit in which p_f approaches its mass shell and $T \to \infty$ simplifies the result to:

$$
i(p_f^2 + m^2) \left\langle p_f \right| - i(S - i\varepsilon)^{-1} \left| x_i \right\rangle = \exp\left(-ip_f x_i\right) f(\infty). \tag{4.28}
$$

The f-function of equation (4.26), in the limit $T \to \infty$ is

$$
\begin{aligned}
f(\infty) = \int_{x(0)=0} \mathcal{D}x \exp\Bigg[i \int_0^\infty dt \Bigg(&\frac{1}{2}\dot{x}^2 + (p + \dot{x}) \cdot A(x_i + pt + x) \\
&+ \frac{i}{2} \partial \cdot A(x_i + pt + x)\Bigg)\Bigg],
\end{aligned}
\tag{4.29}
$$

where $p = p_f$ has been used in the result. The soft contribution to the amplitude using these ingredients is therefore:

$$
S(p_1, ..., p_n) = \int \mathcal{D}A_s^\mu e^{-ip_1 x_1} f_1(\infty) ... e^{-ip_n x_n} f_n(\infty) e^{iS[A_s]}. \tag{4.30}
$$

To clearly isolate the eikonal contribution it is useful to introduce a softness parameter via a rescaling of the momentum such that $p \to \lambda n$ and take the eikonal limit to be that for which $\lambda \to \infty$. In this strict eikonal limit the leading term in λ will be:

$$
f(\infty) = \exp\left(i \int_0^\infty dt \lambda n \cdot A(\lambda n t)\right). \tag{4.31}
$$

Equation (4.31) can be recognised as being proportional to a Wilson line operator where the gauge field acts as a source term for the soft radiation. This demonstrates that in the strict eikonal recoil-less limit we can replace particles with Wilson line operators defined along the classical trajectories of the particle, this was first shown in [27, 28].

4.2.4 Next-to-eikonal Feynman rules

Terms of next-to-eikonal order will arise by keeping next-to-leading order terms in the λ expansion from equation (4.29). These terms can be considered as leading order

fluctuations about the classical path as this is no longer the strictly recoilless limit. Furthermore it is useful to rescale $t \to t/\lambda$ such that equation (4.29) can be rewritten as:

$$f(\infty) = \int_{x(0)=0} \mathcal{D}x \exp\left[i \int_0^\infty dt \left(\frac{\lambda}{2}\dot{x}^2 + (n+\dot{x}) \cdot A(x_i + nt + x) \right.\right. \\ \left.\left. + \frac{i}{2\lambda} \partial \cdot A(x_i + nt + x) \right)\right]. \tag{4.32}$$

The first term may appear to be at a higher soft order than the eikonal term but it will give rise to the x propagator which will be of $\mathcal{O}(\lambda^{-1})$. It will be necessary to calculate the x propagator, using integration by parts the term that's squared in x can be written as a quadratic differential operator:

$$\frac{i}{2}\int_0^\infty dt \dot{x}^2 = -\frac{1}{2}\int_0^\infty dt x_\mu \left(i\eta^{\mu\nu}\frac{\partial^2}{\partial t^2} \right) x_\nu. \tag{4.33}$$

The x propagator is the inverse function of the quadratic operator in equation (4.33)

$$G(t,t') = \frac{i}{\lambda}\min(t,t')\eta_{\mu\nu}. \tag{4.34}$$

To compute the full NE level contribution one must construct all graphs possible from the Feynman rules in the path integral. These are generated when the integration over the soft gauge field path integral in the soft function is performed. Necessary for this calculation will be the correlators between combinations of x and $\dot{x}$:

$$\begin{aligned} \langle x(t)x(t')\rangle =& G(t,t') = \frac{i}{\lambda}\min(t,t'), \\ \langle \dot{x}(t)x(t')\rangle =& \frac{\partial G(t,t')}{\partial t} = \frac{i}{\lambda}\theta(t'-t), \\ \langle \dot{x}(t)\dot{x}(t')\rangle =& \frac{\partial^2 G(t,t')}{\partial t \partial t'} = \frac{i}{\lambda}\delta(t'-t). \end{aligned} \tag{4.35}$$

To construct all NE Feynman rules for the vertices, one must Taylor expand the gauge field in x and perform the path integral in x. Keeping terms that will contribute at next-to-leading order in λ equation (4.32) is

$$f(\infty) = \int_{x(0)=0} \mathcal{D}x \exp\left[i \int_0^\infty dt \left(\frac{\lambda}{2}\dot{x}^2 + n \cdot A(nt) + \frac{i}{2\lambda}\partial A(nt) \right.\right. \\ \left.\left. + \dot{x} \cdot A(nt) + (n+\dot{x})^\nu \partial_\alpha A_\nu(nt) x^\alpha + \frac{1}{2} n^\nu \partial_\alpha \partial_\beta A_\nu(nt) x^\alpha x^\beta \right)\right]. \tag{4.36}$$

We also need the equal time correlator of $\langle \dot{x}(t)x(t)\rangle = 0$ with which we can peform the path integral in x by summing over the possible connected diagrams

$$\begin{aligned} f(\infty) =& \exp\left\{ i\int_0^\infty dt \left[n\cdot A(nt) + \frac{i}{2\lambda}\partial A(nt) + \frac{1}{2}n^\nu \partial_\alpha\partial_\beta A_\nu(nt)\eta^{\alpha\beta}\,\langle x(t)x(t)\rangle \right.\right. \\ &+ \int_0^\infty dt' \left(\langle \dot{x}(t)\dot{x}(t')\rangle\, A_\mu(nt)A^\mu(nt') + \langle x(t)x(t')\rangle\, n^\mu n^\nu \partial_\beta A_\mu(nt)\partial_\alpha A_\nu(nt')\eta^{\alpha\beta} \right. \\ &\left.\left. \left. + \langle \dot{x}(t)x(t')\rangle\, \eta^{\mu\alpha} A_\mu(nt) n^\nu \partial_\alpha A_\nu(nt')\right) \right] \right\}, \\ =& \exp\left\{ i\int_0^\infty dt \left[n\cdot A(nt) + \frac{i}{2\lambda}\partial A(nt) + \frac{it}{2\lambda}n^\nu \partial_\alpha\partial_\beta A_\nu(nt)\eta^{\alpha\beta} \right.\right. \\ &+ \frac{i}{\lambda}A(nt)\cdot A(nt) + \int_0^\infty dt' \left(\langle x(t)x(t')\rangle\, n^\mu n^\nu \partial_\beta A_\mu(nt)\partial_\alpha A_\nu(nt')\eta^{\alpha\beta} \right. \\ &\left.\left. \left. + \langle \dot{x}(t)x(t')\rangle\, \eta^{\mu\alpha} A_\mu(nt) n^\nu \partial_\alpha A_\nu(nt')\right) \right] \right\}, \end{aligned} \tag{4.37}$$

The two NE Feynman rules linear in the gauge field and coupling constant are associated with the single photon emission vertex that we call external emission contributions. The additional vertex correction is a seagull vertex, involving a pair of correlated gluons. Having now isolated the NE Feynman rules we can now set our book-keeping parameter $\lambda = 1$ such that the two Feynman rules we are interested in are

$$\begin{aligned} NE_1 &= \int_0^\infty dt \frac{i}{2}\partial\cdot A(pt), \\ NE_2 &= \int_0^\infty dt \frac{i}{2} t p^\nu \partial^2 A_\nu(pt). \end{aligned} \tag{4.38}$$

The last consideration to be made is in the definition of the limits on the integration. The formulation has been for Wilson lines going from $0 \to \infty$ i.e. outgoing particles from the point of interaction. It will also be necessary to deal with incoming Wilson lines going from $-\infty \to 0$ however this is treated by swapping $p_{\text{in}} \to -p_{\text{in}}$ and keeping the positive integration limits.

4.3 Path integral approach for gravity

Having outlined how a path integral treatment can be implemented to deal with soft and next-to-soft effects in QCD we can develop a similar formalism for quantum gravity. This approach has been performed previously in [82] which will be reproduced here except with the canonical definition of the graviton of equation (4.4). From the previous treatment we see that the same approach can be followed except with the action for

quantum gravity in place of the one we used previously. The action we shall require is the Einstein-Hilbert action of equation (4.2) and we shall be interested in expanding it with respect to small κ. It will be necessary to compute the expanded form of $(\sqrt{-|g|})^{-1}$

$$(-|g|))^{-1/2} = 1 + \frac{\kappa}{2}h^{\alpha}{}_{\alpha} + \frac{\kappa^2}{2}\left[\frac{(h^{\alpha}{}_{\alpha})^2}{(d-2)^2} - \frac{h^{\alpha\beta}h_{\alpha\beta}}{d-2}\right] + \mathcal{O}(\kappa^3 h^3), \tag{4.39}$$

the derivation of which can be found in appendix (A.1). The action for the matter portion of the lagrangian that we shall be concerned with for soft radiation can be written using this expanded form of the metric as:

$$S = -\int d^d x \phi^* \hat{S} \phi, \tag{4.40}$$

where (ignoring surface terms)

$$\hat{S} = -\partial_\mu(\sqrt{-g}g^{\mu\nu})\partial_\nu - \sqrt{-g}g^{\mu\nu}\partial_\mu\partial_\nu + \sqrt{-g}m^2. \tag{4.41}$$

We can use the fact that $-ip_\mu = \partial_\mu$ to rewrite this as

$$\hat{S} = i\partial_\mu(\sqrt{-g}g^{\mu\nu})p_\nu + \sqrt{-g}g^{\mu\nu}p_\mu p_\nu + \sqrt{-g}m^2. \tag{4.42}$$

We require the propagator between a state of known initial position and known final state momentum, which as defined in [34] may be written as

$$\begin{aligned}\langle p_j|(\hat{S} - i\epsilon)^{-1}|x_j\rangle = &\frac{1}{2}\int_0^\infty dT \int_{x(0)=x_j}^{p(T)=p_j} DpDx \exp\Big[-ip(T)\cdot x(T) \\ &+ i\int_0^T dt(p\cdot\dot{x} - \hat{H}(p,x))\Big],\end{aligned} \tag{4.43}$$

where $\hat{H} = \frac{1}{2}\hat{S}$. Substituting in equation (4.42), we can perform an expansion about the classical trajectory to extract out the subeikonal corrections using the substitutions of equation (4.14). The result is

$$\langle p_j|(\hat{S} - i\epsilon)^{-1}|x_j\rangle = \frac{1}{2}\int_0^\infty dT exp\left[-ip_j\cdot x_j - \frac{i}{2}(p_j^2 + m^2)T\right] f(T), \tag{4.44}$$

where we have defined

$$f(T) = \int_{x(0)=0}^{p(T)=0} DpDx \exp\left\{ i \int_0^T dt \left[p\cdot\dot{x} - \frac{i}{2}\partial_\mu(\sqrt{-g}g^{\mu\nu})(p_{j\nu}+p_\nu) \right.\right. \\ - \frac{1}{2}\sqrt{-g}g^{\mu\nu}(p_{j\mu}+p_\mu)(p_{j\nu}+p_\nu) - \frac{m^2}{2}(\sqrt{-g}-1) \\ \left.\left. + \frac{1}{2}\eta^{\mu\nu}p_{j\mu}p_{j\nu} + \frac{1}{2}\eta^{\mu\nu}(p_{j\mu}p_\nu + p_\mu p_{j\nu}) \right] \right\}. \tag{4.45}$$

Expanding out the metric terms, neglecting those of order κ^2 or higher we have:

$$f(T) = \int_{x(0)=0}^{p(T)=0} DpDx \exp\left\{ i \int_0^T dt \left[p\cdot\dot{x} - \frac{i}{2}\partial_\mu\left(\kappa h^{\mu\nu} + \frac{\kappa}{2}h^\alpha{}_\alpha\eta^{\mu\nu}\right)(p_{j\nu}+p_\nu) \right.\right. \\ - \frac{1}{2}(\eta^{\mu\nu} + \kappa h^{\mu\nu} + \frac{\kappa}{2}h^\alpha{}_\alpha\eta^{\mu\nu})(p_{j\mu}+p_\mu)(p_{j\nu}+p_\nu) \\ \left.\left. - \frac{m^2}{2}\left(\frac{\kappa}{2}h^\alpha{}_\alpha\right) + \frac{1}{2}\eta^{\mu\nu}p_{j\mu}p_{j\nu} + \frac{1}{2}\eta^{\mu\nu}(p_{j\mu}p_\nu + p_\mu p_{j\nu}) \right] \right\}. \tag{4.46}$$

This can be written in the form of a Gaussian integral over the momentum

$$f(T) = \int_{x(0)=0}^{p(T)=0} DpDx \exp\left[i \int_0^T dt \left(-\frac{1}{2}p_\mu A^{\mu\nu}p_\nu + B^\mu p_\mu + C \right) \right], \tag{4.47}$$

where we have defined:

$$A^{\mu\nu} = \left(\eta^{\mu\nu} + \kappa h^{\mu\nu} + \frac{\kappa}{2}h^\alpha{}_\alpha\eta^{\mu\nu}\right), \\ B^\mu = \dot{x}^\mu - \frac{i}{2}\partial_\rho\left(\kappa h^{\rho\mu} + \frac{\kappa}{2}h^\alpha{}_\alpha\eta^{\rho\mu}\right) - \left(\kappa h^{\mu\nu} + \frac{\kappa}{2}h^\alpha{}_\alpha\eta^{\mu\nu}\right)p_{j\nu}, \\ C = -\frac{i}{2}\partial_\rho\left(\kappa h^{\rho\mu} + \frac{\kappa}{2}h^\alpha{}_\alpha\eta^{\rho\mu}\right)p_{j\nu} - \frac{1}{2}\left(\kappa h^{\mu\nu} + \frac{\kappa}{2}h^\alpha{}_\alpha\eta^{\mu\nu}\right)p_{j\mu}p_{j\nu} - \frac{m^2}{2}\left(\frac{\kappa}{2}h^\alpha{}_\alpha\right). \tag{4.48}$$

The path integral over momentum gives

$$f(T) = \int Dx \exp\left[i \int_0^T dt (\frac{1}{2}B^\mu(A^{-1})_{\mu\nu}B^\nu + C) \right]. \tag{4.49}$$

The inverse of the quadratic term is

$$(A^{-1})_{\mu\nu} = \eta_{\mu\nu} - \kappa h_{\mu\nu} - \frac{\kappa}{2}h^\alpha{}_\alpha\eta_{\mu\nu} + \mathcal{O}(\kappa^2), \tag{4.50}$$

and therefore the result is:

$$f(T) = \int \mathcal{D}x \exp\left\{ i \int_0^T dt \left[\frac{1}{2}\dot{x}^\mu \left(\left(1 - \frac{\kappa}{2} h^\alpha{}_\alpha \right) \eta_{\mu\nu} - \kappa h_{\mu\nu} \right) \dot{x}^\nu \right.\right.$$
$$+ \dot{x}_\nu \left(-i\partial_\rho \left(\kappa h^{\rho\nu} + \frac{\kappa}{2} h^\alpha{}_\alpha \eta^{\rho\nu} \right) - 2 \left(\kappa h^{\nu\rho} + \frac{\kappa}{2} h^\alpha_\alpha \eta^{\nu\rho} \right) \right) p_{j\rho}$$
$$- \frac{1}{2} \left(\kappa h^{\mu\nu} + \frac{\kappa}{2} h^\alpha{}_\alpha \eta^{\mu\nu} \right) p_{j\mu} p_{j\nu} - \frac{m^2}{2} \left(\frac{\kappa}{2} h^\alpha{}_\alpha \right)$$
$$\left.\left. - \frac{i}{2} \partial_\rho \left(\kappa h^{\rho\mu} + \frac{\kappa}{2} h^\alpha{}_\alpha \eta^{\rho\mu} \right) p_{j\nu} + \mathcal{O}(\kappa^2) \right] \right\}. \tag{4.51}$$

For our purposes of dealing with semi-infinite Wilson lines we can set $T = \infty$, we also make use of $p^2 = -m^2$, neglect terms $\mathcal{O}(x\dot{x})$ and $\mathcal{O}(\dot{x}\dot{x})$ and Taylor expanding the graviton tensor about the classical path $p^\mu t + x^\mu$ where necessary:

$$h^{\mu\nu}(pt + x) = h^{\mu\nu}(pt) + \partial_\sigma h^{\mu\nu}(pt) x^\sigma + \frac{\partial_\sigma \partial_\tau}{2} h^{\mu\nu} x^\sigma x^\tau, \tag{4.52}$$

the NE contribution to equation (4.51) is

$$f(\infty) = \int \mathcal{D}x \exp\left\{ i \int_0^\infty dt \left[\frac{1}{2}\dot{x}^\mu \dot{x}^\nu + \right.\right.$$
$$- \frac{1}{2} \kappa p_{j\mu} p_{j\nu} \left(h^{\mu\nu} + \partial_\sigma h^{\mu\nu} x^\sigma + \frac{\partial_\sigma \partial_\tau}{2} h^{\mu\nu} x^\sigma x^\tau \right) +$$
$$+ \dot{x}_\nu \left(-i\partial_\rho \left(\kappa h^{\rho\nu} + \frac{\kappa}{2} h^\alpha{}_\alpha \eta^{\rho\nu} \right) - 2 \left(\kappa h^{\nu\rho} + \frac{\kappa}{2} h^\alpha_\alpha \eta^{\nu\rho} \right) \right) p_{j\rho} +$$
$$- \frac{i}{2} \partial_\rho \left(\kappa h^{\rho\mu} + \frac{\kappa}{2} h^\alpha{}_\alpha \eta^{\rho\mu} \right) p_{j\nu} -$$
$$- \frac{i}{2} \partial_\sigma \partial_\rho \left(\kappa h^{\rho\mu} + \frac{\kappa}{2} h^\alpha{}_\alpha \eta^{\rho\mu} \right) x^\sigma p_{j\nu}$$
$$\left.\left. + \mathcal{O}(\kappa^2) \right] \right\}. \tag{4.53}$$

Utilising the correlators as per equation (4.35), $\left\langle x^\alpha(t) x^\beta(t') \right\rangle = it\eta^{\alpha\beta}$ for $t \leq t'$, the path integral over x can be performed

$$f(\infty) = \exp\left\{ i \int_0^\infty dt \left[-\frac{1}{2} \kappa p_{j\mu} p_{j\nu} h^{\mu\nu} - \frac{i\kappa}{4} t p_{j\mu} p_{j\nu} \partial^2 h^{\mu\nu} \right.\right.$$
$$\left.\left. - \frac{i}{2} \partial_{(\rho} \left(\kappa h^{\rho\mu} + \frac{\kappa}{2} h^\alpha{}_\alpha \eta^{\rho\mu} \right) p_{j\mu)} + \mathcal{O}(\kappa^2) \right] \right\}, \tag{4.54}$$

where we have used symmetrisation of $\partial_\rho p_{j\mu} \to \frac{\partial_{(\rho} p_{j\mu)}}{2}$. This result gives the eikonal and NE Feynman rules for gravity. To check this result to we can then Fourier transform to momentum space using:

$$h^{\mu\nu}(pt) = \int \frac{d^d k}{(2\pi)^d} h^{\mu\nu}(k) \exp(ik \cdot pt). \tag{4.55}$$

This gives the momentum space Feynman rules:

$$f(\infty) = \int \frac{d^dk}{(2\pi)^d} \exp\left\{ \left[\frac{\kappa}{2} \frac{p_{j\mu}p_{j\nu}}{p\cdot k} h^{\mu\nu}(k) - \frac{\kappa}{4} \frac{p_{j\mu}p_{j\nu}k^2}{(p\cdot k)^2} h^{\mu\nu}(k) \right.\right. \\ \left.\left. -\frac{\kappa}{2} \frac{k_\mu p_{j\nu}}{p\cdot k} h^{\mu\nu}(k) - \frac{\kappa}{4}\eta_{\mu\nu}h^{\mu\nu} \right] \right\}. \tag{4.56}$$

We can introduce the symmetrised term $k_\mu p_{j\nu} \to \frac{k_{(\mu}p_{j\nu)}}{2}$ drop the j subscript and reverse the momentum flow $k \to -k$

$$f(\infty) = \int \frac{d^dk}{(2\pi)^d} \exp\left\{ \frac{\kappa}{2} \left[\frac{p_\mu p_\nu}{p\cdot k} - \frac{1}{2}\frac{p_\mu p_\nu k^2}{(p\cdot k)^2} + \frac{k_{(\mu}p_{\nu)}}{2p\cdot k} - \frac{\eta_{\mu\nu}}{2} \right] h^{\mu\nu}(k) \right\}. \tag{4.57}$$

This result matches that calculated with diagramatic techniques in [77]. We will now go on to use this formulation of the eikonal and next-to-eikonal Feynman rules to compute the soft and next-to-soft behaviour of quantum gravity in position space.

4.4 Regge theory

Soft effects become dominant in certain energy regimes. One that we shall be considering is called the Regge limit where $s \gg -t \gg m^2$. This name comes from Regge Theory which predates the advent of QCD and sought to describe the strong interactions independently of any underlying field theory through considerations of the S-matrix. For the purposes of the coming work it will be useful to know what it means for an exchanged particle to become "Reggeized" and for this a brief introduction to Regge theory will be useful. This introduction follows the work of [83] where a more in depth detailing of Regge theory and its applications can be found.

The S-matrix is considered to have the properties of: Lorentz invariance, unitarity and analytic dependence on Lorentz invariants except at poles required for unitarity. The S-matrix in four dimensional momentum space has the form

$$S_{ab} = \delta_{ab} + i(2\pi)^4\delta^4(p_b - p_a)T_{ab}, \tag{4.58}$$

where T_{ab} is the transition matrix. The transition matrix will be dependent upon Lorentz invariants constructed from the four momenta of the scattering objects. For $2 \to 2$ scattering the possible quantities it can depend upon are the familiar Mandelstam invariants:

$$s = (p_1 + p_2)^2, \qquad t = (p_1 - p_3)^2, \qquad u = (p_1 - p_4)^2, \tag{4.59}$$

which satisfy momentum conservation:

$$s + t + u = \sum_{i=1}^{4} m_i^2. \tag{4.60}$$

Therefore only two are linearly independent and one can say that $T \equiv T(s,t)$. If one implements crossing such that $p_2 \leftrightarrow -p_3$ this has the effect of interchanging $t \leftrightarrow s$ and changes the scattering process being considered. We call this crossed process a t-channel process for which the scattering angle in the centre of mass frame is

$$\cos\theta \approx 1 + \frac{2s}{t}. \tag{4.61}$$

As is done in quantum mechanics one can expand this scattering amplitude using the partial wave expansion as

$$T_t(t,s) = \sum_{l=0}^{\infty}(2l+1)f_l(s)P_l(\cos\theta), \tag{4.62}$$

where $f_l(s)$ is the partial amplitude which can be written in terms of spherical Hankel functions and $P_l(\cos\theta)$ are Legendre polynomials. We can now utilise crossing symmetry to return to the original s-channel process being considered, such that the partial wave expansion is now

$$T\,(s,t) = \sum_{l=0}^{\infty}(2l+1)f_l(t)P_l\left(1 + \frac{2s}{t}\right), \tag{4.63}$$

Using Cauchy's integral theorem this can be re-written using the Sommerfeld-Watson expansion as

$$T\,(s,t) = \frac{1}{2i}\int_C dl \frac{(2l+1)}{\sin(\pi l)} f(l,t)P\left(l, 1 + \frac{2s}{t}\right), \tag{4.64}$$

where the integral is over a contour in the complex plane enclosing the poles at integer values of α and the analytic functions P_l and f_l have been analytically continued. It is necessary to consider the analytic continuations of the even and odd partial wave amplitudes $f^{\pm 1}(l,t)$ respectively and introduce a sum over them

$$T\,(s,t) = \frac{1}{2i}\int_C dl \frac{(2l+1)}{\sin(\pi l)} \sum_{\sigma=\pm 1} \frac{\sigma + e^{-i\pi l}}{2} f^{\sigma}(l,t)P\left(l, 1 + \frac{2s}{t}\right), \tag{4.65}$$

The contour integration encricling the poles along the real axis can be deformed to a contour C' running parallel to the imaginary axis with an offset of $-\frac{1}{2}$ between $\pm i\infty$. In order to do this one must encircle the poles and cuts of the function $f^{\sigma}(l,t)$ at

$l = \alpha_{n_\sigma}(t)$ and add $2\pi i$ multiplied by the residue of the pole. The amplitude will now be in the form

$$T(s,t) = \frac{1}{2i}\int_{-1/2-i\infty}^{-1/2+i\infty} dl \left[\frac{(2l+1)}{\sin(\pi l)}\sum_{\sigma=\pm 1}\frac{\sigma + e^{-i\pi l}}{2} f^{\sigma}(l,t) P\left(l, 1+\frac{2s}{t}\right)\right] + \sum_{\sigma=\pm 1}\sum_{n_\sigma}\frac{\sigma + e^{-i\pi\alpha_{n_\sigma}(t)}}{2}\tilde{\beta}_{n_\sigma}(t) P\left(\alpha_{n_\sigma}(t), 1+\frac{2s}{t}\right), \tag{4.66}$$

where

$$\tilde{\beta}_{n_\sigma}(t) = \frac{\pi(2\alpha_{n_\sigma}(t)+1)}{\sin(\pi\alpha_{n_\sigma}(t))} \times Res(f^{\sigma}(l,t), l = \alpha_{n_\sigma}(t)) \tag{4.67}$$

. The asymptotic form of the Legendre polynomial is

$$P_l(z) \approx z^l \qquad \text{for} \qquad z \gg 1, \tag{4.68}$$

which is applicable in the Regge limit where we can take $s \to \infty$. The result of this limit is that the integration along the contour in equation (4.66) is zero. Through use of the assumptotice form of the Leendre polynomial the high energy behaviour of the scattering amplitude can be isolated. Only the contribution from the leading Regge pole needs to be considered, that with the largest real part of $\alpha_{n_\sigma}(t)$. Therefore the leading contribution to the scattering amplitude takes the form

$$T(s,t) \propto \left(\frac{s}{-t}\right)^{\alpha(t)}, \tag{4.69}$$

where $\alpha(t)$ is the position of the leading Regge pole.

Each pole in the complex angular momentum plane is called a *Regge Pole*, or *Reggeon* for short. The function $\alpha(t)$ is referred to as the *Regge trajectory*. This behaviour is completely general in its derivation from considerations of the S-matrix and should therefore be reproduced by any field theory in the Regge limit.

The Regge limit corresponds to the eikonal limit for each incoming particle as we are considering the soft limit of t-channel exchanges where the exchanged momentum is much less than the centre of mass energy. We shall approach scattering amplitude calculations using the Wilson line approach adopted in QCD following the work of [84, 85]. In this work the use of Wilson line techniques to study Reggeization is demonstrated for $2 \to 2$ scattering. The two particles are in the highly forward scattering (recoilless) limit and can only affect each other by a change of phase. To preserve the gauge-transformation properties of the scattering amplitude this phase must correspond to a Wilson line operator. We can therefore model the $2 \to 2$ scattering as being between two Wilson lines dressing the external legs separated by a transverse

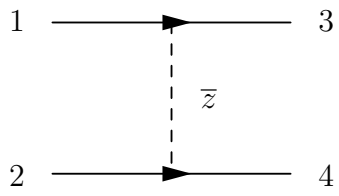

Figure 4.1: Schematic diagram for $2 \to 2$ scattering of massive bodies described by Wilson lines separated by a two (d-2)-dimensional transverse distance $\overline{z}$.

distance $\overline{z}$ over which t-channel exchanges can occur, as in figure (4.1). The behaviour of the Wilson line correlator in the UV limit reproduces the IR singular behaviour of the scattering amplitude.

4.4.1 Reggeization of particles

Many studies exist for Reggeization in perturbative quantum field theory, see references [86–113]. In order to show the Reggeization of amplitudes in QCD it is necessary to show that the fundamental particles themselves Reggeize. The propagator for the gluon becomes dressed by a Regge factor and takes the form of

$$\frac{-\eta_{\mu\nu}}{k^2} \to \frac{-\eta_{\mu\nu}}{k^2} \left(\frac{s}{-t}\right)^{\tilde{\alpha}(t)}, \tag{4.70}$$

where the gluon Regge trajectory $\tilde{\alpha}(-t)$ is related to the Regge trajectory for the full amplitude. The Regge trajectory is known to two loop order [107–112] for the quark and gluon. The one loop contribution is

$$\tilde{\alpha}^{(1)}(t) = \frac{\alpha_s(\mu^2)}{2\pi} \left(\frac{\mu^2}{-t}\right)^{\epsilon} \frac{C_R}{\epsilon}, \tag{4.71}$$

where C_R is the quadratic Casimir operator appropriate for the representation of the particle. To one loop order the Regge trajectory is purely infrared singular, up to scale logs. At two loop order added infrared finite terms appear. The pre-factor is universal and can be written in terms of the one-loop cusp anomalous dimension (see [84, 85]) controlling the UV renormalisation of the Wilson line operators. In the study to follow we regulate the UV divergence via the impact parameter $\overline{z}$ which will appear in the pre-factor.

We shall be interested in examining the Reggeization behaviour of particles in quantum gravity. The one-loop Regge trajectory for the graviton has been derived in [**L82b**, 114, 115] for both Einstein-Hilbert gravity and its supersymmetric extensions. It had been argued in [116] using the KLT relations [117] that the Reggeization of the graviton in $\mathcal{N} = 8$ supergravity consequently follows from the Reggeization of the

gluon in $\mathcal{N} = 4$ super Yang-Mills theory demonstrated in [118, 119] (see also [120, 121]). This was considered using Feynman diagrams in references [122–124] where the structure of potential Regge cut contributions in supergravity was also considered.

4.4.2 Regge limit of Gravity

The Regge limit of gravity is gathering interest firstly for the reason that this corresponds to the regime of transplanckian scattering. In this regime one can explore the existence of a gravitational S-matrix see [125, 126]. The negative mass dimension of the coupling constant for gravity leads to issues in the high energy limit of the theory due to the lack of UV renormalisability. The Regge limit of gravity is dominated by the IR divergent effects and free of the issues of UV renormalisability. We will also demonstrate that in the Regge limit the number of copies of supersymmetry doesn't impact the infrared behaviour.

At high energy we will see that the leading infra-red singular behaviour comes from a complex eikonal phase term responsible for the production of gravitational bound states see [127] and the Reggeization term, the interplay of which left some confusion in reference [128]. The reason becomes clear in what follows in that the Reggeization term becomes kinematically suppressed by the exchanged momentum t. Additional complications arise due to the presence of double logarithmic terms in $s/(-t)$ discussed in detail in [127].

We will also see that this limit is a regime in which there is correspondence between gauge and gravity theories. The all order validity of BCJ duality [53–55] was examined in the high energy limit in [129, 130]. The soft limit of quantum gravity was first studied in [131] and more extensively studied in [78, 82, 132–136].

Chapter 5

Wilson line approach to the soft limit of Gravity

This chapter will now investigate high energy scattering in QCD and quantum gravity using the Wilson line picture of figure (4.1) with the aim of investigating the IR singularities of the Regge trajectory. Before examining the Regge limit of quantum gravity it is instructive to perform the calculation in QCD as it will prove very similar to the quantum gravity calculation. As discussed we consider scattering between two Wilson lines separated by a constant transverse distance $\overline{z}$ that follow straight line trajectories. The appropriate scattering amplitude is

$$\tilde{M} = \int d^2\overline{z} \exp(-i\overline{z}\cdot\overline{p}) \left\langle 0|\Phi(p_1,0)\Phi(p_2,z)|0\right\rangle , \tag{5.1}$$

where the tilde denotes that this is a momentum space Fourier transform of the position space amplitude. The Wilson line operator used here is

$$\Phi(p,z) = \mathcal{P}\exp\left[ig_s p^\mu \int_C ds A_\mu(sp+z)\right] . \tag{5.2}$$

The path ordering symbol $\mathcal{P}$ is to maintain the correct ordering of the colour matrices. z^μ is the four-vector form of the separation vector related to the transverse separation via $z^2 = -\overline{z}^2$. The Wilson line follows an infinite contour along the classical trajectory of the particle mapped out by $sp^\mu + z^\mu$.

As mentioned in chapter (3) eikonal integrals are zero due to an exact cancellation between UV and IR poles. The amplitude above will not exhibit the same UV, IR cancellation as the $\overline{z}$ offset acts as a UV regulator. This becomes more intuitive when one considers the UV behaviour of amplitudes described by Wilson lines. UV poles for such amplitudes arise if there is a cusp present at the origin of the Wilson lines and

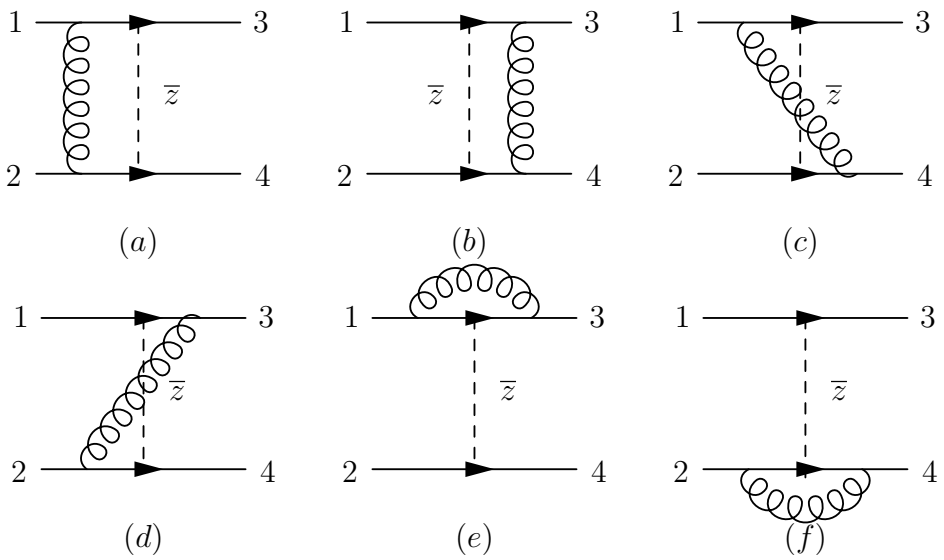

Figure 5.1: Feynman diagrams arising at one-loop order for the calculation of leading soft amplitudes in QCD.

the UV pole becomes dominant for the gluon emission being vanishingly close to this cusp. The transverse separation removes the cusp altogether and so along with it the UV pole.

5.1 1 loop diagrams

To calculate the amplitude we must calculate all 1 loop diagrams that are shown in figure (5.1). It will be necessary to use the position space gluon propagator (see e.g. [27])

$$D_{\mu\nu}(x-y) = -\eta_{\mu\nu}\frac{\Gamma(d/2-1)}{4\pi^{d/2}}\left[-(x-y)^2+i\varepsilon\right]^{1-d/2}. \tag{5.3}$$

Firstly we shall calculate the amplitude associated with diagram (a) which is given by

$$M_a^{(1)} = \frac{g_s^2\Gamma(1-\epsilon)\mu^{2\epsilon}}{4\pi^{2-\epsilon}}\mathbf{T}_1\cdot\mathbf{T}_2(p_1\cdot p_2)\int_\infty^0 ds\int_\infty^0 dt[-(sp_1-tp_2)^2+\overline{z}^2+i\varepsilon]^{\epsilon-1}, \tag{5.4}$$

where $\mathbf{T}_i$ is the Catani-Seymour notation [137] for the color generator on leg i. The cusp angle between lines i and j is defined as

$$\cosh\gamma_{i,j} = \frac{p_i\cdot p_j}{m_i m_j}. \tag{5.5}$$

We can reparameterise to $s = sm_1$ and $t = tm_2$ and use the definition of the cusp angle to write the diagram as

$$M_a^{(1)} = \frac{g_s^2\Gamma(1-\epsilon)\mu^{2\epsilon}}{4\pi^{2-\epsilon}}\mathbf{T}_1\cdot\mathbf{T}_2\cosh\gamma_{1,2}\int_0^\infty ds\int_0^\infty dt[-s^2-t^2-2st\cosh\gamma_{1,2}+\overline{z}^2+i\varepsilon]^{\epsilon-1}. \tag{5.6}$$

We can reparameterise again such that $s \to \sqrt{\overline{z}^2}s$ and $t \to \sqrt{\overline{z}^2}t$ to extract the factor of $\overline{z}^2$:

$$M_a^{(1)} = \frac{g_s^2\Gamma(1-\epsilon)(\mu^2\overline{z}^2)^\epsilon}{4\pi^{2-\epsilon}}\mathbf{T}_1\cdot\mathbf{T}_2\cosh\gamma_{1,2}\int_0^\infty ds\int_0^\infty dt[-s^2-t^2-2st\cosh\gamma_{1,2}+1+i\varepsilon]^{\epsilon-1}. \tag{5.7}$$

In order to perform the integral over s perform the reparameterisation $t \to st$ giving

$$M_a^{(1)} = \frac{g_s^2\Gamma(1-\epsilon)(\mu^2\overline{z}^2)^\epsilon}{4\pi^{2-\epsilon}}\mathbf{T}_1\cdot\mathbf{T}_2\cosh\gamma_{1,2}\int_0^\infty ds\int_0^\infty dts[s^2(-1-t^2-2t\cosh\gamma_{1,2})+1+i\varepsilon]^{\epsilon-1}. \tag{5.8}$$

The integral in s can now be performed yielding

$$M_a^{(1)} = \frac{g_s^2\Gamma(1-\epsilon)(\mu^2\overline{z}^2)^\epsilon}{4\pi^{2-\epsilon}}\mathbf{T}_1\cdot\mathbf{T}_2\cosh\gamma_{1,2}\int_0^\infty dt\frac{1}{1+2\cosh\gamma_{1,2}t+t^2-i\varepsilon}. \tag{5.9}$$

In order to solve this integral reparameterise to $t = u\sinh\gamma_{1,2}+\cosh\gamma_{1,2}$ leading to

$$M_a^{(1)} = \frac{g_s^2\Gamma(1-\epsilon)(\mu^2\overline{z}^2)^\epsilon}{4\pi^{2-\epsilon}}\mathbf{T}_1\cdot\mathbf{T}_2\coth\gamma_{1,2}\int_\infty^{-\coth\gamma_{1,2}} du\frac{1}{u^2-1-i\varepsilon}. \tag{5.10}$$

To get the correct factor of $i\pi$ we need to make sure to correctly implement the Feynman $i\varepsilon$ prescription when performing the integral to obtain:

$$\int_{\sigma\coth\gamma_{1,2}}^\infty du\frac{1}{u^2-1-i\varepsilon} = \begin{cases} i\pi-\gamma_{1,2} & \text{for } \sigma\text{=-1} \\ \gamma_{1,2} & \text{for } \sigma\text{=+1} \end{cases}. \tag{5.11}$$

Inserting this into equation (5.10) gives

$$M_a^{(1)} = \frac{g_s^2\Gamma(1-\epsilon)(\mu^2\overline{z}^2)^\epsilon}{4\pi^{2-\epsilon}}\mathbf{T}_1\cdot\mathbf{T}_2\frac{1}{2\epsilon}(i\pi-\gamma_{1,2})\coth\gamma_{1,2}. \tag{5.12}$$

Diagram (b) is similar to calculate except that the exchange is occurring between the two outgoing legs 3 and 4. The resulting contribution is

$$M_b^{(1)} = \frac{g_s^2\Gamma(1-\epsilon)(\mu^2\overline{z}^2)^\epsilon}{4\pi^{2-\epsilon}}\mathbf{T}_3\cdot\mathbf{T}_4\frac{1}{2\epsilon}(i\pi-\gamma_{3,4})\coth\gamma_{3,4}. \tag{5.13}$$

Diagrams (c) and (d) differ due to the exchange occurring between one incoming and one outgoing leg. The effect this has is to swap the sign on the lower limit of the final integration step. The result for diagram (c) is therefore

$$M_c^{(1)} = \frac{g_s^2\Gamma(1-\epsilon)(\mu^2\overline{z}^2)^\epsilon}{4\pi^{2-\epsilon}}\mathbf{T}_1\cdot\mathbf{T}_4\frac{1}{2\epsilon}\gamma_{1,4}\coth\gamma_{1,4}. \tag{5.14}$$

Diagram (d) is similar to (c) except with the exchange being between legs 2 and 3:

$$M_d^{(1)} = \frac{g_s^2\Gamma(1-\epsilon)(\mu^2\overline{z}^2)^\epsilon}{4\pi^{2-\epsilon}}\mathbf{T}_2\cdot\mathbf{T}_3\frac{1}{2\epsilon}\gamma_{2,3}\coth\gamma_{2,3}. \tag{5.15}$$

The two graphs (e) and (f) must be calculated differently due to the lack of z separation between the emitting and absorbing lines. Diagram (e) is given by

$$M_e^{(1)} = \frac{g_s^2\Gamma(1-\epsilon)\mu^{2\epsilon}}{4\pi^{2-\epsilon}}\mathbf{T}_1\cdot\mathbf{T}_3(-p_1\cdot p_3)\int_\infty^0 ds\int_0^\infty dt[-(-sp_1-tp_3)^2+i\varepsilon]^{\epsilon-1}. \tag{5.16}$$

Performing the rescaling $s\to s/m_1$ and $t\to t/m_3$ the integral becomes

$$M_e^{(1)} = \frac{g_s^2\Gamma(1-\epsilon)\mu^{2\epsilon}}{4\pi^{2-\epsilon}}\mathbf{T}_1\cdot\mathbf{T}_3\cosh\gamma_{1,3}\int_0^\infty ds\int_0^\infty dt[-s^2-t^2-2st\cosh\gamma_{1,3}+i\varepsilon]^{\epsilon-1}. \tag{5.17}$$

Making the reparameterisation $t\to ts$ gives

$$M_e^{(1)} = \frac{g_s^2\Gamma(1-\epsilon)\mu^{2\epsilon}}{4\pi^{2-\epsilon}}\mathbf{T}_1\cdot\mathbf{T}_3\cosh\gamma_{1,3}\int_0^\infty dss^{2\epsilon-1}\int_0^\infty dt[-1-t^2-2t\cosh\gamma_{1,3}+i\varepsilon]^{\epsilon-1}. \tag{5.18}$$

The integral over the s parameter is zero due to the cancellation between UV and IR poles. This is due to the absence of $\overline{z}^2$ acting as a UV regulator. This can be approached by extracting just the IR pole or by introducing a UV cutoff. The dimension of s after the reparameterising is that of a length. Therefore it is possible to use $\sqrt{\vec{z^2}}$ as a limit of integration to regulate the result, similarly to the previously calculated diagrams $(a)\to(d)$. The s integral is then

$$\int_0^\infty dss^{2\epsilon-1}\to\int_{\sqrt{\vec{z^2}}}^\infty dss^{2\epsilon-1} = -\frac{[(\overline{z})^2]^\epsilon}{2\epsilon} \tag{5.19}$$

Inserting this into equation (5.18) one obtains

$$M_e^{(1)} = \frac{g_s^2\Gamma(1-\epsilon)(\mu^2\overline{z}^2)^\epsilon}{4\pi^{2-\epsilon}}\mathbf{T}_1\cdot\mathbf{T}_3\cosh\gamma_{1,3}\frac{1}{2\epsilon}\int_0^\infty dt[-1-t^2-2t\cosh\gamma_{1,3}+i\varepsilon]^{\epsilon-1}. \tag{5.20}$$

Performing the integral over t one obtains the final result for diagram (e):

$$M_e^{(1)} = \frac{g_s^2\Gamma(1-\epsilon)(\mu^2\overline{z}^2)^\epsilon}{4\pi^{2-\epsilon}}\mathbf{T}_1\cdot\mathbf{T}_3\gamma_{1,3}\coth\gamma_{1,3}\frac{1}{2\epsilon}+\mathcal{O}(\epsilon^0). \tag{5.21}$$

Diagram (f) is very similar except that the exchange is between the lines labelled 2 and 4

$$M_f^{(1)} = \frac{g_s^2\Gamma(1-\epsilon)(\mu^2\overline{z}^2)^\epsilon}{4\pi^{2-\epsilon}}\mathbf{T}_2\cdot\mathbf{T}_4\gamma_{2,4}\coth\gamma_{2,4}\frac{1}{2\epsilon}+\mathcal{O}(\epsilon^0). \tag{5.22}$$

Before summing over the diagrams to obtain the one-loop amplitude the Regge limit can be employed to rewrite the cusp angles. To this end we can use

$$\gamma_{i,j} = \cosh^{-1}\left(\frac{p_i\cdot p_j}{m_i m_j}\right)\to\log\left(\frac{2p_i\cdot p_j}{m_i m_j}\right), \tag{5.23}$$

valid in the Regge limit of $p_i\cdot p_j \gg m_i m_j$. In this limit it is also the case that $(p_i+p_j)^2\approx 2p_i\cdot p_j$ which yields the relations:

$$\begin{aligned}
\gamma_{1,2},\gamma_{3,4}&\to\log\left(\frac{s}{m_1m_2}\right),\\
\gamma_{1,4},\gamma_{2,3}&\to\log\left(-\frac{u}{m_1m_2}\right),\\
\gamma_{1,3}&\to\log\left(-\frac{t}{m_1^2}\right),\qquad \gamma_{2,4}\to\log\left(-\frac{t}{m_2^2}\right),
\end{aligned} \tag{5.24}$$

where $m_1=m_3$ and $m_2=m_4$ have been used. Due to the momentum conservation constraint the Regge limit also means that $s\approx -u$ such that $\gamma_{1,2},\gamma_{3,4}\approx\gamma_{1,4},\gamma_{2,3}$, and due to the choice of scale orderings we can also make the simplification that $\coth\gamma_{i,j}\to 1$. The sum of diagrams in the Regge limit is now

$$\begin{aligned}
\sum_i M_i^{(1)} =& \frac{g_s^2\Gamma(1-\epsilon)}{4\pi^{2-\epsilon}}\frac{(\mu^2\overline{z}^2)^\epsilon}{2\epsilon}\Big\{i\pi\left[\mathbf{T}_1\cdot\mathbf{T}_2+\mathbf{T}_3\cdot\mathbf{T}_4\right]\\
&+\log\left(\frac{s}{m_1m_2}\right)\left[-\mathbf{T}_1\cdot\mathbf{T}_2-\mathbf{T}_3\cdot\mathbf{T}_4+\mathbf{T}_1\cdot\mathbf{T}_4+\mathbf{T}_2\cdot\mathbf{T}_3\right]\\
&+\log\left(-\frac{t}{m_1^2}\right)\mathbf{T}_1\cdot\mathbf{T}_3+\log\left(-\frac{t}{m_2^2}\right)\mathbf{T}_2\cdot\mathbf{T}_4\Big\}+\mathcal{O}(\epsilon^0).
\end{aligned} \tag{5.25}$$

It is useful to introduce color operators to simplify these expressions:

$$\mathbf{T}_s^2=(\mathbf{T}_1+\mathbf{T}_2)^2,\qquad \mathbf{T}_t^2=(\mathbf{T}_1-\mathbf{T}_3)^2. \tag{5.26}$$

The eigenstates of these operators relate to pure s and t channel exchanges respectively and the eigenvalues are the quadratic Casimir operators for the representation the

particle being exchanged is in. Using color conservation $\mathbf{T}_1 + \mathbf{T}_2 = \mathbf{T}_3 + \mathbf{T}_4$ we can write:

$$\begin{aligned}
\mathbf{T}_1 \cdot \mathbf{T}_2 + \mathbf{T}_3 \cdot \mathbf{T}_4 &= \frac{1}{2}\left[(\mathbf{T}_1 + \mathbf{T}_2)^2 + (\mathbf{T}_3 + \mathbf{T}_4)^2 - \sum_{i=1}^{4} C_i\right] = \mathbf{T}_s^2 - \frac{1}{2}\sum_{i=1}^{4} C_i, \\
-\mathbf{T}_1 \cdot \mathbf{T}_2 - \mathbf{T}_3 \cdot \mathbf{T}_4 + \mathbf{T}_1 \cdot \mathbf{T}_4 + \mathbf{T}_2 \cdot \mathbf{T}_3 &= (\mathbf{T}_1 - \mathbf{T}_3) \cdot (\mathbf{T}_4 - \mathbf{T}_2) = \mathbf{T}_t^2, \\
\mathbf{T}_1 \cdot \mathbf{T}_3 + \mathbf{T}_2 \cdot \mathbf{T}_4 &= -\frac{1}{2}\left[(\mathbf{T}_1 - \mathbf{T}_3)^2 + (\mathbf{T}_2 - \mathbf{T}_4)^2 - \sum_{i=1}^{4} C_i\right] = -\mathbf{T}_t^2 + \frac{1}{2}\sum_{i=1}^{4} C_i,
\end{aligned} \tag{5.27}$$

where C_i is the representation-dependent quadratic Casimir operator. This simplifies the expression of the one-loop amplitude to be

$$\begin{aligned}
\sum_i M_i^{(1)} = \frac{g_s^2 \Gamma(1-\epsilon)}{4\pi^{2-\epsilon}} \frac{(\mu^2 \overline{z}^2)^\epsilon}{2\epsilon} \Bigg[& i\pi \left(\mathbf{T}_s^2 - \frac{1}{2}\sum_{i=1}^{4} C_i\right) + \log\left(\frac{s}{m_1 m_2}\right) \mathbf{T}_t^2 + \\
& + \frac{1}{2}\log\left(-\frac{t}{m_1^2}\right)\left(\mathbf{T}_t^2 - 2C_1^2\right) + \frac{1}{2}\log\left(-\frac{t}{m_2^2}\right)\left(\mathbf{T}_t^2 - 2C_2^2\right)\Bigg] + \mathcal{O}(\epsilon^0),
\end{aligned} \tag{5.28}$$

where we have used $C_1 = C_3$ and $C_2 = C_4$. This result can be simplified further to

$$\begin{aligned}
\sum_i M_i^{(1)} = & \frac{g_s^2 \Gamma(1-\epsilon)}{4\pi^{2-\epsilon}} \frac{(\mu^2 \overline{z}^2)^\epsilon}{2\epsilon} \Bigg[i\pi \mathbf{T}_s^2 + \log\left(-\frac{s}{t}\right) \mathbf{T}_t^2 - i\pi \frac{1}{2}\sum_{i=1}^{4} C_i \\
& + \log\left(-\frac{t}{m_1^2}\right) C_1^2 + \log\left(-\frac{t}{m_2^2}\right) C_2^2\Bigg] + \mathcal{O}(\epsilon^0).
\end{aligned} \tag{5.29}$$

The calculation of diagrams (e) and (f) gave a $-\log\left(\frac{-t}{m^2}\right)\mathbf{T}_t^2$ term. Choosing the UV cut-off to be $\overline{z}^2$ enabled the summation with the term $\log\left(\frac{s}{m^2}\right)\mathbf{T}_t^2$ arising from diagrams $(a) \to (d)$ giving $\log\left(\frac{s}{-t}\right)\mathbf{T}_t^2$ in the total. This choice is useful for comparison to literature considering the massless limit, as we have cancelled the mass dependence from the terms that are not proportional to color diagonal factors.

It is well known that expectation values of Wilson lines exponentiate (see [36] for a review). We can use this knowledge to immediately resum the amplitude by writing

$$\begin{aligned}
\mathcal{A}_E = \exp\Bigg\{ & \frac{g_s^2 \Gamma(1-\epsilon)}{4\pi^{2-\epsilon}} \frac{(\mu^2 \overline{z}^2)^\epsilon}{2\epsilon} \Bigg[i\pi \mathbf{T}_s^2 + \log\left(-\frac{s}{t}\right) \mathbf{T}_t^2 - i\pi \frac{1}{2}\sum_{i=1}^{4} C_i \\
& + \log\left(-\frac{t}{m_1^2}\right) C_1^2 + \log\left(-\frac{t}{m_2^2}\right) C_2^2\Bigg]\Bigg\}.
\end{aligned} \tag{5.30}$$

From the definition of the Regge limit, the term proportional to $\log\left(\frac{s}{-t}\right)$ will dominate

such that the above combination becomes

$$\left(\frac{s}{-t}\right)^{K\mathbf{T}_t^2}, \tag{5.31}$$

where we have defined

$$K = \frac{g_s^2\Gamma(1-\epsilon)}{4\pi^{2-\epsilon}}\frac{(\mu^2\overline{z}^2)^\epsilon}{2\epsilon}. \tag{5.32}$$

In the Regge limit we are dealing with a Born interaction dominated by the t-channel exchange and this operator acts to Reggeize the exchanged particle. The resulting amplitude factor is then

$$\left(\frac{s}{-t}\right)^{J+KC_R}, \tag{5.33}$$

where C_R is the quadratic Casimir for the representation of the exchanged particle and J is the spin of the particle from the Born amplitude.

In some cases the Reggeization term vanishes, and the complex eikonal phase term dominates. One such example is QED. If we consider an electron scattering mediated by a photon exchange in the t-channel its squared charge is zero and therefore $C_R = 0$. Using $\mathbf{T_s}^2 = 2$ and $\gamma_{1,2} = \gamma_{3,4}$ the QED amplitude can be obtained by re-summing the integral results that gave equation (5.30) but using these QED values to obtain

$$\exp\left[\frac{i\alpha}{\epsilon}(\mu^2\overline{z}^2)^\epsilon\right], \qquad \alpha = \frac{e^2\Gamma(1-\epsilon)}{4\pi^{1-\epsilon}}\coth\gamma_{1,2}. \tag{5.34}$$

Inserting the definition of the cusp angle gives

$$\coth\gamma_{1,2} = \coth\left[\cosh^{-1}\left(\frac{p_1\cdot p_2}{m^2}\right)\right] = \frac{s-2m^2}{\sqrt{s(s-4m^2)}}. \tag{5.35}$$

It is now possible to define the ϵ independent factor of the trajectory in terms of the Mandelstam invariants

$$\alpha' = \frac{e^2}{4\pi}\frac{s-2m^2}{\sqrt{s(s-4m^2)}}. \tag{5.36}$$

This factor is described as the eikonal phase in gravitational literature, and we can examine its relevance in QED. Inserting equation (5.36) into equation (5.34) and expanding in ϵ gives

$$\begin{aligned}\exp\left[\frac{i\alpha'}{\epsilon}\Gamma(1-\epsilon)(\mu^2\overline{z}^2\pi)^\epsilon\right] =& \exp\left[i\frac{\alpha'}{\epsilon} + i\alpha'\log(\mu^2\overline{z}^2) + \gamma_E + \log(\pi) + \mathcal{O}(\epsilon)\right],\\ =&(\mu^2\overline{z}^2)^{i\alpha'}\exp(i\alpha'/\epsilon),\end{aligned} \tag{5.37}$$

where we have neglected the two constant terms between the first and second lines

as they will not be important in what follows. We can now Fourier transform to momentum space as in equation (5.1). Making use of a Hankel transform of order zero and $t = -\overline{q}^2$ gives

$$\begin{aligned}\tilde{M} &= \int d^2\overline{z}\exp(-i\overline{q}\cdot\overline{z})(\mu^2\overline{z}^2)^{i\alpha'}\exp(i\alpha'/\epsilon),\\ &= \frac{4\pi i\alpha'}{t}\exp(i\alpha'/\epsilon)\left(\frac{-t}{4\mu^2}\right)^{-i\alpha'}\frac{\Gamma(1+i\alpha')}{\Gamma(1-i\alpha')}.\end{aligned} \tag{5.38}$$

The Gamma functions will have poles occurring at points when $i\alpha' = -N$ where $N = 1, 2, \ldots$. Using our definition for α' in equation (5.36) these poles are found to occur at:

$$s = 2m^2\left[1 - \left(1 + \frac{e^4}{16\pi^2 N^2}\right)^{-1/2}\right]. \tag{5.39}$$

These are the physical poles in the scattering amplitude representing bound states. Equation (5.39) gives the spectrum of s-channel bound states creatable in electron-positron scattering (i.e. the spectrum of positronium states) reproducing equation (17) of reference [138].

It has been shown that in the Regge limit in both QCD and QED at one loop level, scattering processes dominated by t-channel exchanges Reggeize. Also explained is the appearance of the eikonal phase term relating to the spectrum of s-channel bound states that can be created in this scattering. Reggeization arises from vertical ladder Feynman diagrams whereas the eikonal phase arises from horizontal ladder diagrams. Which of these effects is kinematically dominant depends upon the squared charge of the exchanged particle. If it is zero such as for the photon the eikonal phase term dominates; in QCD the Reggeization term does. This will be an important consideration for the gravity study detailed in the next section.

5.2 Wilson line approach for gravity

Having demonstrated the use of Wilson line techniques to investigate the Regge limit in QCD and QED, a similar approach will now be constructed for gravity. In this case the relevant Wilson line operators are obtained from equation (4.54):

$$\Phi_g(p, z) = \exp\left[i\frac{\kappa}{2}p^\mu p^\nu\int_C dsh_{\mu\nu}(sp + z)\right]. \tag{5.40}$$

The graviton propagator in the de Donder gauge is

$$D_{\mu\nu,\alpha\beta}(x-y) = P_{\mu\nu,\alpha\beta}\frac{\Gamma(d/2-1)}{4\pi^{d/2}}[-(x-y)^2+i\varepsilon]^{1-d/2},$$
$$P_{\mu\nu,\alpha\beta} = \frac{1}{2}\left(\eta_{\mu\alpha}\eta_{\nu\beta}+\eta_{\nu\alpha}\eta_{\mu\beta}-\frac{2}{d-2}\eta_{\mu\nu}\eta_{\alpha\beta}\right). \tag{5.41}$$

By analogy with equation (5.1), the one-loop amplitude for the soft limit of gravity is

$$\tilde{M}_g = \int d^2\overline{z}\exp(-i\overline{z}\cdot\overline{q})\,\langle 0|\Phi_g(p_1,0)\Phi_g(p_2,z)|0\rangle\,. \tag{5.42}$$

The diagrams contributing at 1-loop are the same as for QCD except with the different Feynman rules for the graviton used. The numerator for (5.41) differs from the gluon propagator but the denominator factor is the same such that the necessary integrations are also the same. The pre-factor to the integration will be different in necessitating the replacement of $p_i\cdot p_j$ from the QCD case with:

$$p_i^\mu p_i^\nu P_{\mu\nu,\alpha\beta}p_j^\alpha p_j^\beta = (p_i\cdot p_j)^2 - \frac{1}{d-2}m^4. \tag{5.43}$$

The result for diagram (a) in the gravity case can then be written as:

$$M_{g,a}^{(1)} = -\left(\frac{\kappa}{2}\right)^2\frac{\Gamma(1-\epsilon)}{4\pi^{2-\epsilon}}(\mu^2\overline{z}^2)^\epsilon\left[p_1\cdot p_2-\frac{m^4}{2(1-\epsilon)}\frac{1}{p_1\cdot p_2}\right]\frac{1}{2\epsilon}(i\pi-\gamma_{1,2})\coth\gamma_{1,2}. \tag{5.44}$$

This diagram can be obtained from equation (5.12) by switching the overall sign and making the replacements:

$$g_s\to\frac{\kappa}{2}, \qquad \mathbf{T}_i\to p_i. \tag{5.45}$$

The other diagrams exhibit similar relations such that the sum of the diagrams for gravity in the Regge limit can be obtained by switching the overall sign and making the replacements (as $m\to 0$) of:

$$g_s\to\frac{\kappa}{2}, \qquad \mathbf{T}_s^2\to s, \qquad \mathbf{T}_t^2\to t, \qquad C_i\to 0, \tag{5.46}$$

doing so yields

$$\sum_i M_{g,i}^{(1)} = -\left(\frac{\kappa}{2}\right)^2\frac{\Gamma(1-\epsilon)}{4\pi^{2-\epsilon}}\frac{(\mu^2\overline{z}^2)^\epsilon}{2\epsilon}\left[i\pi s+t\log\left(\frac{s}{-t}\right)\right]+\mathcal{O}(\epsilon^0). \tag{5.47}$$

The $\mathcal{O}(m^2)$ terms have been neglected as they vanish in the Regge limit and there are no mass logarithms, as expected due to the absence of collinear singularities in quantum gravity (see [131]). Quantum gravity also has the feature of one loop exactness such that there are no perturbative corrections to this result (see [139, 140]).

There are two terms in the square bracket. The first term, $i\pi s$, is the eikonal phase factor (see [141]). The second, logarithmically dependent, term acts to Reggeize the graviton being exchanged in the t-channel. Expanding this result about small ϵ and exponentiating the result gives

$$\mathcal{A}_g = \exp(-i\pi s K_g/\epsilon)\left(\frac{s}{-t}\right)^{-K_g t/\epsilon}(\mu^2\overline{z}^2)^{-K_g[i\pi s + t\log(s/-t)]}, \tag{5.48}$$

where

$$K_g = \left(\frac{\kappa}{2}\right)^2 \frac{\Gamma(1-\epsilon)}{8\pi^{2-\epsilon}}. \tag{5.49}$$

The power like term in $(s/-t)$ when acting on the Born amplitude will Reggeize the graviton with a Regge trajectory of

$$\alpha_g(t) = 2 - \frac{tK_g}{\epsilon}. \tag{5.50}$$

This one-loop Regge trajectory has a number of expected features e.g. it is infrared singular like in the QED and QCD cases. As in the latter theories, the Regge trajectory is proportional to the quadratic casimir of the particle being exchanged in the t-channel. For the case of gravity this corresponds to the squared momentum of the graviton, which is t itself.

The amplitude also exhibits an eikonal phase factor where s is the quadratic Casimir for s-channel exchanges. In the strict Regge limit of $s \gg -t$ the eikonal phase will dominate, kinematically suppressing the Reggeization term.

Performing the Fourier transform of the exponentiated amplitude gives the momentum space amplitude

$$\begin{aligned}\tilde{M}_g =& \frac{-4\pi K_g}{t}\exp(-i\pi s K_g/\epsilon)\left(\frac{s}{-t}\right)^{-K_g t/\epsilon}\left[i\pi s + t\log\left(\frac{s}{-t}\right)\right]\left(\frac{-t}{4\mu^2}\right)^{K_g[i\pi s + t\log(s/-t)]} \\ &\times \frac{\Gamma(1-K_g(i\pi s + t\log(s/-t))}{\Gamma(1+K_g(i\pi s + t\log(s/-t))}.\end{aligned} \tag{5.51}$$

The Gamma functions will no longer give a pure phase and instead of poles in the s plane here we will have cuts. This has ramifications in Regge theory where the high-energy behaviour of the amplitude $A(s,t)$ is related to its analytically continued partial wave coefficients $F(t,j)$ where the angular momentum j is complex, via the relation

[142]

$$F(t,j) = \int_1^\infty ds s^{-j-1} A(s,t). \tag{5.52}$$

Therefore cuts in the s-plane give rise to Regge cuts in the complex angular momentum plane. The cuts arise due to the cross talk between the Reggeization term and the eikonal phase term.

Neglecting the Reggeization term and restoring the full mass dependence in the eikonal phase term the amplitude is

$$\tilde{M}_g = -\frac{4\pi i G(s)}{t} \exp(-iG(s)/\epsilon) \left(\frac{-t}{4\mu^2}\right)^{iG(s)} \frac{\Gamma[1-iG(s)]}{\Gamma[1+iG(s)]}, \tag{5.53}$$

where we have defined

$$G(s) = G_n \left(\frac{s^2 - 4m^2 s + 2m^4}{\sqrt{s(s-4m^2)}}\right). \tag{5.54}$$

We now find poles instead of cuts and these poles correspond to the Newtonian bound states relating to the $1/r$ part of the gravitational potential, an example of which is the earth-moon system.

So far this investigation has been into the nature of the infra-red singular behaviour of scattering amplitudes. But recent research has sought to clarify the nature of infra-red finite contributions. The infra-red finite terms turn out to be different in the different supersymmetric extensions of Einstein-Hilbert gravity. This is investigated in the following section.

5.3 Infrared-finite contributions in supergravity

Supergravity will be considered with $\mathcal{N} = M$ copies of supersymmetry where $4 \leq M \leq 8$. One-loop results are obtained in references [143–146]. Following reference [147] the one-loop four graviton amplitude can be written as

$$\begin{aligned}\mathcal{M}_4^{(1),\mathcal{N}=M} = &\left(\frac{\kappa}{8\pi}\right)^2 \left(\frac{4\pi e^{-\gamma_E}\mu^2}{|s|}\right)^\epsilon \mathcal{M}_4^{tree} \\ &\times \left\{\frac{2}{\epsilon}[s\log(-s) + t\log(-t) + u\log(-u)] + F_4^{(1),\mathcal{N}=M}\right\},\end{aligned} \tag{5.55}$$

where $F_4^{(1),\mathcal{N}=M}$ is IR finite and depends upon the degree of supersymmetry. The IR singular part is universal at one loop and in the physical region of $s > 0$ and $t, u < 0$

it is

$$\mathcal{M}_{4,IR}^{(1),\mathcal{N}=M} = \left(\frac{\kappa}{8\pi}\right)^2 \left(\frac{4\pi e^{-\gamma_E}\mu^2}{|s|}\right)^{\epsilon} \frac{2}{\epsilon}[s\log(s) - i\pi s + t\log(-t) + u\log(-u)]\mathcal{M}_4^{tree}, \tag{5.56}$$

where we have used that $\log(-s) = \log|s| - i\pi$. In the massless limit the choice can be made that $u = -s - t$ and equation (5.56) can be expanded about the Regge limit to obtain

$$\mathcal{M}_{4,IR}^{(1),\mathcal{N}=M} = \left(\frac{\kappa^2}{32\pi^2\epsilon}\right) \left(\frac{4\pi e^{-\gamma_E}\mu^2}{|s|}\right)^{\epsilon} \left[i\pi s + t\log\left(\frac{s}{-t}\right) + t + \mathcal{O}\left(\frac{t^2}{s}\right)\right] \mathcal{M}_4^{tree}, \tag{5.57}$$

This result demonstrates the insensitivity of scattering ampltidues to the level of supersymmetry in the strict Regge limit and has an eikonal phase and Reggieization term as we found previously. We can define a parameter for the Regge limit as

$$x \equiv \frac{-t}{s}. \tag{5.58}$$

Adding on the IR finite terms relating to different supergravity theories given in the appendix of [147] to equation (5.57) and expand the resulting amplitude to next-to-leading order in x gives

$$\begin{aligned}
\mathcal{M}_4^{(1),\mathcal{N}=8} &= \left(\frac{\kappa}{8\pi}\right)^2 \left(\frac{4\pi e^{-\gamma_E}\mu^2}{-t}\right)^{\epsilon} \left\{\frac{s}{\epsilon}\left[-2i\pi + 2x(L+1)\right] + sx\left[-2L^2 + 2i\pi L\right]\right\} \mathcal{M}_4^{tree}, \\
\mathcal{M}_4^{(1),\mathcal{N}=6} &= \left(\frac{\kappa}{8\pi}\right)^2 \left(\frac{4\pi e^{-\gamma_E}\mu^2}{-t}\right)^{\epsilon} \left\{\frac{s}{\epsilon}\left[-2i\pi + 2x(L+1)\right] + sx\left[-L^2 + 2i\pi L + \pi^2\right]\right\} \mathcal{M}_4^{tree}, \\
\mathcal{M}_4^{(1),\mathcal{N}=5} &= \left(\frac{\kappa}{8\pi}\right)^2 \left(\frac{4\pi e^{-\gamma_E}\mu^2}{-t}\right)^{\epsilon} \left\{\frac{s}{\epsilon}\left[-2i\pi + 2x(L+1)\right] + sx\left[-\frac{L^2}{2} + 2i\pi L + \frac{3\pi^2}{2}\right]\right\} \mathcal{M}_4^{tree}, \\
\mathcal{M}_4^{(1),\mathcal{N}=4} &= \left(\frac{\kappa}{8\pi}\right)^2 \left(\frac{4\pi e^{-\gamma_E}\mu^2}{-t}\right)^{\epsilon} \left\{\frac{s}{\epsilon}\left[-2i\pi + 2x(L+1)\right] + sx\left[2i\pi L - L + 2\pi^2 + 1\right]\right\} \mathcal{M}_4^{tree},
\end{aligned} \tag{5.59}$$

where we have defined $L = \log(s/-t)$. From the results of equation (5.59) it is possible to write a general amplitude at this order for different amounts of supersymmetry

$$\begin{aligned}
\mathcal{M}_4^{(1),\mathcal{N}=M} = \left(\frac{\kappa}{8\pi}\right)^2 \left(\frac{4\pi e^{-\gamma_E}\mu^2}{-t}\right)^{\epsilon} \Bigg\{ & \frac{s}{\epsilon}[-2i\pi + 2xL + 2x] \\
& + sx\left[\left(\frac{4-M}{2}\right)L^2 + \left(\frac{8-M}{2}\right)\pi^2 + 2i\pi L + \delta_{M4}(1-L)\right] \\
& + \mathcal{O}(sx^2) + \mathcal{O}(\epsilon)\Bigg\} \mathcal{M}_4^{tree}.
\end{aligned} \tag{5.60}$$

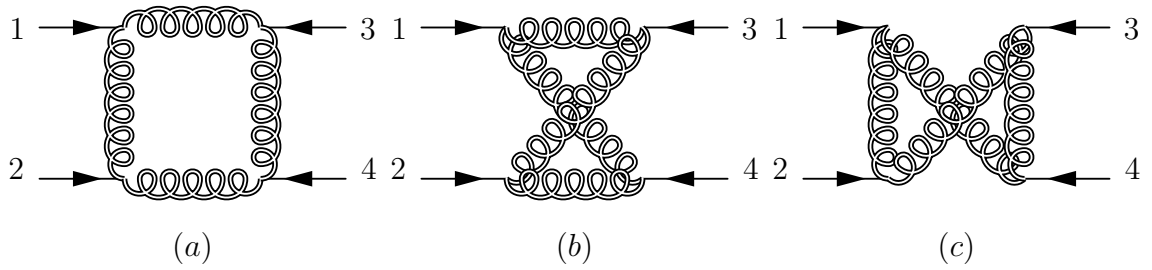

Figure 5.2: The complete set of diagrams contributing to the one-loop four-graviton amplitude arising in $\mathcal{N}=8$ supergravity. Diagram (a) is the dressed s-channel exchange, (b) the dressed t-channel and (c) the dressed u-channel. All bubble and triangle graphs cancel out.

In the infrared singular part of equation (5.60) there is the eikonal phase term and the Reggeization term as before. However, in the infrared finite part there is a double log contribution

$$sx\left(\frac{4-M}{2}\right)L^2=\left(\frac{M-4}{2}\right)t\log^2\left(\frac{s}{-t}\right), \tag{5.61}$$

first observed in [127]. The double logarithm is super-leading over the Reggeization term in the Regge parameter expansion by a factor of $L(x)$. The prefactor to the double logarithm term is dependent upon the degree of supersymmetry therefore this term cannot be obtained from the Wilson line approach which is insensitive to the matter content of the theory and only manages graviton-related contributions.

It is important to note that the double logarithm term is not connected to the Reggeization factor for the graviton. This can be demonstrated by considering the Feynman diagrams contributing to the amplitude. If we consider $\mathcal{N}=8$ supergravity the graphs contributing to the amplitude are shown in figure (5.2) and the corresponding amplitude can be written as [148]

$$\mathcal{M}_4^{(1),\mathcal{N}=8}=-i\left(\frac{\kappa}{2}\right)^2 stu\left[\mathcal{I}_4^{(1)}(s,t)+\mathcal{I}_4^{(1)}(t,u)+\mathcal{I}_4^{(1)}(s,u)\right]\mathcal{M}_4^{tree}, \tag{5.62}$$

where

$$\mathcal{I}_4^{(1)}(s,t)=\mu^{4-d}\int\frac{d^dk}{(2\pi)^d}\frac{1}{k^2(k-p_2)^2(k-p_1-p_2)^2(k+p_4)^2}. \tag{5.63}$$

This integral corresponds to the first box diagram, and $\mathcal{I}_4^{(1)}(t,u)$ and $\mathcal{I}_4^{(1)}(s,u)$ then correspond to the second and third diagrams respectively. The result for the integral is

$$\begin{aligned}\mathcal{I}_4^{(1)}(s,t)=\frac{ie^{-\epsilon\gamma_E}(4\pi)^{\epsilon-2}}{st}\Bigg\{&\frac{4}{\epsilon^2}-\frac{2}{\epsilon}\log\left(\frac{-s}{\mu^2}\right)-\frac{2}{\epsilon}\log\left(\frac{-t}{\mu^2}\right)\\&+2\log\left(\frac{-s}{\mu^2}\right)\log\left(\frac{-t}{\mu^2}\right)-\frac{4\pi^2}{3}+\mathcal{O}(\epsilon)\Bigg\}.\end{aligned} \tag{5.64}$$

From this result we can see that the double logarithmic contribution comes from the dressed u-channel diagram which contributes to neither the eikonal phase or the Reggeization term by not being a ladder type diagram.

The origin of these double logarithms is important when considering if they exponentiate and two such sources exist as discussed in [127]. One source is from finite terms in ladder diagrams (see [**L82b**, 114, 115]), and the other is from backward scattering. Backward scattering contributions arise from dressed u-channel graphs where $|k_\perp|^2 > -t$ which are important at this order in x. The authors of [127] write an evolution equation for the leading partial wave contributing to the amplitude in the limit in which the double logarithms are important whose solution is argued to resum these contributions

$$\left[\kappa^2 t \log^2\left(\frac{s}{-t}\right)\right]^n \approx \kappa^{2n} s^n x^n L^{2n}, \tag{5.65}$$

indicating that such contributions become more kinematically suppressed at higher orders in perturbation theory.

5.3.1 Two loop results

In order to investigate the exponentiation properties of the terms derived at one loop it is worth doing a two-loop analysis as this will give information on the double logarithm term. From [147] we can write the two-loop amplitude as

$$\frac{\mathcal{M}_4^{(2),\mathcal{N}=M}(\epsilon)}{\mathcal{M}_4^{tree}} = \frac{1}{2}\left[\frac{\mathcal{M}_4^{(1),\mathcal{N}=M}(\epsilon)}{\mathcal{M}_4^{tree}}\right]^2 + \left(\frac{\kappa}{8\pi}\right)^4 F_4^{(2),\mathcal{N}=M} + \mathcal{O}(\epsilon), \tag{5.66}$$

where $F_4^{(2),\mathcal{N}=M}$ is the two-loop remainder function not generated from the exponentiation of one-loop results. This function has been calculated for $\mathcal{N}=8$ supergravity in references [149, 150] using results of [148, 151, 152], and for $\mathcal{N}=M<8$ supergravity in [147]. The behaviour of these functions expanded about the Regge limit is:

$$\begin{aligned}
F_4^{(2),\mathcal{N}=8} =& s^2 x\left\{-2\pi^2\log^2 x - 4\pi^2\log x + \pi^4 + 4\pi^2 + \right.\\
&\left. + i\pi\left[\frac{4}{3}\log^3 x + 4\log^2 x - \left(8+\frac{8\pi^2}{3}\right)\log x + 16\zeta_3 + \frac{8\pi^2}{3} + 8\right]\right\} + ...,\\
F_4^{(2),\mathcal{N}=6} =& s^2 x\left\{-2\pi^2\log^2 x - 4\pi^2\log x + \frac{59\pi^4}{90} + 4\pi^2 + \right.\\
&\left. + i\pi\left[\frac{2}{3}\log^3 x + 4\log^2 x - \left(8+\frac{6\pi^2}{3}\right)\log x + 4\zeta_3 + \frac{16\pi^2}{3} + 8\right]\right\} + ...,\\
F_4^{(2),\mathcal{N}=5} =& s^2 x\left\{-2\pi^2\log^2 x - 4\pi^2\log x + \frac{2\pi^4}{3} + 4\pi^2 + \right.
\end{aligned}$$

$$
\begin{aligned}
&+i\pi\left[\frac{1}{3}\log^3 x+4\log^2 x-\left(8+\frac{5\pi^2}{3}\right)\log x+4\zeta_3+\frac{20\pi^2}{3}+8\right]\Bigg\}+...,\\
F_4^{(2),\mathcal{N}=4}=&s^2x\left\{-2\pi^2\log^2 x-4\pi^2\log x+\frac{13\pi^4}{30}+\frac{22\pi^2}{3}-1+\right.\\
&\left.+i\pi\left[3\log^2 x-\left(14+\frac{4\pi^2}{3}\right)\log x+4\zeta_3+\frac{71\pi^2}{9}+\frac{32}{3}\right]\right\}+...\ .
\end{aligned}
\tag{5.67}
$$

These remainder terms vanish in the strict Regge limit of $x \to 0$. In the Regge limit the amplitude is dominated by the eikonal phase dressing the tree level result. This is to be expected as the eikonal phase is known to exponentiate at this order and therefore these terms have to vanish.

The logarithmic contributions can be written in general $\mathcal{N} = M$ form

$$
\begin{aligned}
F_4^{(2),\mathcal{N}=M}=&s^2x\left\{-2\pi^2\log^2 x-4\pi^2\log x+\right.\\
&\left.+i\pi\left[\left(\frac{M-4}{3}\right)\log^3 x+(4-\delta_{M4})\log^2 x-\left(8+\frac{M_\pi^2}{3}+6\delta_{M4}\right)\log x\right]\right\}+...
\end{aligned}
\tag{5.68}
$$

where terms independent of the amount of supersymmetry can be interpreted as involving the graviton alone. Such terms are UV divergent in Einstein-Hilbert gravity at two loops however the added matter content in supergravity makes them finite.

To investigate the exponentiation of the double logarithm we need to include the quartic logarithmic terms that can arise at this loop order noted in [127], they are not shown above as they are of $\mathcal{O}(s^2x^2)$. The terms are known to be of the form

$$
F_4^{(2),\mathcal{N}=M}=...+c_M s^2x^2\log^4\left(\frac{s}{-t}\right)+... \qquad \text{where}\begin{cases} c_8 &= -\frac{1}{3}\\ c_6 &= 0\\ c_5 &= \frac{1}{24}\\ c_4 &= 0\end{cases}\ . \tag{5.69}
$$

This shows that for $M = 5$ and 8 the double logarithm term does not formally exponentiate even though it has been argued in [127] that they can be resummed to all orders. Such terms as these will be subleading to those of $\mathcal{O}(s^2x)$. The terms in the remainder function of $\mathcal{O}(s^2x)$ also are kinematically superleading over the graviton Reggeization term.

In the strict Regge limit $x \to 0$ the two-loop remainder function vanishes and therefore the two-loop amplitude is obtainable in full from exponentiation of the one-loop amplitude. At three-loop level however there is evidence to indicate the possible

breaking of the one-loop exactness by infra-red finite terms that survive in the Regge limit. If one expands the ratio of gamma functions in equation (5.53) we get

$$\frac{\Gamma[1-iG]}{\Gamma[1+iG]} = e^{2i\gamma_E G}\left[1+\frac{i}{3}\Psi^{(2)}(1)G^3+\mathcal{O}(G^4)\right], \tag{5.70}$$

where we have defined

$$\Psi(x) = \frac{d}{dx}\log\Gamma(x). \tag{5.71}$$

This lack of pure exponentiation at three-loop order is the term is evidence for one-loop exactness being broken. There could arise additional terms at this loop order not captured by the eikonal approximation that correct for this and restore the one-loop exactness.

5.4 The Regge limit of multi-particle amplitudes

The previous work will be extended in this chapter to examine the Regge behaviour of multigraviton amplitudes. Multi-Regge scattering considers the scattering of $2 \to (L-2)$ particles. The outgoing particles all have similar transverse momenta but are strongly ordered in rapidities. This restriction allows one to construct a hierachy of Lorentz invariants such that $s_{ij} = (p_i + p_j)^2 \gg -t_{1,\ldots L}$ for all i, j where there can still be a hierachy in the s_{ij} such as $s_{12} \gg s_{3,L-2}$. In the theory of QCD Reggeization has been studied for general L-point scattering for $L \geq 4$ (see reference [153] for a pedagogical review). It has been confirmed in [154, 155] that in the Regge Limit of QCD, scattering of this type is dominated by t-channel exchanges. The Feynman diagrams for such graphs as that shown in figure (5.3) are ladder type graphs. Each possible exchange between the rungs on the ladder should exhibit Reggeization through a Reggeized propagator factor dependant upon the quadratic Casimir operator of the exchanged object. We will examine this scattering at the one loop level as previously.

It would be a natural extension of the above work to demonstrate that this will occur also for gravitons in the theories of quantum gravity we discussed. Again we will perform the calculation using the Wilson line approach for comparison to the existing results for non-abelian gauge theory. It will also help to have more insight into the behaviour of the eikonal phase term in this scenario.

We can take the result for the four particle non-exponentiated QCD amplitude of equation (5.25) and generalise it to the L-point case. To do so we consider the sum over all one-loop diagrams that can occur for the diagram of figure (5.3). To simplify

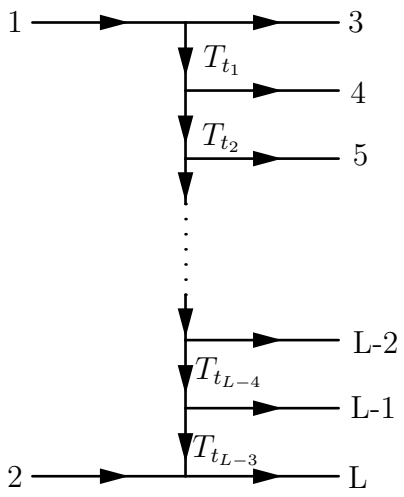

Figure 5.3: The ladder diagram being computed when considering $2 \to (L-2)$ scattering in the Multi-Regge-Kinematic limit. T_{t_i} is the quadratic Casimir operator associated with each strut on the ladder

things we consider all the masses to be the same. The resulting amplitude is

$$M_L^{(1)} = \frac{g_s^2 \Gamma(1-\epsilon)}{4\pi^{2-\epsilon}} \frac{(\mu^2 \Lambda_{UV}^2)^\epsilon}{2\epsilon} \left\{ i\pi \left(\mathbf{T}_1 \cdot \mathbf{T}_2 + \sum_{i=3}^{L-1} \sum_{j>i} \mathbf{T}_i \cdot \mathbf{T}_j \right) - \mathbf{T}_1 \cdot \mathbf{T}_2 \log\left(\frac{s}{m^2}\right) \right.$$
$$\left. - \sum_{i=3}^{L-1} \sum_{i>j} \mathbf{T}_i \cdot \mathbf{T}_j \log\left(\frac{s_{ij}}{m^2}\right) - \sum_{i=3}^{L} \left[\mathbf{T}_1 \cdot \mathbf{T}_i \log\left(-\frac{s_{1i}}{m^2}\right) + \mathbf{T}_2 \cdot \mathbf{T}_i \log\left(-\frac{s_{2i}}{m^2}\right) \right] \right\}, \tag{5.72}$$

where the color operators for the incoming particles $\mathbf{T}_{1,2}$ have had their signs reversed from equation (5.25), Λ_{UV} is a UV regulator and:

$$s = (p_1+p_2)^2, \quad s_{ij} = (p_i+p_j)^2, \quad s_{1i} = (p_1-p_i)^2, \quad s_{2i} = (p_2-p_i)^2; \quad i,j > 3. \tag{5.73}$$

The high energy limit of multiparton scattering corresponds to the multi-Regge-kinematic (MRK) regime where the outgoing particles have widely separated rapidities. If we rewrite the invariants in equation (5.73) in terms of the rapidity and transverse momenta of the particles, see [153], we can make use of the approximations:

$$\begin{aligned} s &\approx |k_{3\perp}||k_{L\perp}| e^{y_3 - y_L}, \\ -s_{1i} &\approx |k_{3\perp}||k_{i\perp}| e^{y_3 - y_i}, \\ -s_{2i} &\approx |k_{L\perp}||k_{i\perp}| e^{y_L - y_i}, \\ s_{ij} &\approx |k_{i\perp}||k_{j\perp}| e^{y_i - y_j}, \qquad 3 \le i \le j \le L, \end{aligned} \tag{5.74}$$

where y_i and $k_{i\perp}$ are the rapidity and the transverse momentum of particle i respec-

tively. As we did earlier we can set the UV cutoff as the impact parameter $\overline{z}$ being the distance of closest approach between the two incoming particles. A different choice will introduce additional logarithms of the chosen cut off in equation (5.72). We can substitute the results of equation (5.74) into equation (5.72) to obtain

$$M_L^{(1)} = \frac{g_s^2\Gamma(1-\epsilon)}{4\pi^{2-\epsilon}}\frac{(\mu^2\Lambda_{UV}^2)^\epsilon}{2\epsilon}\left\{-\sum_{i=1}^{L-1}\sum_{j>i}|y_i-y_j|\mathbf{T}_i\cdot\mathbf{T}_j + i\pi\left(\mathbf{T}_1\cdot\mathbf{T}_3+\sum_{i=3}^{L-1}\sum_{j>i}\mathbf{T}_i\cdot\mathbf{T}_j\right)\right.$$
$$\left.+\sum_{i=1}^{L}C_i\log\left(\frac{|k_{i\perp}|}{m}\right)\right\}, \tag{5.75}$$

where we have introduced the quadratic Casimirs associated with the external lines, used color conservation

$$\sum_{i=1}^{L}\mathbf{T}_i = 0, \tag{5.76}$$

and introduced the unphysical rapidities $y_1 \equiv y_3$, $y_2 \equiv y_L$, in order to simplify the notation. The s-channel quadratic Casimir can also be written in terms of the color generators of the extra emissions via

$$\mathbf{T}_s^2 = (\mathbf{T}_1+\mathbf{T}_2)^2 = \left(\sum_{i=3}^{L}\mathbf{T}_i\right)^2. \tag{5.77}$$

Using the above we can rewrite equation (5.75) as

$$M_L^{(1)} = \frac{g_s^2\Gamma(1-\epsilon)}{4\pi^{2-\epsilon}}\frac{(\mu^2\Lambda_{UV}^2)^\epsilon}{2\epsilon}\left\{-\sum_{i=1}^{L-1}\sum_{j>i}|y_i-y_j|\mathbf{T}_i\cdot\mathbf{T}_j + i\pi\mathbf{T}_s^2+\sum_{i=1}^{L}C_i\left[\log\left(\frac{|k_{i\perp}|}{m}\right)-\frac{i\pi}{2}\right]\right\}. \tag{5.78}$$

Making use of the identity proven in [155]

$$\sum_{i=1}^{L-1}\sum_{j>i}|y_i-y_j|\mathbf{T}_i\cdot\mathbf{T}_j = -\sum_{k=3}^{L-1}\mathbf{T}_{t_{k-2}}^2\Delta y_k, \tag{5.79}$$

where $\mathbf{T}_{t_i}$ is a quadratic Casimir operator for a given strut of the t-channel ladder and $\Delta y_k = y_k - y_{k+1}$ is the associated rapidity difference. Using these we can re-write equation (5.78) as

$$M_L^{(1)} = \frac{g_s^2\Gamma(1-\epsilon)}{4\pi^{2-\epsilon}}\frac{(\mu^2\Lambda_{UV}^2)^\epsilon}{2\epsilon}\left\{\sum_{k=3}^{L-1}\mathbf{T}_{t_{k-2}}^2\Delta y_k + i\pi\mathbf{T}_s^2+\sum_{i=1}^{L}C_i\left[\log\left(\frac{|k_{i\perp}|}{m}\right)-\frac{i\pi}{2}\right]\right\}. \tag{5.80}$$

We can exponentiate this one-loop function to obtain

$$\exp\left\{\frac{g_s^2\Gamma(1-\epsilon)}{4\pi^{2-\epsilon}}\frac{(\mu^2\Lambda_{UV}^2)^\epsilon}{2\epsilon}\left\{\sum_{k=3}^{L-1}\mathbf{T}^2_{t_{k-2}}\Delta y_k + i\pi\mathbf{T}_s^2 + \sum_{i=1}^{L}C_i\left[\log\left(\frac{|k_{i\perp}|}{m}\right)-\frac{i\pi}{2}\right]\right\}\right\}, \tag{5.81}$$

which will act to dress the L-point tree-level hard interaction. We see that this result contains an eikonal phase term corresponding to the production of s-channel bound states. The first term in the exponent is the Reggeization term, it is the leading high energy behaviour and corresponds to leading contributions in rapidity. The t-channel operators for each strut on the ladder will commute with each other (see [155]) such that this term shows that each strut on the ladder Reggeizes independently.

We will now consider the gravity case. Either through explicit calculation or using the previously indicated replacements of equation (5.46) we can find the exponentiated one-loop eikonal amplitude

$$\exp\left\{-\left(\frac{\kappa}{2}\right)^2\frac{\Gamma(1-\epsilon)}{4\pi^{2-\epsilon}}\frac{(\mu^2\overline{z}^2)^\epsilon}{2\epsilon}\left[\sum_{k=3}^{L-1}t_{k_2}\Delta y_k + i\pi s\right]\right\}, \tag{5.82}$$

where t_k is the squared momentum that is flowing through the k^{th} strut of the ladder. We see again that there is an eikonal phase term and a Reggeization term. The quadratic Casimir is now the squared momentum transfer in the strut and the Reggeization term acts to Reggeize each transferred graviton independently. Once again the Reggeization term is kinematically subleading to the eikonal phase term in the Regge limit by virtue of the quadratic Casimir being the momentum t of the exchanged particle.

It is likely to be the case in L-point scattering as it was for four that there will be added infra-red finite terms that are kinematically superleading in such a way as to affect the Reggeization of the graviton.

Chapter 6

Next-to-Soft gravity

We have investigated the soft limit of QCD and quantum gravity utilising the Wilson line technique. Now this work can be extended utilising the NE Feynman rules in the Wilson line approach given in equations (4.54) and (4.38) to investigate the external next-to-soft contributions to quantum gravity. Again we shall investigate QCD first and utilise it for comparison in the following quantum gravity calculation.

6.1 External contributions in QCD

The external next-to-soft diagrams will be constructed by considering the scattering processes depicted in figure (5.1) but with one of the external legs involved in the virtual exchange dressed with a next-to-eikonal Wilson line. The resulting diagram contributions will be of the form:

$$\begin{aligned}
\mathcal{M}_{NE1} &= (\mu^2)^\epsilon (ig_s)^2 \mathbf{T}_i \cdot \mathbf{T}_j \frac{i}{2} \int_0^\infty dt_i \int_0^\infty dt_j p_{j\mu} \frac{\partial}{\partial x_i^\nu} \left\langle A^\nu(x_i) A^\mu(x_j) \right\rangle , \\
&= -\frac{ig_s^2}{2} (\mu^2)^\epsilon \mathbf{T}_i \cdot \mathbf{T}_j \int_0^\infty dt_i \int_0^\infty dt_j p_{j\mu} \frac{\partial}{\partial x_i^\nu} D^{\mu\nu}(x_i - x_j), \\
\mathcal{M}_{NE2} &= (\mu^2)^\epsilon (ig_s)^2 \mathbf{T}_i \cdot \mathbf{T}_j \frac{i}{2} \int_0^\infty dt_i \int_0^\infty dt_j t_i p_{i\nu} p_{j\mu} \partial^2 \left\langle A^\nu(x_i) A^\mu(x_j) \right\rangle , \\
&= -\frac{ig_s^2}{2} (\mu^2)^\epsilon \mathbf{T}_i \cdot \mathbf{T}_j \int_0^\infty dt_i \int_0^\infty dt_j t_i p_{i\nu} p_{j\mu} \partial^2 D^{\mu\nu}(x_i - x_j),
\end{aligned} \tag{6.1}$$

where $x_i = p_i t_i$ or $x_i = p_i t_i + z$ and we have used the definition of the gluon propagator of equation (5.3). The derivatives of the propagator give

$$\begin{aligned}
\frac{\partial}{\partial x_i^\nu} D^{\mu\nu}(x_i - x_j) &= -\frac{(d-2)\Gamma(d/2-1)}{4\pi^{d/2}} (x_i - x_j)^\mu \left[-(x_i - x_j)^2 + i\varepsilon \right]^{-d/2} , \\
\partial^2 D^{\mu\nu}(x_i - x_j) &= \eta^{\mu\nu} \delta^{(d)}(x_i - x_j),
\end{aligned} \tag{6.2}$$

where the second result is due to it being a Green's function of the Klein-Gordon equation. We are using a non-zero impact vector separating the two Wilson lines and consequently $x_i \neq x_j$ at any point such that the second term will always be zero. We therefore must compute all such diagrams with integral definitions of the form $\mathcal{M}_{NE1}$ to develop all of the external contributions.

6.1.1 Master integral

We can now look to compute a master integral for the NE case applicable for all possible insertions of the NE Feynman rule. The integral we will compute is

$$\begin{aligned} V^\mu(\sigma_i p_i, \sigma_j p_j, z) =& \frac{\Gamma(d/2)}{2\pi^{d/2}} \int_0^\infty ds_i \int_0^\infty ds_j (s_i \sigma_i p_i + s_j \sigma_j p_j)^\mu \\ & \times \left[-(z + s_i \sigma_i p_i + s_j \sigma_j p_j)^2 + i\varepsilon \right]^{-d/2}, \\ =& \frac{\Gamma(d/2)}{2\pi^{d/2}} \int_0^\infty ds_i \int_0^\infty ds_j (s_i \sigma_i p_i + s_j \sigma_j p_j)^\mu \\ & \times \left[\overline{z}^2 - (s_i m_i)^2 - 2(s_i m_i)(s_j m_j)\sigma \cosh \gamma_{i,j} - (s_j m_j)^2 + i\varepsilon \right]^{-d/2}, \end{aligned} \tag{6.3}$$

where σ_k is a sign keeping track of whether line k is incoming (-1) or outgoing $(+1)$ and $\sigma = \sigma_i \sigma_j$. We can perform the re-parameterisations:

$$s_i = \frac{\sqrt{\overline{z}^2}}{m_i} st, \qquad s_j = \frac{\sqrt{\overline{z}^2}}{m_j} s, \tag{6.4}$$

and rescale ε by $(s^2+1)\overline{z}^2$ to give

$$\begin{aligned} =& \frac{\Gamma(d/2)}{2\pi^{d/2}} \frac{(\overline{z}^2)^{(3-d)/2}}{m_i m_j} \int_0^\infty dt \int_0^\infty ds s \left(st \sigma_i \frac{p_i^\mu}{m_i} + s \sigma_j \frac{p_j^\mu}{m_j} \right) \\ & \times \left[1 - s^2(t^2 + 2\sigma t \cosh \gamma_{i,j} + 1 - i\varepsilon) + i\varepsilon \right]^{-d/2}. \end{aligned} \tag{6.5}$$

There are two different integrals one proportional to p_i^μ and one proportional to p_j^μ. We shall firstly compute the one proportional to p_j^μ the integration for which we define as V_j:

$$\begin{aligned} V_j &= \int_0^\infty dt \int_0^\infty ds s^2 \left[1 - s^2(t^2 + 2\sigma t \cosh \gamma_{i,j} + 1 - i\varepsilon) + i\varepsilon \right]^{-d/2} \\ &= \sinh \gamma_{i,j} \int_{\sigma \coth \gamma_{i,j}}^\infty dx \int_0^\infty ds s^2 \left[1 - s^2 \sinh^2 \gamma_{i,j} (x^2 - 1 - i\epsilon) + i\varepsilon \right]^{-d/2}. \end{aligned} \tag{6.6}$$

To put the integral into the recognisable form of a hypergeometric function we perform the transformation of

$$s = \sqrt{\frac{u}{1-u}}, \qquad ds = \frac{1}{2}\sqrt{\frac{1}{u(1-u)^3}}. \tag{6.7}$$

This allows us to rewrite the s integral as:

$$\begin{aligned} I_u &= \frac{1}{2}\int_0^1 u^{1/2}(1-u)^{(d-5)/2}\left[1-u(1+\sinh^2\gamma_{i,j}(x^2-1-i\varepsilon))+i\varepsilon\right]^{-d/2}, \\ &= \frac{\Gamma(3/2)\Gamma((d-3)/2)}{2\Gamma(d/2)}\,{}_2F_1\left(\frac{d}{2},\frac{3}{2},\frac{d}{2},1+\sinh^2\gamma_{i,j}(x^2-1-i\varepsilon)\right), \\ &= \frac{\Gamma(3/2)\Gamma((d-3)/2)}{2\Gamma(d/2)}\left(-\sinh^2\gamma_{i,j}(x^2-1-i\varepsilon)\right)^{-3/2}. \end{aligned} \tag{6.8}$$

Inserting this result into equation (6.6) we obtain

$$V_j = \frac{\Gamma(3/2)\Gamma(d/2-3/2)}{2\Gamma(d/2)\sinh^2\gamma_{i,j}}\int_{\sigma\coth\gamma_{i,j}}^{\infty}\frac{dx}{(-x^2+1+i\varepsilon)^{3/2}}. \tag{6.9}$$

For $\sigma = 1$ we can take $\varepsilon \to 0$ and get

$$\begin{aligned} \int_{\coth\gamma_{i,j}}^{\infty}\frac{dx}{(-x^2+1+i\epsilon)^{3/2}} &= -i\frac{x}{\sqrt{x^2-1}}\Bigg|_{\coth\gamma_{i,j}}^{\infty} \\ &= i(\cosh\gamma_{i,j}-1). \end{aligned} \tag{6.10}$$

For $\sigma = -1$ the integration contour encounters the poles at $x = \pm\sqrt{1-i\varepsilon}$. We can split the integral into pieces to manage this

$$\int_{-\coth\gamma_{i,j}}^{\infty}\frac{dx}{(-x^2+1+i\epsilon)^{3/2}} = I_1+I_2+I_3+I_4+I_5, \tag{6.11}$$

where we have defined

$$\begin{aligned} I_1 &= \int_{-\coth\gamma_{i,j}}^{-1-\varepsilon}\frac{dx}{(1-x^2)^{3/2}} = -i\left(-\frac{1}{\sqrt{2\varepsilon}}+\cosh\gamma_{i,j}\right), \\ I_2 &= \int_{|x+1|=\varepsilon}\frac{dx}{[-(x-1-i\varepsilon)(x+1+i\varepsilon)]^{3/2}} = \int_{\pi}^{0}\frac{\varepsilon i e^{i\theta}d\theta}{(2\varepsilon e^{i\theta})^{3/2}} \\ &= \frac{-1}{\sqrt{2\varepsilon}}e^{-i\theta/2}\Big|_{\pi}^{0} = \frac{1}{\sqrt{2\epsilon}}(-i-1), \\ I_3 &= \int_{-1+\varepsilon}^{1-\varepsilon}\frac{dx}{(1-x)^{3/2}} = \frac{2}{\sqrt{2\varepsilon}}, \end{aligned}$$

$$
\begin{aligned}
I_4 &= \int_{|x-1|=\varepsilon} \frac{dx}{\left[-(x-1-i\varepsilon)(x+1+i\varepsilon)\right]^{3/2}} = \int_{\pi}^{2\pi} \frac{-\varepsilon i e^{i(\theta-\pi)d\theta}}{(2\varepsilon e^{i(\theta-\pi)})^{3/2}} \\
&= \frac{1}{\sqrt{2\epsilon}} e^{-i(\theta-\pi)/2}\Big|_{\pi}^{2\pi} = \frac{1}{\sqrt{2\epsilon}}\left(-i-1\right), \\
I_5 &= \int_{1+\varepsilon}^{\infty} \frac{dx}{(1-x^2)^{3/2}} = -i\left(1-\frac{1}{\sqrt{2\varepsilon}}\right),
\end{aligned} \tag{6.12}
$$

and worked to leading order in ε. The contour goes over the pole at $x=-1$ so in I_2 we use $x=-1+\varepsilon e^{i\theta}$. Similarly, it goes under the pole at $x=1$ so for I_4 we use $x=1-\varepsilon e^{i(\theta-\pi)}$. The sum over the integration parts is

$$
I_1+I_2+I_3+I_4+I_5 = i(-\cosh\gamma_{i,j}-1), \tag{6.13}
$$

thus we find that all divergent pieces cancel. The result for the integral is

$$
V_j = \frac{i\Gamma(3/2)\Gamma(d/2-3/2)}{2\Gamma(d/2)(1+\sigma\cosh\gamma_{i,j})}. \tag{6.14}
$$

6.1.2 V_i

Next we need to compute the integral proportional to p_i^{μ}, which we denote by:

$$
\begin{aligned}
V_i &= \int_0^{\infty} dt t \int_0^{\infty} ds s^2 \left[1-s^2(t^2+2\sigma t\cosh\gamma_{i,j}+1-i\varepsilon)+i\varepsilon\right]^{-d/2}, \\
&= \frac{\Gamma(3/2)\Gamma(d/2-3/2)}{2\Gamma(d/2)\sinh^2\gamma_{i,j}} \int_{\sigma\coth\gamma_{i,j}}^{\infty} dx \frac{(x\sinh\gamma_{i,j}-\sigma\cosh\gamma_{i,j})}{(-x^2+1+i\varepsilon)^{3/2}},
\end{aligned} \tag{6.15}
$$

where the computation follows the same procedure as for V_j. For $\sigma=1$ we have

$$
\begin{aligned}
\int_{\coth\gamma_{i,j}}^{\infty} dx \frac{x}{(-x^2+1+i\varepsilon)^{3/2}} &= i\int_{\coth\gamma_{i,j}}^{\infty} dx \frac{x}{(x^2-1)^{3/2}} \\
&= \frac{i}{(x^2-1)^{1/2}}\Big|_{\coth\gamma_{i,j}}^{\infty} = i\sinh\gamma_{i,j}.
\end{aligned} \tag{6.16}
$$

For $\sigma=-1$ we can follow the same procedure of splitting the integration into parts as for equation (6.11), the result is

$$
\int_{-\coth\gamma_{i,j}}^{\infty} dx \frac{x}{(-x^2+1+i\varepsilon)^{3/2}} = i\sinh\gamma_{i,j}, \tag{6.17}
$$

again we find all divergent pieces cancel. The result for V_i is now

$$V_i = \frac{i\Gamma(3/2)\Gamma(d/2-3/2)}{2\Gamma(d/2)\sinh^2\gamma_{i,j}}\left[(i\sinh\gamma_{i,j})\sinh\gamma_{i,j} - i(\sigma\cosh\gamma_{i,j}-1)\sigma\cosh\gamma_{i,j}\right],$$
$$= \frac{\Gamma(3/2)\Gamma(d/2-3/2)}{2\Gamma(d/2)(1+\sigma\cosh\gamma_{i,j})}. \tag{6.18}$$

From this calculation we see that $V_i = V_j$. This is the expected result as can be seen from considering equation (6.3) which is symmetric under interchange of $i \leftrightarrow j$. We can now insert the result above into equation (6.3) to obtain the result for the master integral

$$V^\mu(\sigma_i p_i, \sigma_j p_j, z) = \frac{i\Gamma(3/2)\Gamma((d-3)/2)}{4\pi^{d/2}}\frac{(\overline{z}^2)^{(3-d)/2}}{m_i m_j}\left(\frac{p_i^\mu}{m_i}+\frac{p_j^\mu}{m_j}\right)\frac{1}{1+\sigma\cosh\gamma_{i,j}}. \tag{6.19}$$

6.1.3 Vertex correction master integral

We will also need to consider the case of the vertex correction where the emission and absorption of the soft gluon occurs between two lines not separated by the physical impact parameter. Starting from the same integral as before but with $z \to 0$

$$V(\sigma_i p_i, \sigma_j p_j, 0) = \frac{\Gamma(d/2)}{2\pi^{d/2}}\int_0^\infty ds_i \int_0^\infty ds_j (s_i p_i\cdot p_j + s_j\sigma p_j^2) \times \left[-(s_i\sigma_i p_i + s_j\sigma_j p_j)^2 + i\varepsilon\right]^{-d/2}. \tag{6.20}$$

Performing the re-parameterisations:

$$s_i = \frac{s}{m_i}, \qquad s_j = \frac{st}{m_j}, \tag{6.21}$$

puts the integral in the form

$$V(\sigma_i p_i, \sigma_j p_j, 0) = \frac{\Gamma(d/2)}{2\pi^{d/2}}\frac{1}{m_i m_j}\int_0^\infty dt\int_0^\infty ds s\left(s\frac{p_i\cdot p_j}{m_i}+st\sigma\frac{p_j^2}{m_j}\right) \times\left[-s^2(t^2+1+2\sigma t\cosh(\gamma_{i,j}))+i\varepsilon\right]^{\epsilon-2},$$
$$= \frac{\Gamma(d/2)}{2\pi^{d/2}}\frac{1}{m_i}\int_0^\infty ds s^{2\epsilon-2}\int_0^\infty dt\,(\cosh(\gamma_{i,j})+\sigma t) \times\left[-(t^2+1+2\sigma t\cosh(\gamma_{i,j}))+i\varepsilon\right]^{\epsilon-2}. \tag{6.22}$$

The s integral contains the cancellation between the spurious UV and IR divegences this time in $d=3$ or equivalently $\epsilon = 1/2$. We can introduce a short distance cut off to regulate the UV divergence, doing so will introduce logarithms of the regulator in the final result as in the soft case of the previous chapter. We therefore use $\sqrt{\overline{z}^2}$ for the

same reasons as discussed in the previous chapter allowing us to perform the s integral,

$$\int_{\sqrt{\overline{z}^2}}^{\infty} ds s^{2\epsilon-2} = -\frac{(\overline{z}^2)^\epsilon}{(2\epsilon-1)\sqrt{\overline{z}^2}}. \tag{6.23}$$

We can insert this into equation (6.22) and complete the square in t:

$$\begin{aligned} V(\sigma_i p_i, \sigma_j p_j, 0) =& -\frac{\Gamma(d/2)}{2\pi^{d/2}} \frac{(\overline{z}^2)^\epsilon}{(2\epsilon-1)\sqrt{\overline{z}^2}} \frac{1}{m_i} \int_0^\infty dt \left(\cosh(\gamma_{i,j}) + \sigma t\right) \\ & \times \left[-((t+\sigma\cosh(\gamma_{i,j}))^2 - \cosh^2(\gamma_{i,j}) + 1) + i\varepsilon\right]^{\epsilon-2}, \\ =& -\frac{\Gamma(d/2)}{2\pi^{d/2}} \frac{(\overline{z}^2)^\epsilon}{(2\epsilon-1)\sqrt{\overline{z}^2}} \frac{1}{m_i} \int_0^\infty dt \left(\cosh(\gamma_{i,j}) + \sigma t\right) \\ & \times \left[-(t+\sigma\cosh(\gamma_{i,j}))^2 + \sinh^2(\gamma_{i,j}) + i\varepsilon\right]^{\epsilon-2}. \end{aligned} \tag{6.24}$$

Rescale $t = x\sinh(\gamma_{i,j}) - \sigma\cosh(\gamma_{i,j})$ gives the integral:

$$\begin{aligned} V(\sigma_i p_i, \sigma_j p_j, 0) =& -\frac{\Gamma(d/2)}{2\pi^{d/2}} \frac{(\overline{z}^2)^\epsilon}{(2\epsilon-1)\sqrt{\overline{z}^2}} \frac{1}{m_i} \int_{\sigma\coth(\gamma_{i,j})}^\infty dx \left(\sigma x \sinh^2(\gamma_{i,j})\right) \\ & \times \left[-(x\sinh(\gamma_{i,j}))^2 + \sinh^2(\gamma_{i,j}) + i\varepsilon\right]^{\epsilon-2}, \\ =& -\frac{\Gamma(d/2)}{2\pi^{d/2}} \frac{(\overline{z}^2)^\epsilon}{(2\epsilon-1)\sqrt{\overline{z}^2}} \frac{1}{m_i} \frac{\sigma}{\sinh^2(\gamma_{i,j})} \\ & \times \int_{\sigma\coth(\gamma_{i,j})}^\infty dx \frac{x}{\left[-x^2+1+i\varepsilon\right]^2}. \end{aligned} \tag{6.25}$$

For $\sigma = 1$, true for all vertex correction diagrams, we can send $\varepsilon \to 0$ to obtain

$$\begin{aligned} \int_{\sigma\coth(\gamma_{i,j})}^\infty dx \frac{x}{\left[-x^2+1+i\varepsilon\right]^2} &= \frac{-1}{2(x^2-1)}\Big|_{\coth(\gamma_{i,j})}^\infty \\ &= \frac{\sinh^2(\gamma_{i,j})}{2}. \end{aligned} \tag{6.26}$$

Inserting the result into equation (6.25) gives the master integral as

$$\begin{aligned} V(\sigma_i p_i, \sigma_j p_j, 0) &= -\frac{\Gamma(d/2)}{4\pi^{d/2}} \frac{(\overline{z}^2)^\epsilon}{(2\epsilon-1)\sqrt{\overline{z}^2}} \frac{1}{m_i}, \\ &= \frac{\Gamma(2-\epsilon)}{4\pi^{2-\epsilon}} \frac{(\overline{z}^2)^\epsilon}{(1-2\epsilon)\sqrt{\overline{z}^2}} \frac{1}{m_i}. \end{aligned} \tag{6.27}$$

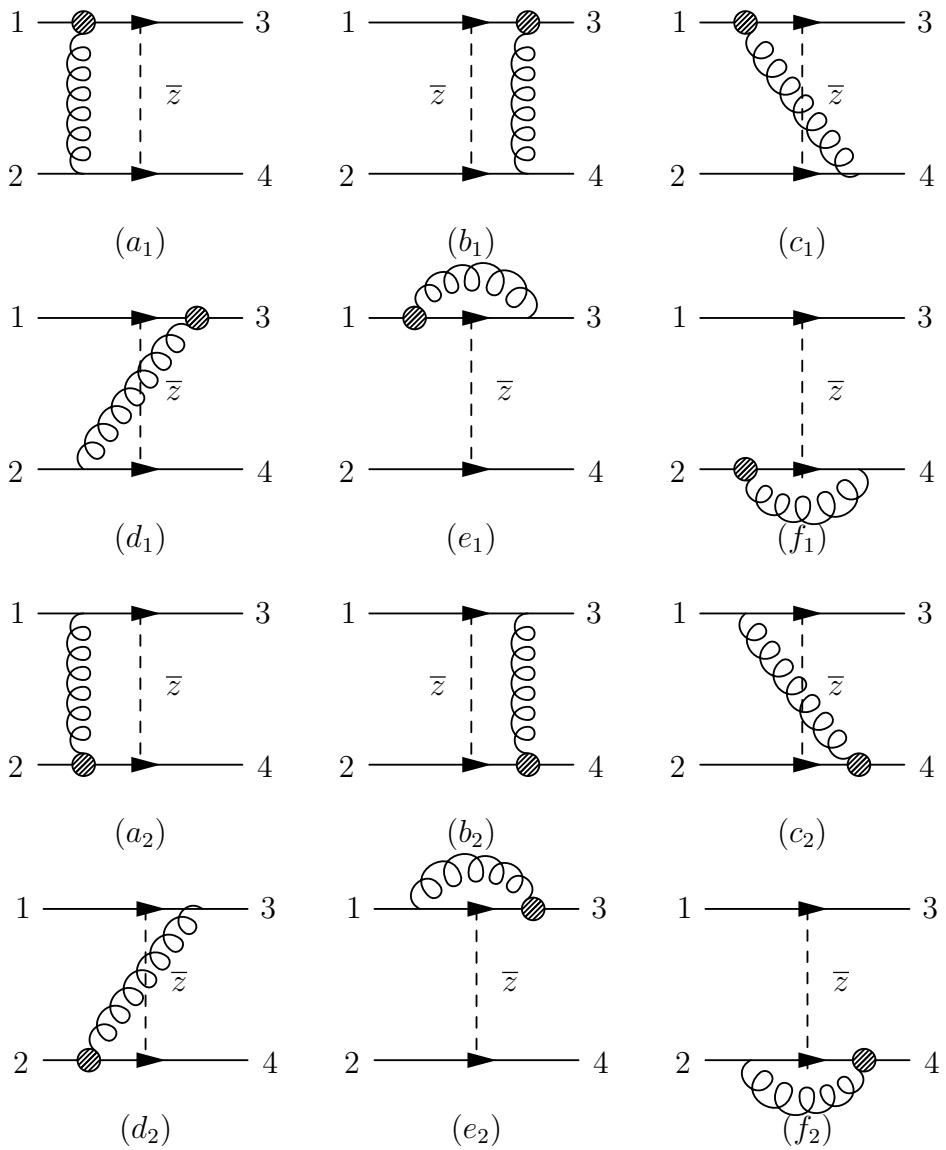

Figure 6.1: Feynman diagrams arising at one-loop order for the calculation of NE (external) next-to-soft amplitudes in QCD. The blob vertex represents the NE vertex and the other gluonic vertex is eikonal.

6.1.4 Sum over diagrams

We have now calculated master integrals for the purposes of computing all the external emission contributions. Using these the integrals associated with the diagrams shown in figure (6.1) can be written as:

$$\mathcal{M}_{a_1} = \frac{ig_s^2}{2}(\mu^2)^\epsilon \mathbf{T}_1 \cdot \mathbf{T}_2 V(-p_1, p_2, z),$$
$$\mathcal{M}_{b_1} = \frac{ig_s^2}{2}(\mu^2)^\epsilon \mathbf{T}_3 \cdot \mathbf{T}_4 V(p_3, -p_4, z),$$

$$
\begin{aligned}
\mathcal{M}_{c_1} &= \frac{ig_s^2}{2}(\mu^2)^\epsilon \mathbf{T}_1 \cdot \mathbf{T}_4 V(-p_1, -p_4, z),\\
\mathcal{M}_{d_1} &= \frac{ig_s^2}{2}(\mu^2)^\epsilon \mathbf{T}_3 \cdot \mathbf{T}_2 V(p_3, p_2, z),\\
\mathcal{M}_{e_1} &= \frac{ig_s^2}{2}(\mu^2)^\epsilon \mathbf{T}_1 \cdot \mathbf{T}_3 V(-p_1, -p_3, 0),\\
\mathcal{M}_{f_1} &= \frac{ig_s^2}{2}(\mu^2)^\epsilon \mathbf{T}_2 \cdot \mathbf{T}_4 V(-p_2, -p_4, 0),\\
\mathcal{M}_{a_2} &= \frac{ig_s^2}{2}(\mu^2)^\epsilon \mathbf{T}_1 \cdot \mathbf{T}_2 V(-p_2, p_1, z),\\
\mathcal{M}_{b_2} &= \frac{ig_s^2}{2}(\mu^2)^\epsilon \mathbf{T}_3 \cdot \mathbf{T}_4 V(p_4, -p_3, z),\\
\mathcal{M}_{c_2} &= \frac{ig_s^2}{2}(\mu^2)^\epsilon \mathbf{T}_1 \cdot \mathbf{T}_4 V(p_4, p_1, z),\\
\mathcal{M}_{d_2} &= \frac{ig_s^2}{2}(\mu^2)^\epsilon \mathbf{T}_3 \cdot \mathbf{T}_2 V(-p_2, -p_3, z),\\
\mathcal{M}_{e_2} &= \frac{ig_s^2}{2}(\mu^2)^\epsilon \mathbf{T}_1 \cdot \mathbf{T}_3 V(p_3, p_1, 0),\\
\mathcal{M}_{f_2} &= \frac{ig_s^2}{2}(\mu^2)^\epsilon \mathbf{T}_2 \cdot \mathbf{T}_4 V(p_4, p_2, 0).
\end{aligned}
\tag{6.28}
$$

For clarity we introduce the combined pre-factor:

$$
\overline{C}(\mu, \epsilon, \overline{z}) = \frac{-g_s^2}{2} \frac{\Gamma\left(\frac{1-2\epsilon}{2}\right)}{8\pi^{(3-2\epsilon)/2}} \frac{(\mu^2 \overline{z}^2)^\epsilon}{\sqrt{\overline{z}^2}}. \tag{6.29}
$$

The sum over the two possible insertions for diagrams $(a) \to (d)$ gives

$$
\begin{aligned}
\sum_{i=1}^{2} \sum_{\alpha \in a,b,c,d} \mathcal{M}_{\alpha_i} =& \overline{C}(\mu, \epsilon, \overline{z}) \left[-\mathbf{T}_1 \cdot \mathbf{T}_2 \left(\frac{1}{m_1} + \frac{1}{m_2} \right) - \mathbf{T}_3 \cdot \mathbf{T}_4 \left(\frac{1}{m_3} + \frac{1}{m_4} \right) + \right.\\
&\left. + \mathbf{T}_1 \cdot \mathbf{T}_4 \left(\frac{1}{m_1} + \frac{1}{m_4} \right) + \mathbf{T}_2 \cdot \mathbf{T}_3 \left(\frac{1}{m_2} + \frac{1}{m_3} \right) \right].
\end{aligned}
\tag{6.30}
$$

We can use the fact that $m_1 = m_3$, $m_2 = m_4$ and the color operators of equation (5.26) to write this as

$$
\sum_{i=1}^{2} \sum_{\alpha \in a,b,c,d} \mathcal{M}_{\alpha_i} = \overline{C}(\mu, \epsilon, \overline{z}) \left(\frac{1}{m_1} + \frac{1}{m_2} \right) \mathbf{T}_t^2. \tag{6.31}
$$

Similarly we can define another pre-factor for the vertex correction diagrams

$$
\tilde{C}(\mu, \epsilon, \overline{z}) = \frac{-g_s^2}{2} \frac{\Gamma(2-\epsilon)}{4\pi^{2-\epsilon}} \frac{(\mu^2 \overline{z}^2)^\epsilon}{\sqrt{\overline{z}^2}} + \mathcal{O}(\epsilon). \tag{6.32}
$$

The sum of the two insertions for both diagrams (e) and (f) therefore gives

$$\begin{aligned}\sum_{i=1}^{2}\sum_{\alpha\in e,f}\mathcal{M}_{\alpha_i} =&\tilde{C}(\mu,\epsilon,\overline{z})\left[\mathbf{T}_1\cdot\mathbf{T}_3\left(\frac{1}{m_1}+\frac{1}{m_3}\right)+\mathbf{T}_2\cdot\mathbf{T}_4\left(\frac{1}{m_2}+\frac{1}{m_4}\right)\right],\\ =&2\tilde{C}(\mu,\epsilon,\overline{z})\left[\mathbf{T}_1\cdot\mathbf{T}_3\frac{1}{m_1}+\mathbf{T}_2\cdot\mathbf{T}_4\frac{1}{m_2}\right],\\ =&\tilde{C}(\mu,\epsilon,\overline{z})\left[\mathbf{T}_t^2\left(\frac{1}{m_1}+\frac{1}{m_2}\right)-\frac{2C_1}{m_1}-\frac{2C_2}{m_2}\right].\end{aligned}\tag{6.33}$$

The result for the amplitude is proportional to $1/m_i$ for $i=1,2$ which prevents taking the massless limit of the incoming particles. The interpretation of this requires comparison with the eikonal result. If we consider the eikonal result with diagrams (e) and (f) removed we have terms proportional to $\log(s/m_1m_2)$ as appear in equation (5.28) differing from our previous result where they were $\log(s/-t)$. At eikonal level we see that there is a logarithmic divergence associated with $m_i\to 0$ in $d=4$. From our earlier discussion of spurious cancellation of UV and IR poles we can see that the NE result of equation (6.31) is divergent in $d=3$. The mass divergence for the NE result is powerlike in $d=4$ however in $d=3$ it is logarithmic. Terms logarithmically divergent in the mass are due to collinear singularities so we can therefore interpret the mass divergence in equation (6.31) as being due to the virtual next-to-soft gluon being collinear with one of the external lines.

It is worth noting that the choice of UV regulator being $\sqrt{\overline{z}^2}$ in diagrams (e) and (f) in the eikonal case allowed us to shift the mass divergence from the Regge trajectory term into the color diagonal terms in the amplitude. The choice of regulator was such as to compare with massless results, the diagrams contain scaleless integrals if unregulated and consequently are zero in dimensional regularisation. The choice of how to include the graphs (e) and (f) comes down to a choice of regularisation scheme. This scheme dependence is a well-known ambiguity as to whether the mass singularities should be absorbed into the Regge trajectory or into the *impact factor* of the external line as discussed in [153].

We can exponentiate this one loop result to gain all order resummation as demonstrated in [34]. The result of exponentiating the diagrams $(a)\to(f)$ and combining with the eikonal result gives

$$\begin{aligned}\mathcal{A}_{E+NE}=\exp\Bigg\{\frac{g_s^2}{8\pi^{2-\epsilon}}(\mu^2\overline{z}^2)^\epsilon\Bigg[\frac{\Gamma(1-\epsilon)}{\epsilon}\Bigg(i\pi\mathbf{T}_s^2+\log\left(-\frac{s}{t}\right)\mathbf{T}_t^2-\frac{i\pi}{2}\sum_{i=1}^{4}C_i\\ +\log\left(-\frac{t}{m_1^2}\right)C_1^2+\log\left(-\frac{t}{m_2^2}\right)C_2^2\Bigg)-\end{aligned}$$

$$-\frac{\pi}{2\sqrt{\bar{z}^2}}\left(\frac{1}{m_1}+\frac{1}{m_2}\right)\mathbf{T}_t^2-\frac{1}{\sqrt{\bar{z}^2}}\left(\mathbf{T}_t^2\left(\frac{1}{m_1}+\frac{1}{m_2}\right)-\frac{2C_1}{m_1}-\frac{2C_2}{m_2}\right)\Bigg]\Bigg\}. \tag{6.34}$$

We see that the NE external additions contribute to the gluon Reggeization term proportional to $\mathbf{T}_t^2$. The absence of an imaginary term means there is no contribution to the eikonal phase factor from these NE additions.

6.2 External contributions in quantum gravity

Having computed the external corrections in the path integral formulation for QCD we will now go on to examine gravity utilising the calculation from QCD. The NE gravity Feynman rules one must consider are obtained from equation(4.54) and are restated here

$$\begin{aligned} NE_{g1} &= \frac{\kappa}{4}p_{j(\mu}\partial_{\rho)}\left(\kappa h^{\rho\mu}+\frac{\kappa}{2}h^{\alpha}{}_{\alpha}\eta^{\rho\mu}\right), \\ NE_{g2} &= \frac{\kappa}{4}tp_{j\mu}p_{j\nu}\partial^2 h^{\mu\nu}. \end{aligned} \tag{6.35}$$

As for QCD we know that the propagator for the graviton is a Green's function of the Klein-Gordon equation therefore $NE_{g2}=0$. The first term can be rewritten as

$$NE_{g1}=\frac{\kappa}{4}p_{j\mu}\partial_{\rho}\left(\eta^{\rho\alpha}\eta^{\mu\beta}+\eta^{\rho\beta}\eta^{\mu\alpha}-\eta^{\alpha\beta}\eta^{\rho\mu}\right)h_{\alpha\beta}, \tag{6.36}$$

where $h^{\alpha\beta}$ is symmetric in its indices. The diagrams to be computed are the same as for QCD except with the exchanged object being the graviton. The contribution from a general diagram where the graviton is exchanged between legs i and j can be written as

$$\begin{aligned} \mathcal{M}_{NEg1} =& -\frac{i}{2}\left(\frac{\kappa}{2}\right)^2(\mu^2)^{\epsilon}p_i^{\mu}p_i^{\nu}p_{j\sigma}\left(\eta^{\rho\alpha}\eta^{\mu\beta}+\eta^{\rho\beta}\eta^{\mu\alpha}-\eta^{\alpha\beta}\eta^{\rho\mu}\right) \\ &\times\int_0^{\infty}ds_i\int_0^{\infty}ds_j\frac{\partial}{\partial x_j^{\rho}}\left\langle h_{\mu\nu}(x_i)h_{\alpha\beta}(x_j)\right\rangle. \end{aligned} \tag{6.37}$$

We can insert the graviton propagator used previously from equation (5.41)

$$\begin{aligned} \mathcal{M}_{NEg1} =& -\frac{i}{2}\left(\frac{\kappa}{2}\right)^2(\mu^2)^{\epsilon}p_i^{\mu}p_i^{\nu}p_{j\sigma}\left(\eta^{\rho\alpha}\eta^{\mu\beta}+\eta^{\rho\beta}\eta^{\mu\alpha}-\eta^{\alpha\beta}\eta^{\rho\mu}\right)P_{\mu\nu\alpha\beta} \\ &\times\int_0^{\infty}ds_i\int_0^{\infty}ds_j\frac{\Gamma(d/2-1)}{4\pi^{d/2}}\frac{\partial}{\partial x_j^{\rho}}\left[-(x_i-x_j)^2+i\varepsilon\right]^{1-d/2}. \end{aligned} \tag{6.38}$$

Using $x_i = s_i p_i + z$ and $x_j = s_j p_j$ this integration can be recognised as being the same as that from the QCD case given in equation (6.3) such the result for a general diagram is now

$$\mathcal{M}_{NEg1} = -\frac{i}{2}\left(\frac{\kappa}{2}\right)^2 (\mu^2)^\epsilon p_i^\mu p_i^\nu p_{j\sigma} \left(\eta^{\rho\alpha}\eta^{\mu\beta} + \eta^{\rho\beta}\eta^{\mu\alpha} - \eta^{\alpha\beta}\eta^{\rho\mu}\right) P_{\mu\nu\alpha\beta} \times V_\rho(\sigma_i p_i, \sigma_j p_j, z). \tag{6.39}$$

We can also recognise that this diagram could be constructed by using the replacements of equation (5.45) in the QCD result of equation (6.1) multiplied by an overall factor of 2. This factor of 2 is consistent with the double copy [53–55] and arises from combinatorics. It is due to the numerator in the gravitational integrals being constructed from combining two copies of a gauge theory numerator. If we consider expanding a gauge theory numerator in the virtual soft momentum we have

$$N_{gauge} = N^{(0)}_{gauge} + N^{(1)}_{gauge} + \mathcal{O}(k^2), \tag{6.40}$$

where (0) and (1) correspond to leading and next-to-leading in soft momentum terms respectively. Gravity numerators in the double copy are constructed from two insertions of these such that

$$N_{grav} = N^2_{gauge} = {N^{(0)}_{gauge}}^2 + 2N^{(0)}_{gauge}N^{(1)}_{gauge} + \mathcal{O}(k^2). \tag{6.41}$$

We see that the factor of two arises in the term of $\mathcal{O}(k)$. We can therefore use this observation with the replacements of equation (5.46) to immediately write the exponentiated 1-loop amplitude for the external next-to-soft contribution to quantum gravity using equations (6.31) and (6.33) as

$$\mathcal{M}_{g(a\to f)} = -\left(\frac{\kappa}{2}\right)^2 \frac{1}{4\pi^{(2-\epsilon)}} \frac{(\mu^2\overline{z}^2)^\epsilon}{\sqrt{\overline{z}^2}} t \left(\frac{1}{m_1} + \frac{1}{m_2}\right) \left[\Gamma\left(\frac{1-2\epsilon}{2}\right)\Gamma\left(\frac{3}{2}\right) + \Gamma(2-\epsilon)\right]. \tag{6.42}$$

We see that the result in gravity gives a term proportional to $\frac{t}{m_{1,2}}$ which means this is a contribution to the Regge trajectory term from the soft analysis. This is the same conclusion as was reached for the external next-to-soft contributions in QCD but as discussed in chapter 5, the Regge trajectory is kinematically subleading with respect to the eikonal phase term in quantum gravity. Recent studies into the next-to-soft contributions to quantum gravity neglected these contributions [156]. In that work they considered large masses therefore it is justified to do so, as they are doubly suppressed in the Regge limit.

Chapter 7

Conclusions

The work of this thesis has been to demonstrate a correct treatment of all contributions to next-to-soft enhancements to scattering cross sections. Using the language of Feynman diagrams we have fully captured all added contributions to scattering amplitudes that need to be calculated and where necessary shown the calculations. A next-to-soft treatment of scattering will give information into the behaviour of theories in the infra-red limit beyond just examining the poles, this is particularly interesting for the theory of quantum gravity due to the infra-red limit being that observed on large, astronomical scales allowing insights into phenomena such as black holes. This can be demonstrated graphically in figure (7.1) produced in the work of Giddings [126] discussing the gravitational S-matrix. The figure indicates that the next-to-soft analysis extends into the regions of phase space adjacent to black hole physics. The issues of unitarity that arise when considering black hole evaporation and the existence of a gravitational S-matrix will require next-to-soft analysis of quantum gravity. Therefore the work produced in developing next-to-soft formalisms and techniques for quantum gravity in this thesis will help to guide work in these fields.

In chapter two we detailed that through a modification of the LBKDD theorem one can construct a generalised formalism for computing all Abelian like NLP logarithms contributing at NNLO in the Drell-Yan electroweak annihilation cross section. This process was selected for two reason: firstly, the real-virtual gluon contributions test all terms in the formalism; secondly, there is an absence of final state jets when compared to DIS and other processes. This builds upon previous work of [157] which considered the contributions of double real emission contributions through extending the soft expansion to next-to-soft level. The formalism is written in terms of familiar components from soft-collinear factorisation but with the additional inclusion of a radiative jet contribution first defined in [37] but here computed to NLO. The computation of the radiative jet function was performed using light like reference vectors

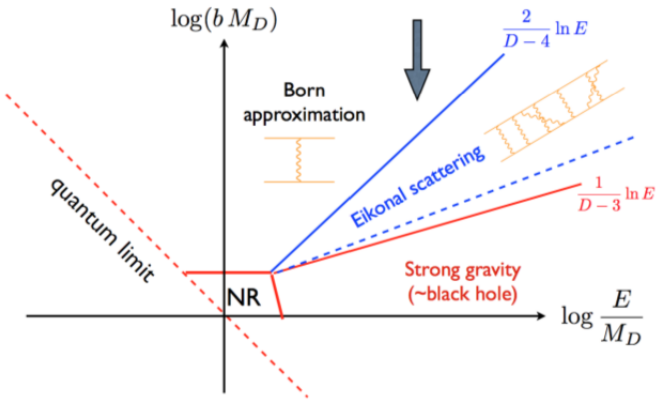

Figure 7.1: A plot of the impact parameter and interaction energy phase space to indicate the regions of physics probed by the next-to-soft extensions in quantum gravity. The next-to-soft region is the area between the dashed eikonal line and the solid strong gravity line.

$n_i^2 = 0$ which leads to a much simplified expression for the general NLP formalism. It is demonstrated that doing so introduces no double counting of poles or other issues due to the simple renormalisation properties of equation (2.74).

This method can be extended to other scattering processes that arise in collider physics that are gluon-initiated. A necessary extension of this work will be to generalise the technique for abelian like terms to the full non-abelian case which will have immediate applications to Higgs production via gluon fusion. The application of this formalism to inclusive cross sections for Higgs production will be of clear use for currently interesting phenomenological calculations. In order to accomplish this a fully systematic treatment of the factorisation of the multi-gluon phase space will be required. An important line of future work will be to see which components of this formalism are amenable to all order resummation techniques to go beyond NNLO in the perturbative expansion. As well as the reproduction of the logarithmically enhanced terms at NNLO the formalism correctly reproduced the constant term in the infra-red finite part giving evidence that the formalism will be applicable at higher, non divergent orders. The resummation of next-to-soft effects will lead to increased accuracy in theoretical predictions of scattering cross sections in collider physics this has been examined from an effective theory (SCET) point of view in [158]. In the future it would be useful for the formalism to be applied to final state jets to extend the applicability of the formalism to more processes relevant to collider physics.

The formalism constructed has correctly disentangled hard-collinear and soft divergent effects at NLP level. This has created a simple recipe by which to fully reproduce all NLP logarithms in scattering processes such that in the future one will not need to be concerned with lost or double counted contributions at this level. The general

nature of the work should also be useful when considering what parts of it exponentiate or can other-wise be itteratively resummed to gain all order information on NLP effects.

The generality of the formalism constructed gave it applicability to other theories and in this thesis attention was turned to quantum gravity. In chapter three we demonstrated a leading order soft calculation in quantum gravity using techniques familiar from QCD, that of Wilson lines applicable in the Regge limit. This treatment is very natural due to its position space formalism being very intuitive to interpret for gravitational scattering. To demonstrate the technique, clarify similarities between quantum gravity and QCD and to show the ease with which it is applied to quantum gravity we performed the calculation in QCD too.

The Wilson line technique first utilised in the Regge limit of gauge theories is a natural way of describing transplanckian gravitational scattering. This approach to gravitational scattering naturally makes manifest the term which Reggeizes the t-channel exchanged object even if it is sub-leading in the strict Regge limit. In QCD the Reggeization term is the dominant contribution to the amplitude in the Regge limit superleading over the eikonal phase term. In quantum gravity the exchanged object is the graviton and it was demonstrated using this formalism that the graviton does Reggeize. It was shown that in the Regge limit the amplitude for the t-channel exchange of a graviton has terms kinematically superleading over the Reggeization term. The leading term is that of the eikonal phase. It was also demonstrated that non-logarithmic terms arising in $\mathcal{N} = 4, 5, 6, 8$ supergravity can also be of the same order as the Reggeization term. This clarification of the nature of the Reggeization of the graviton made manifest by the Wilson line formalism is a demonstration of the potential insight one can gain by the application of gauge theory techniques to quantum gravity. The difference in the kinematically leading nature of the Regge term is due to the interchange of color factors from QCD for kinematic factors in quantum gravity given in equation (5.46). Multi-Reggeon exchange for both QCD and gravity was also demonstrated again showing that the Reggeization term is subleading to the eikonal phase term in quantum gravity. This clarification of the Reggiezation behaviour of gravitons gives evidence that the approach of using the Wilson line decription of eikonal scattering can give insight into expected features in quantum gravity that have been lost by previous approaches to the eikonal limit. Reggiezation phenomena occuring in quantum gravity is another example of similarities between the theories of quantum gravity and QCD and it is an example of how one can hope to gain insight into quantum gravity by using QCD technologies.

Beyond leading order in perturbation theory cross-talk occurs between the Reggeization and eikonal phase terms and in QCD there will arise added terms from perturbative

contributions to the exponent of the soft function. The soft function is known to be one-loop exact in (super-)gravity [78, 82, 131, 132] and in the strict Regge limit we see that the contribution arises just from the eikonal phase term. By computing the Regge-limit of the logarithm of the known two loop amplitudes in $\mathcal{N} = 4, 5, 6, 8$ supergravity it is possible to find any correction terms to the result obtained from exponentiating the one-loop result, testing one loop exactness. We know that the eikonal phase term is of $\mathcal{O}(s^2)$ and we have shown that the Reggeization term is of $\mathcal{O}(t^2)$ owing to its lack of contribution in the Regge limit. We find correction terms are $\mathcal{O}(st)$ and therefore in the strict Regge limit vanish with respect to the eikonal phase term, demonstrating the validity of one loop exactness at this two loop order. Further study into whether this holds for the interesting case of $\mathcal{N} = 4$ supergravity at three-loops and beyond requires the evaluation of the contributing non-planar integrals. Further study into the higher loop levels of supergravity in the Regge limit would be a natural extension of this work and may shed light onto issues of black hole formation and unitarity in quantum gravity.

The combination of these areas of work into creating a full treatment of next-to-soft contributions in quantum gravity is the next area of work to be completed. The method detailed in chapter 2 where the extended version of the LBKDD theorem was constructed for gauge theory amplitudes should reproduce all NLP logarithms in the scattering cross sections. The first thing to complete is to clarify and compute all relevant Feynman diagrams. It has been explained how contributions can be split into internal and external contributions and chapter 6 has outlined how to calculate the external corrections in QCD and quantum gravity. It has been demonstrated that the external emission contributions at next-to-soft level give color (kinematically) suppressed contributions to the Reggeization term found in the soft limit of QCD (gravity). Such results were found to be divergent in the limit of massless emitting particle due to the virtual boson becoming collinear with an external line. The next task will be to compute the internal emission contributions that will involve computations of the seagull and 3-graviton vertex graphs. Combining these results should then give a full treatment of next-to-soft effects free of constraints on the masses of the emitters. It will then be possible to take limits of the masses to try and make connection with previous results obtained for next-to-soft quantum gravity calculations such as those of [156]. This will both test our formalism and demonstrate it's capacity to examine such scenarios as test particle scattering in the region of black holes.

Appendix A

Appendix

A.1 Expansion of metric determinant

It has been necessary to use the expanded form of the metric determinant. The method by which we have done so for the work in this thesis is detailed below

$$
\begin{aligned}
(-|g|))^{1/2} &= -\exp\left(\frac{1}{2}\ln(|g|)\right), \\
&= -\exp\left(\frac{1}{2}\,\mathrm{Tr}(\ln(g))\right), \\
&= -\exp\left(\frac{1}{2}\,\mathrm{Tr}(\ln(\eta^{\mu\nu}+\kappa h^{\mu\nu}))\right), \\
&= (-|\eta^{\mu\nu}|)^{1/2}\exp\left(\frac{1}{2}\,\mathrm{Tr}(\ln(1+\kappa\eta_{\mu\nu}h^{\mu\nu}))\right), \\
&= \exp\left(\frac{1}{2}(\kappa\eta_{\mu\nu}h^{\mu\nu}-(\kappa\eta_{\mu\nu})h^{\mu\nu})^2\frac{1}{2}+\wr(\kappa^3h^3)\right), \\
&= 1+\frac{1}{2}\,\mathrm{Tr}\left(\kappa\eta_{\mu\nu}h^{\mu\nu}-(\kappa\eta_{\mu\nu}h^{\mu\nu})^2\frac{1}{2}\right)+\frac{1}{8}(\mathrm{Tr}(\kappa\eta_{\mu\nu}h^{\mu\nu}))^2+\mathcal{O}((\kappa h)^3), \\
&= 1+\frac{1}{2}\kappa h^{\mu}{}_{\mu}-\frac{1}{4}\kappa^2 h_{\mu}{}^{\nu}h_{\nu}{}^{\mu}+\frac{1}{8}\kappa^2(h^{\mu}{}_{\mu})^2, \\
&= 1+\frac{\kappa}{2}h^{\alpha}{}_{\alpha}+\frac{\kappa^2}{2}\left[\frac{(h^{\alpha}{}_{\alpha})^2}{4}-\frac{h^{\alpha\beta}h_{\alpha\beta}}{2}\right]+\mathcal{O}(k^3h^3). \qquad \text{(A.1)}
\end{aligned}
$$

A.2 Integral techniques

Some useful integral techniques and the definitions used for the thesis calculations are detailed below.

A.2.1 Feynman parameters

Feynman parameters have been used for computing integrals throughout the thesis. The general implementation of this that has been used is:

$$\frac{1}{D_1^{\alpha_1}...D_n^{\alpha_n}} = \frac{\Gamma(\alpha_1+...+\alpha_n)}{\Gamma(\alpha_1)...\Gamma(\alpha_n)}\int_0^1 dx_1..\int_0^1 dx_n \frac{\delta(\sum_{k=1}^n \alpha_k - 1)x_1^{\alpha_1-1}...x_n^{\alpha_n-1}}{(x_1D_1+...+x_nD_n)^{\sum_{k=1}^n \alpha_k}}. \quad (A.2)$$

A.2.2 Schwinger parameter

A useful trick for performing loop momentum integrals is the Schwinger parameter, it can be shown that

$$\frac{i}{A} = \int_0^\infty ds \exp(isA). \quad (A.3)$$

Performing derivatives with respect to A one arrives at the all order form

$$\left(\frac{i}{A}\right)^n = \int_0^\infty ds \frac{s^{n-1}}{\Gamma(n)} \exp(isA). \quad (A.4)$$

A.2.3 Gaussian integrals

The use of d dimensional Gaussian integrals is ubiquitous throughout this work and included are those with pre-factors that are linear, quadratic and higher orders in the integration variable. Those that have odd integer powers in the pre-factor are necessarily zero due to the symmetry of the exponential term and of the integration limits. Even powers can be tackled using parameter differentiation, i.e.

$$\begin{aligned} I_g =& \int dx (x^2)^n \exp(-\alpha x^2), \\ =&(-1)^n \frac{\partial^n}{\partial(\alpha)^n}\int dx \exp(-\alpha x^2), \\ =&(-1)^n \frac{\partial^n}{\partial(\alpha)^n}\sqrt{\frac{\pi}{\alpha}}, \\ =&\frac{\Gamma(n+1/2)}{\Gamma(1/2)}\alpha^{-n}\sqrt{\frac{\pi}{\alpha}}. \end{aligned} \quad (A.5)$$

The d-dimensional generalisation of this is

$$I_{gn} = -\left(\frac{\pi}{\alpha}\right)^{d/2}\frac{\Gamma(n+d/2)}{\Gamma(d/2)}\alpha^{-n}. \quad (A.6)$$

A.2.4 Quadratic numerator identity

I shall derive here the integration identity utilised in computing the quadratic numerator term in the one-loop radiative jet function calculation. Consider the starting

point

$$\int d^d k \frac{\partial}{\partial k^\mu} \frac{k^\nu}{(k^2 - m^2)^n} = 0$$
$$= \int d^d k \frac{\eta^{\mu\nu}}{(k^2 - m^2)^n} - 2n \frac{k^\nu k^\mu}{(k^2 - m^2)^{n+1}}. \tag{A.7}$$

Giving the identity

$$\frac{\eta^{\mu\nu}}{2n} \int d^d k \frac{1}{(k^2 - m^2)^n} = \int d^d k \frac{k^\nu k^\mu}{(k^2 - m^2)^{n+1}} \tag{A.8}$$

A.2.5 Plus distribution

The plus distribution function is used in equation (2.67). When convoluted with a smooth test function the plus distribution acts such that

$$\int_0^1 dz D_+(z) F(z) = \int_0^1 dz D(z) \left[F(z) - F(1) \right]. \tag{A.9}$$

The purpose of the plus distribution function in equation (2.67) is to overcome the divergent nature of the function $D_n(z)$ at $z = 1$ when integrating over the threshold parameter space ($z \in [0, 1]$).

Bibliography

[1] D. Bonocore et al. "A factorization approach to next-to-leading-power threshold logarithms". In: *JHEP 1506 (2015) 008* (2015). arXiv: 1503.05156 [hep-ph].

[2] S. Melville et al. "Wilson line approach to gravity in the high energy limit". In: *Phys.Rev. D89 (2014) no.2, 025009* (2014). arXiv: 1306.6019 [hep-th].

[3] A. Luna et al. *Next-to-soft corrections to high energy scattering in QCD and gravity*. Pre Print November 2016.

[4] A. Nordsieck and F. Bloch. "Note on the Radiation Field of the Electron". In: *Phys. Rev. 52, 54* (1937).

[5] T. Kinoshita. "Mass Singularities of Feynman Amplitudes". In: *J. Math. Phys. 3, 650* (1962).

[6] T.D. Lee and M. Nauenberg. "Degenerate Systems and Mass Singularities". In: *Phys. Rev. 133, B1549* (1964).

[7] N. Nakanishi. "General Theory of Infrared Divergence". In: *Prog. Theor. Phys. (1958) 19 (2): 159-168.* (1958).

[8] J.G.M. Gatheral. "Exponentiation of eikonal cross sections in nonabelian gauge theories". In: *Phys.Lett.* B133 (1983), p. 90. DOI: 10.1016/0370-2693(83)90112-0.

[9] J. Frenkel and J.C. Taylor. "Nonabelian eikonal exponentiation". In: *Nucl.Phys.* B246 (1984), p. 231. DOI: 10.1016/0550-3213(84)90294-3.

[10] George Sterman. "Infrared divergences in perturbative QCD". In: *AIP Conference Proceedings* 74.1 (1981), pp. 22–40. DOI: http://dx.doi.org/10.1063/1.33099. URL: http://scitation.aip.org/content/aip/proceeding/aipcp/10.1063/1.33099.

[11] Alexander Mitov, George Sterman, and Ilmo Sung. "Diagrammatic Exponentiation for Products of Wilson Lines". In: *Phys.Rev.* D82 (2010), p. 096010. DOI: 10.1103/PhysRevD.82.096010. arXiv: 1008.0099 [hep-ph].

[12] A. A. Vladimirov. "Generating function for web diagrams". In: *Phys. Rev. D* 90 (6 2014), p. 066007. DOI: 10.1103/PhysRevD.90.066007. arXiv: 1406.6253 [hep-th]. URL: http://link.aps.org/doi/10.1103/PhysRevD.90.066007.

[13] A. A. Vladimirov. *Exponentiation for products of Wilson lines within the generating function approach*. 2015. arXiv: 1501.03316 [hep-th].

[14] Einan Gardi et al. "Webs in multiparton scattering using the replica trick". In: *JHEP* 1011 (2010), p. 155. DOI: 10.1007/JHEP11(2010)155. arXiv: 1008.0098 [hep-ph].

[15] Einan Gardi and Chris D. White. "General properties of multiparton webs: Proofs from combinatorics". In: *JHEP* 1103 (2011), p. 079. DOI: 10.1007/JHEP03(2011)079. arXiv: 1102.0756 [hep-ph].

[16] Einan Gardi, Jennifer M. Smillie, and Chris D. White. *The Non-Abelian Exponentiation theorem for multiple Wilson lines*. 2013. arXiv: 1304.7040 [hep-ph].

[17] Einan Gardi, Jennifer M. Smillie, and Chris D. White. "On the renormalization of multiparton webs". In: *JHEP* 1109 (2011), p. 114. DOI: 10.1007/JHEP09(2011)114. arXiv: 1108.1357 [hep-ph].

[18] Mark Dukes et al. *Web worlds, web-colouring matrices, and web-mixing matrices*. 2013. arXiv: 1301.6576 [math.CO].

[19] Einan Gardi. "From webs to polylogarithms". In: *Journal of High Energy Physics* 2014.4 (2014), pp. 1–65. ISSN: 1029-8479. DOI: 10.1007/JHEP04(2014)044. arXiv: 1310.5268 [hep-ph]. URL: http://dx.doi.org/10.1007/JHEP04(2014)044.

[20] Giulio Falcioni et al. "Multiple gluon exchange webs". In: *Journal of High Energy Physics* 2014.10 (2014), pp. 1–63. ISSN: 1029-8479. DOI: 10.1007/JHEP10(2014)010. arXiv: 1407.3477 [hep-ph]. URL: http://dx.doi.org/10.1007/JHEP10(2014)010.

[21] C D White. "An introduction to webs". In: *Journal of Physics G: Nuclear and Particle Physics* 43.3 (2016), p. 033002. arXiv: 1507.02167 [hep-ph]. URL: http://stacks.iop.org/0954-3899/43/i=3/a=033002.

[22] J.C. Collins. "Sudakov form-factors". In: *Adv.Ser.Direct.High Energy Phys. 5 (1989) 573614* (1989). arXiv: 0312336 [hep-ph].

[23] Lance J. Dixon, Lorenzo Magnea, and George F. Sterman. "Universal structure of subleading infrared poles in gauge theory amplitudes". In: *JHEP* 0808 (2008), p. 022. DOI: 10.1088/1126-6708/2008/08/022. arXiv: 0805.3515 [hep-ph].

[24] G. Sterman. "Summation of large corrections to short distance hadronic cross-sections". In: *Nucl. Phys. B281 (1987) 310* (1987).

[25] S. Catani and L. Trentadue. "Resummation of the QCD Perturbative Series for Hard Processes". In: *Nucl. Phys. B327 (1989) 323* (1989).

[26] H. Contopanagos, E. Laenen, and G. Sterman. "Sudakov factorization and resummation". In: *Nucl. Phys. B484 (1997) 303330* (1997). arXiv: 9604313 [hep-ph].

[27] G.P. Korchemsky and G. Marchesini. "Structure function for large x and renormalization of Wilson loop". In: *Nucl.Phys.* B406 (1993), pp. 225–258. DOI: 10.1016/0550-3213(93)90167-N. arXiv: hep-ph/9210281 [hep-ph].

[28] G.P. Korchemsky and G. Marchesini. "Resummation of large infrared corrections using Wilson loops". In: *Phys. Lett. B313 (1993) 433440* (1993).

[29] S. Forte and G. Ridolfi. "Renormalization group approach to soft gluon resummation". In: *Nucl. Phys. B650 (2003) 229270* (2003). arXiv: 0209154 [hep-ph].

[30] T. Becher and M. Neubert. "Threshold resummation in momentum space from effective field theory". In: *Phys. Rev. Lett. 97 (2006) 082001* (2006). arXiv: 0605050 [hep-ph].

[31] M.D. Schwartz. "Resummation and NLO matching of event shapes with effective field theory". In: *Phys.Rev. D77 (2008) 014026* (2008). arXiv: 0709.2709 [hep-ph].

[32] C.W. Bauer et al. "Factorization of e+e- Event Shape Distributions with Hadronic Final States in Soft Collinear Effective Theory". In: *Phys.Rev. D78 (2008) 034027* (2008). arXiv: 0801.4569 [hep-ph].

[33] Jui-yu Chiu et al. "Factorization Structure of Gauge Theory Amplitudes and Application to Hard Scattering Processes at the LHC". In: *Phys.Rev.* D80 (2009), p. 094013. DOI: 10.1103/PhysRevD.80.094013. arXiv: 0909.0012 [hep-ph].

[34] Eric Laenen, Gerben Stavenga, and Chris D. White. "Path integral approach to eikonal and next-to-eikonal exponentiation". In: *JHEP* 0903 (2009), p. 054. DOI: 10.1088/1126-6708/2009/03/054. arXiv: 0811.2067 [hep-ph].

[35] Einan Gardi and Lorenzo Magnea. "Factorization constraints for soft anomalous dimensions in QCD scattering amplitudes". In: *JHEP* 0903 (2009), p. 079. DOI: 10.1088/1126-6708/2009/03/079. arXiv: 0901.1091 [hep-ph].

[36] Einan Gardi and Lorenzo Magnea. "Infrared singularities in QCD amplitudes". In: *Nuovo Cim.* 032C (2009), pp. 137–157. DOI: 10.1393/ncc/i2010-10528-x. arXiv: 0908.3273 [hep-ph].

[37] V. Del Duca. "High-energy bremsstrahlung theorems for soft photons". In: *Nucl. Phys. B345 (1990) 369388* (1990).

[38] M. Kramer, E. Laenen, and M. Spira. "Soft gluon radiation in Higgs boson production at the LHC". In: *Nucl. Phys. B511 (1998) 523549* (1998). arXiv: 9611272 [hep-ph].

[39] R.V. Harlander and W.B. Kilgore. "Soft and virtual corrections to pp H + X at NNLO". In: *Phys. Rev. D64 (2001) 013015* (2001). arXiv: 0102241 [hep-ph].

[40] R.V. Harlander and W.B. Kilgore. "Next-to-next-to-leading order higgs production at hadron colliders". In: *Phys. Rev. Lett. 88 (2002) 201801* (2002). arXiv: 0201206 [hep-ph].

[41] S. Catani, D. de Florian, and M. Grazzini. "Higgs production in hadron collisions: Soft and virtual QCD corrections at NNLO". In: *JHEP 0105 (2001) 025* (2001). arXiv: 0102227 [hep-ph].

[42] S. Catani et al. "Soft-gluon resummation for Higgs boson production at hadron colliders". In: *JHEP 0307 (2003) 028* (2003). arXiv: 0306211 [hep-ph].

[43] F. Herzog and B. Mistlberger. "The Soft-Virtual Higgs Cross-section at N^3LO and the Convergence of the Threshold Expansion". In: *Proceedings of Moriond QCD 2014* (2014). arXiv: 1405.5685 [hep-ph].

[44] F.E. Low. "Bremsstrahlung of very low-energy quanta in elementary particle collisions". In: *Phys. Rev. 110 (1958) 974977* (1958).

[45] T.H. Burnett and N.M. Kroll. "Extension of the low soft photon theorem". In: *Phys. Rev. Lett. 20 (1968) 86* (1968).

[46] Jr. Grammer G. and D.R. Yennie. "Improved treatment for the infrared divergence problem in quantum electrodynamics". In: *Phys.Rev.* D8 (1973), pp. 4332–4344. DOI: 10.1103/PhysRevD.8.4332.

[47] E. Laenen et al. "Next-to-eikonal corrections to soft gluon radiation: a diagrammatic approach". In: *JHEP 1101 (2011) 141* (2011). arXiv: 1010.1860 [hep-ph].

[48] C. Anastasiou et al. "Real-virtual contributions to the inclusive Higgs cross-section at N^3LO". In: *JHEP 1312 (2013) 088* (2013). arXiv: 1311.1425 [hep-ph].

[49] R. Hamberg, W.L. van Neerven, and T. Matsuura. "A complete calculation of the order s2 correction to the Drell-Yan K-factor". In: *Nuclear Physics B* 359.2 (1991), pp. 343 –405. ISSN: 0550-3213. DOI: http://dx.doi.org/10.1016/0550-3213(91)90064-5. URL: http://www.sciencedirect.com/science/article/pii/0550321391900645.

[50] D. Bonocore et al. "The method od regions and next-to-soft corrections in Drell-Yan production". In: *Phys.Lett. B742 (2015) 375-382* (2015). arXiv: 1410.6406 [hep-ph].

[51] D.B. Kaplan, M.J. Savage, and M.B. Wise. "A New Expansion for the Nucleon-Nucleon Interactions". In: *Phys.Lett. B424 (1998) 390-396* (1998). arXiv: 9801034 [nucl-th].

[52] G. Sterman. *An introduction to quantum field theory.* Cambridge University Press, 1993.

[53] Zvi Bern, John Joseph M. Carrasco, and Henrik Johansson. "Perturbative Quantum Gravity as a Double Copy of Gauge Theory". In: *Phys.Rev.Lett.* 105 (2010), p. 061602. DOI: 10.1103/PhysRevLett.105.061602. arXiv: 1004.0476 [hep-th].

[54] Zvi Bern et al. "Gravity as the Square of Gauge Theory". In: *Phys.Rev.* D82 (2010), p. 065003. DOI: 10.1103/PhysRevD.82.065003. arXiv: 1004.0693 [hep-th].

[55] Z. Bern, J.J.M. Carrasco, and Henrik Johansson. "New Relations for Gauge-Theory Amplitudes". In: *Phys.Rev.* D78 (2008), p. 085011. DOI: 10.1103/PhysRevD.78.085011. arXiv: 0805.3993 [hep-ph].

[56] Freddy Cachazo, Song He, and Ellis Ye Yuan. "Scattering of Massless Particles in Arbitrary Dimensions". In: *Phys. Rev. Lett.* 113 (17 2014), p. 171601. DOI: 10.1103/PhysRevLett.113.171601. URL: http://link.aps.org/doi/10.1103/PhysRevLett.113.171601.

[57] Freddy Cachazo, Song He, and Ellis Ye Yuan. "Scattering of massless particles: scalars, gluons and gravitons". In: *Journal of High Energy Physics* 2014.7 (2014), pp. 1–33. ISSN: 1029-8479. DOI: 10.1007/JHEP07(2014)033. URL: http://dx.doi.org/10.1007/JHEP07(2014)033.

[58] Andrew Strominger. "On BMS invariance of gravitational scattering". In: *Journal of High Energy Physics* 2014.7 (2014), pp. 1–20. ISSN: 1029-8479. DOI: 10.1007/JHEP07(2014)152. URL: http://dx.doi.org/10.1007/JHEP07(2014)152.

[59] Temple He et al. "BMS supertranslations and Weinberg's soft graviton theorem". In: *Journal of High Energy Physics* 2015.5 (2015), pp. 1–17. ISSN: 1029-8479. DOI: 10.1007/JHEP05(2015)151. URL: http://dx.doi.org/10.1007/JHEP05(2015)151.

[60] Freddy Cachazo and Andrew Strominger. *Evidence for a New Soft Graviton Theorem.* arXiv: 1404.4091 [hep-th].

[61] Eduardo Casali. "Soft sub-leading divergences in Yang-Mills amplitudes". In: *Journal of High Energy Physics* 2014.8 (2014), pp. 1–5. ISSN: 1029-8479. DOI: 10.1007/JHEP08(2014)077. URL: http://dx.doi.org/10.1007/JHEP08(2014)077.

[62] Burkhard U. W. Schwab and Anastasia Volovich. "Subleading Soft Theorem in Arbitrary Dimensions from Scattering Equations". In: *Phys. Rev. Lett.* 113 (10 2014), p. 101601. DOI: 10.1103/PhysRevLett.113.101601. URL: http://link.aps.org/doi/10.1103/PhysRevLett.113.101601.

[63] Zvi Bern, Scott Davies, and Josh Nohle. "On loop corrections to subleading soft behavior of gluons and gravitons". In: *Phys. Rev. D* 90 (8 2014), p. 085015. DOI: 10.1103/PhysRevD.90.085015. URL: http://link.aps.org/doi/10.1103/PhysRevD.90.085015.

[64] Song He, Yu-tin Huang, and Congkao Wen. "Loop corrections to soft theorems in gauge theories and gravity". In: *Journal of High Energy Physics* 2014.12 (2014), pp. 1–21. ISSN: 1029-8479. DOI: 10.1007/JHEP12(2014)115. URL: http://dx.doi.org/10.1007/JHEP12(2014)115.

[65] Andrew J. Larkoski. "Conformal invariance of the subleading soft theorem in gauge theory". In: *Phys. Rev. D* 90 (8 2014), p. 087701. DOI: 10.1103/PhysRevD.90.087701. URL: http://link.aps.org/doi/10.1103/PhysRevD.90.087701.

[66] Freddy Cachazo and E. Y. Yuan. *Are Soft Theorems Renormalized?* arXiv: 1405.3413 [hep-th].

[67] Nima Afkhami-Jeddi. *Soft Graviton Theorem in Arbitrary Dimensions.* arXiv: 1405.3533 [hep-th].

[68] Tim Adamo, Eduardo Casali, and David Skinner. "Perturbative gravity at null infinity". In: *Classical and Quantum Gravity* 31.22 (2014), p. 225008. URL: http://stacks.iop.org/0264-9381/31/i=22/a=225008.

[69] Massimo Bianchi et al. "More on soft theorems: Trees, loops, and strings". In: *Phys. Rev. D* 92 (6 2015), p. 065022. DOI: 10.1103/PhysRevD.92.065022. URL: http://link.aps.org/doi/10.1103/PhysRevD.92.065022.

[70] Zvi Bern et al. "Low-energy behavior of gluons and gravitons from gauge invariance". In: *Phys. Rev. D* 90 (8 2014), p. 084035. DOI: 10.1103/PhysRevD.90.084035. URL: http://link.aps.org/doi/10.1103/PhysRevD.90.084035.

[71] Johannes Broedel et al. "Constraining subleading soft gluon and graviton theorems". In: *Phys. Rev. D* 90 (6 2014), p. 065024. DOI: 10.1103/PhysRevD.90.065024. URL: http://link.aps.org/doi/10.1103/PhysRevD.90.065024.

[72] Temple He et al. "New symmetries of massless QED". In: *Journal of High Energy Physics* 2014.10 (2014), pp. 1–17. ISSN: 1029-8479. DOI: 10.1007/JHEP10(2014)112. URL: http://dx.doi.org/10.1007/JHEP10(2014)112.

[73] Michael Zlotnikov. "Sub-sub-leading soft-graviton theorem in arbitrary dimension". In: *Journal of High Energy Physics* 2014.10 (2014), pp. 1–20. ISSN: 1029-8479. DOI: 10.1007/JHEP10(2014)148. URL: http://dx.doi.org/10.1007/JHEP10(2014)148.

[74] Chrysostomos Kalousios and Francisco Rojas. "Next to subleading soft-graviton theorem in arbitrary dimensions". In: *Journal of High Energy Physics* 2015.1 (2015), pp. 1–16. ISSN: 1029-8479. DOI: 10.1007/JHEP01(2015)107. URL: http://dx.doi.org/10.1007/JHEP01(2015)107.

[75] Yi-Jian Du et al. "Note on soft graviton theorem by KLT relation". In: *Journal of High Energy Physics* 2014.11 (2014), pp. 1–25. ISSN: 1029-8479. DOI: 10.1007/JHEP11(2014)090. URL: http://dx.doi.org/10.1007/JHEP11(2014)090.

[76] Hui Luo, Pierpaolo Mastrolia, and William J. Torres Bobadilla. "Subleading soft behavior of QCD amplitudes". In: *Phys. Rev. D* 91 (6 2015), p. 065018. DOI: 10.1103/PhysRevD.91.065018. URL: http://link.aps.org/doi/10.1103/PhysRevD.91.065018.

[77] C.D. White. "Diagrammatic insights into next-to-soft corrections". In: *Physics Letters B* 737 (2014), pp. 216 –222. ISSN: 0370-2693. DOI: http://dx.doi.org/10.1016/j.physletb.2014.08.041. URL: http://www.sciencedirect.com/science/article/pii/S037026931400608X.

[78] Ratindranath Akhoury, Ryo Saotome, and George Sterman. "Collinear and Soft Divergences in Perturbative Quantum Gravity". In: *Phys.Rev.* D84 (2011), p. 104040. DOI: 10.1103/PhysRevD.84.104040. arXiv: 1109.0270 [hep-th].

[79] M.J. Strassler. "Field theory without Feynman diagrams: One loop effective actions". In: *Nucl.Phys. B385 145-184* (1992). arXiv: 9205205 [hep-ph].

[80] Michael G. Sotiropoulos and George F. Sterman. "Color exchange in near forward hard elastic scattering". In: *Nucl.Phys.* B419 (1994), pp. 59–76. DOI: 10.1016/0550-3213(94)90357-3. arXiv: hep-ph/9310279 [hep-ph].

[81] J.W. van Holten. "Propagators and path integrals". In: *Nucl.Phys. B457 375-407* (1995). arXiv: 9508136 [hep-th].

[82] Chris D. White. "Factorization Properties of Soft Graviton Amplitudes". In: *JHEP* 1105 (2011), p. 060. DOI: 10.1007/JHEP05(2011)060. arXiv: 1103.2981 [hep-th].

[83] J.R. Forshaw and D.A. Ross. *Quantum Chromodynamics and the Pomeron.* Cambridge Univeristy Press, 1997.

[84] I.A. Korchemskaya and G.P. Korchemsky. "High-energy scattering in QCD and cross singularities of Wilson loops". In: *Nucl.Phys.* B437 (1995), pp. 127–162. DOI: 10.1016/0550-3213(94)00553-Q. arXiv: hep-ph/9409446 [hep-ph].

[85] I. A. Korchemskaya and G. P. Korchemsky. "Evolution equation for gluon Regge trajectory". In: *Phys. Lett.* B387 (1996), pp. 346–354. DOI: 10.1016/0370-2693(96)01016-7. arXiv: hep-ph/9607229.

[86] P. D. B. Collins, ed. *An Introduction to Regge Theory and High-Energy Physics*. Cambridge University Press, 1977.

[87] R. J. Eden et al., eds. *The Analytic S-Matrix*. Cambridge University Press, 2002.

[88] V. N. Gribov, ed. *The Theory of Complex Angular Momenta: Gribov Lectures on Theoretical Physics*. Cambridge University Press, 2003.

[89] S. Mandelstam. "Non-Regge Terms in the Vector-Spinor Theory". In: *Phys. Rev.* 137 (1965), B949–B954. DOI: 10.1103/PhysRev.137.B949.

[90] Ernest Abers and Vigdor L. Teplitz. "Kinematic Constraints, Crossing, and the Reggeization of Scattering Amplitudes". In: *Phys. Rev.* 158 (1967), pp. 1365–1376. DOI: 10.1103/PhysRev.158.1365.

[91] B. M. McCoy and Tai Tsun Wu. "Theory of Fermion Exchange in Massive Quantum Electrodynamics at High-Energy. 6. Summation of Diagrams". In: *Phys. Rev.* D13 (1976), pp. 508–512. DOI: 10.1103/PhysRevD.13.508.

[92] G. V. Frolov, V. N. Gribov, and L. N. Lipatov. "On Regge poles in quantum electrodynamics". In: *Phys. Lett.* B31 (1970), p. 34. DOI: 10.1016/0370-2693(70)90013-4.

[93] G. V. Frolov, V. N. Gribov, and L. N. Lipatov. "The leading singularity in the j plane in quantum electrodynamics". In: *Sov. J. Nucl. Phys.* 12 (1971), p. 543.

[94] Hung Cheng and Tai Tsun Wu. "High-energy collision processes in quantum electrodynamics. I". In: *Phys. Rev.* 182 (1969), pp. 1852–1867. DOI: 10.1103/PhysRev.182.1852.

[95] I. I. Balitsky, L. N. Lipatov, and Victor S. Fadin, eds. *Regge Processes in Nonabelian Gauge Theories. (IN RUSSIAN)*. In *Leningrad 1979, Proceedings, Physics Of Elementary Particles*, Leningrad 1979, 109-149. 1979.

[96] A. V. Bogdan and V. S. Fadin. "A proof of the reggeized form of amplitudes with quark exchanges". In: *Nucl. Phys.* B740 (2006), pp. 36–57. DOI: 10.1016/j.nuclphysb.2006.01.033. arXiv: hep-ph/0601117.

[97] Lawrence Tyburski. "Reggeization of the Fermion-Fermion Scattering Amplitude in Nonabelian Gauge Theories". In: *Phys. Rev.* D13 (1976), p. 1107. DOI: 10.1103/PhysRevD.13.1107.

[98] L. N. Lipatov. "Reggeization of the Vector Meson and the Vacuum Singularity in Nonabelian Gauge Theories". In: *Sov. J. Nucl. Phys.* 23 (1976), pp. 338–345.

[99] A. L. Mason. "Radiation Gauge Calculation of High-Energy Scattering Amplitudes". In: *Nucl. Phys.* B120 (1977), p. 275. DOI: 10.1016/0550-3213(77)90044-X.

[100] Hung Cheng and C. Y. Lo. "High-Energy Amplitudes of Yang-Mills Theory in Arbitrary Perturbative Orders. 1". In: *Phys. Rev.* D15 (1977), p. 2959. DOI: 10.1103/PhysRevD.15.2959.

[101] Victor S. Fadin, E. A. Kuraev, and L. N. Lipatov. "On the Pomeranchuk Singularity in Asymptotically Free Theories". In: *Phys. Lett.* B60 (1975), pp. 50–52. DOI: 10.1016/0370-2693(75)90524-9.

[102] E. A. Kuraev, L. N. Lipatov, and Victor S. Fadin. "The Pomeranchuk Singularity in Nonabelian Gauge Theories". In: *Sov. Phys. JETP* 45 (1977), pp. 199–204.

[103] E. A. Kuraev, L. N. Lipatov, and Victor S. Fadin. "Multi-Reggeon Processes in the Yang-Mills Theory". In: *Sov. Phys. JETP* 44 (1976), pp. 443–450.

[104] A. L. Mason. "Factorization and Hence Reggeization in Yang-Mills Theories". In: *Nucl. Phys.* B117 (1976), p. 493. DOI: 10.1016/0550-3213(76)90411-9.

[105] Ashoke Sen. "Asymptotic Behavior of the Wide Angle On-Shell Quark Scattering Amplitudes in Nonabelian Gauge Theories". In: *Phys. Rev.* D28 (1983), p. 860. DOI: 10.1103/PhysRevD.28.860.

[106] Victor S. Fadin and V. E. Sherman. "Processes Involving Fermion Exchange in Nonabelian Gauge Theories". In: *Zh. Eksp. Teor. Fiz.* 72 (1977), pp. 1640–1658.

[107] Victor S. Fadin, M. I. Kotsky, and R. Fiore. "Gluon Reggeization in QCD in the next-to-leading order". In: *Phys. Lett.* B359 (1995), pp. 181–188. DOI: 10.1016/0370-2693(95)01016-J.

[108] Victor S. Fadin, R. Fiore, and M. I. Kotsky. "Gribov's theorem on soft emission and the Reggeon-Reggeon- gluon vertex at small transverse momentum". In: *Phys. Lett.* B389 (1996), pp. 737–741. DOI: 10.1016/S0370-2693(96)01331-7. arXiv: hep-ph/9608229.

[109] Victor S. Fadin, R. Fiore, and A. Quartarolo. "Reggeization of quark quark scattering amplitude in QCD". In: *Phys. Rev.* D53 (1996), pp. 2729–2741. DOI: 10.1103/PhysRevD.53.2729. arXiv: hep-ph/9506432.

[110] J. Blumlein, V. Ravindran, and W. L. van Neerven. "On the gluon Regge trajectory in O(alpha(s)**2)". In: *Phys. Rev.* D58 (1998), p. 091502. DOI: 10.1103/PhysRevD.58.091502. arXiv: hep-ph/9806357.

[111] Vittorio Del Duca and E. W. Nigel Glover. "The high energy limit of QCD at two loops". In: *JHEP* 10 (2001), p. 035. arXiv: hep-ph/0109028.

[112] A. V. Bogdan et al. "The quark Regge trajectory at two loops". In: *JHEP* 03 (2002), p. 032. arXiv: hep-ph/0201240.

[113] V. S. Fadin et al. "Proof of the multi-Regge form of QCD amplitudes with gluon exchanges in the NLA". In: *Phys. Lett.* B639 (2006), pp. 74–81. DOI: 10.1016/j.physletb.2006.03.031. arXiv: hep-ph/0602006.

[114] L.N. Lipatov. *Multi - Regge Processes in Gravitation*. 1982.

[115] L.N. Lipatov. "Graviton Reggeization". In: *Phys.Lett.* B116 (1982), pp. 411–413. DOI: 10.1016/0370-2693(82)90156-3.

[116] Howard J. Schnitzer. *Reggeization of N=8 supergravity and N=4 Yang-Mills theory.* 2007. arXiv: hep-th/0701217 [hep-th].

[117] H. Kawai, D.C. Lewellen, and S.H.H. Tye. "A Relation Between Tree Amplitudes of Closed and Open Strings". In: *Nucl.Phys.* B269 (1986), p. 1. DOI: 10.1016/0550-3213(86)90362-7.

[118] G.P. Korchemsky, J.M. Drummond, and E. Sokatchev. "Conformal properties of four-gluon planar amplitudes and Wilson loops". In: *Nucl.Phys.* B795 (2008), pp. 385–408. DOI: 10.1016/j.nuclphysb.2007.11.041. arXiv: 0707.0243 [hep-th].

[119] Stephen G. Naculich and Howard J. Schnitzer. "Regge behavior of gluon scattering amplitudes in N=4 SYM theory". In: *Nucl.Phys.* B794 (2008), pp. 189–194. DOI: 10.1016/j.nuclphysb.2007.10.026. arXiv: 0708.3069 [hep-th].

[120] Stephen G. Naculich and Howard J. Schnitzer. "IR divergences and Regge limits of subleading-color contributions to the four-gluon amplitude in N=4 SYM Theory". In: *JHEP* 0910 (2009), p. 048. DOI: 10.1088/1126-6708/2009/10/048. arXiv: 0907.1895 [hep-th].

[121] Vittorio Del Duca and E. W. N. Glover. "Testing high-energy factorization beyond the next-to- leading-logarithmic accuracy". In: *JHEP* 05 (2008), p. 056. DOI: 10.1088/1126-6708/2008/05/056. arXiv: 0802.4445.

[122] Howard J. Schnitzer. *Reggeization of N=8 Supergravity and N=4 Yang-Mills theory. II.* 2007. arXiv: 0706.0917 [hep-th].

[123] Johannes M. Henn et al. "More loops and legs in Higgs-regulated N=4 SYM amplitudes". In: *JHEP* 1008 (2010), p. 002. DOI: 10.1007/JHEP08(2010)002. arXiv: 1004.5381 [hep-th].

[124] Johannes M. Henn et al. "Higgs-regularized three-loop four-gluon amplitude in N=4 SYM: exponentiation and Regge limits". In: *JHEP* 1004 (2010), p. 038. DOI: 10.1007/JHEP04(2010)038. arXiv: 1001.1358 [hep-th].

[125] Steven B. Giddings and Rafael A. Porto. "The Gravitational S-matrix". In: *Phys.Rev.* D81 (2010), p. 025002. DOI: 10.1103/PhysRevD.81.025002. arXiv: 0908.0004 [hep-th].

[126] Steven B. Giddings. *The gravitational S-matrix: Erice lectures.* 2011. arXiv: 1105.2036 [hep-th].

[127] Jochen Bartels, Lev N. Lipatov, and Agustin Sabio Vera. *Double-logarithms in Einstein-Hilbert gravity and supergravity.* 2012. arXiv: 1208.3423 [hep-th].

[128] Steven B. Giddings, Maximilian Schmidt-Sommerfeld, and Jeppe R. Andersen. "High energy scattering in gravity and supergravity". In: *Phys.Rev.* D82 (2010), p. 104022. DOI: 10.1103/PhysRevD.82.104022. arXiv: 1005.5408 [hep-th].

[129] Ryo Saotome and Ratindranath Akhoury. "Relationship Between Gravity and Gauge Scattering in the High Energy Limit". In: *JHEP* 1301 (2013), p. 123. DOI: 10.1007/JHEP01(2013)123. arXiv: 1210.8111 [hep-th].

[130] Agustin Sabio Vera, Eduardo Serna Campillo, and Miguel A. Vazquez-Mozo. "Color-Kinematics Duality and the Regge Limit of Inelastic Amplitudes". In: *J. High Energy Phys.* 04 (2013), p. 086. DOI: 10.1007/JHEP04(2013)086. arXiv: 1212.5103 [hep-th].

[131] Steven Weinberg. "Infrared photons and gravitons". In: *Phys.Rev.* 140 (1965), B516–B524. DOI: 10.1103/PhysRev.140.B516.

[132] Stephen G. Naculich and Howard J. Schnitzer. "Eikonal methods applied to gravitational scattering amplitudes". In: *JHEP* 1105 (2011), p. 087. DOI: 10.1007/JHEP05(2011)087. arXiv: 1101.1524 [hep-th].

[133] Martin Beneke and Grisha Kirilin. "Soft-collinear gravity". In: *JHEP* 1209 (2012), p. 066. DOI: 10.1007/JHEP09(2012)066. arXiv: 1207.4926 [hep-ph].

[134] D.J. Miller and C.D. White. "The Gravitational cusp anomalous dimension from AdS space". In: *Phys.Rev.* D85 (2012), p. 104034. DOI: 10.1103/PhysRevD.85.104034. arXiv: 1201.2358 [hep-th].

[135] S. Oxburgh and C.D. White. "BCJ duality and the double copy in the soft limit". In: *JHEP* 1302 (2013), p. 127. DOI: 10.1007/JHEP02(2013)127. arXiv: 1210.1110 [hep-th].

[136] Camille Boucher-Veronneau and Andrew J. Larkoski. "Constructing Amplitudes from Their Soft Limits". In: *JHEP* 1109 (2011), p. 130. DOI: 10.1007/JHEP09(2011)130. arXiv: 1108.5385 [hep-th].

[137] S. Catani and M.H. Seymour. "A General algorithm for calculating jet cross-sections in NLO QCD". In: *Nucl.Phys.* B485 (1997), pp. 291–419. DOI: 10.1016/S0550-3213(96)00589-5. arXiv: hep-ph/9605323 [hep-ph].

[138] E. Brezin, C. Itzykson, and Jean Zinn-Justin. "Relativistic balmer formula including recoil effects". In: *Phys.Rev.* D1 (1970), pp. 2349–2355. DOI: 10.1103/PhysRevD.1.2349.

[139] Ratindranath Akhoury, Ryo Saotome, and George Sterman. "Collinear and soft divergences in perturbative quantum gravity". In: *Phys. Rev. D* 84 (10 2011), p. 104040. DOI: 10.1103/PhysRevD.84.104040. URL: http://link.aps.org/doi/10.1103/PhysRevD.84.104040.

[140] Stephen G. Naculich and Howard J. Schnitzer. "Eikonal methods applied to gravitational scattering amplitudes". In: *Journal of High Energy Physics* 2011.5 (2011), pp. 1–16. DOI: 10.1007/JHEP05(2011)087. URL: http://dx.doi.org/10.1007/JHEP05(2011)087.

[141] Daniel N. Kabat and Miguel Ortiz. "Eikonal quantum gravity and Planckian scattering". In: *Nucl.Phys.* B388 (1992), pp. 570–592. DOI: 10.1016/0550-3213(92)90627-N. arXiv: hep-th/9203082 [hep-th].

[142] R.L. Crawford and R. Jennings, eds. *Phenomenology of Particles at High Energies. Proceedings: 14th Scottish Universities Summer School in Physics, Edinburgh.* 1973.

[143] Michael B. Green, John H. Schwarz, and Lars Brink. "N=4 Yang-Mills and N=8 Supergravity as Limits of String Theories". In: *Nucl.Phys.* B198 (1982), pp. 474–492. DOI: 10.1016/0550-3213(82)90336-4.

[144] David C. Dunbar and Paul S. Norridge. "Calculation of graviton scattering amplitudes using string based methods". In: *Nucl.Phys.* B433 (1995), pp. 181–208. DOI: 10.1016/0550-3213(94)00385-R. arXiv: hep-th/9408014 [hep-th].

[145] David C. Dunbar and Paul S. Norridge. "Infinities within graviton scattering amplitudes". In: *Class.Quant.Grav.* 14 (1997), pp. 351–365. DOI: 10.1088/0264-9381/14/2/009. arXiv: hep-th/9512084 [hep-th].

[146] Z. Bern, C. Boucher-Veronneau, and H. Johansson. "$N \geq 4$ Supergravity Amplitudes from Gauge Theory at One Loop". In: *Phys.Rev.* D84 (2011), p. 105035. DOI: 10.1103/PhysRevD.84.105035. arXiv: 1107.1935 [hep-th].

[147] C. Boucher-Veronneau and L.J. Dixon. "$N \geq 4$ Supergravity Amplitudes from Gauge Theory at Two Loops". In: *JHEP* 1112 (2011), p. 046. DOI: 10.1007/JHEP12(2011)046. arXiv: 1110.1132 [hep-th].

[148] Z. Bern et al. "On the relationship between Yang-Mills theory and gravity and its implication for ultraviolet divergences". In: *Nucl.Phys.* B530 (1998), pp. 401–456. DOI: 10.1016/S0550-3213(98)00420-9. arXiv: hep-th/9802162 [hep-th].

[149] Stephen G. Naculich, Horatiu Nastase, and Howard J. Schnitzer. "Two-loop graviton scattering relation and IR behavior in N=8 supergravity". In: *Nucl.Phys.* B805 (2008), pp. 40–58. DOI: 10.1016/j.nuclphysb.2008.07.001. arXiv: 0805.2347 [hep-th].

[150] Andreas Brandhuber et al. "Four-point Amplitudes in N=8 Supergravity and Wilson Loops". In: *Nucl.Phys.* B807 (2009), pp. 290–314. DOI: 10.1016/j.nuclphysb.2008.09.010. arXiv: 0805.2763 [hep-th].

[151] Vladimir A. Smirnov. "Analytical result for dimensionally regularized massless on shell double box". In: *Phys.Lett.* B460 (1999), pp. 397–404. DOI: 10.1016/S0370-2693(99)00777-7. arXiv: hep-ph/9905323 [hep-ph].

[152] J.B. Tausk. "Nonplanar massless two loop Feynman diagrams with four on-shell legs". In: *Phys.Lett.* B469 (1999), pp. 225–234. DOI: 10.1016/S0370-2693(99)01277-0. arXiv: hep-ph/9909506 [hep-ph].

[153] Vittorio Del Duca. *An introduction to the perturbative QCD pomeron and to jet physics at large rapidities*. 1995. arXiv: hep-ph/9503226 [hep-ph].

[154] Vittorio Del Duca et al. "An infrared approach to Reggeization". In: *Phys.Rev.* D85 (2012), p. 071104. DOI: 10.1103/PhysRevD.85.071104. arXiv: 1108.5947 [hep-ph].

[155] Vittorio Del Duca et al. "The Infrared structure of gauge theory amplitudes in the high-energy limit". In: *JHEP* 1112 (2011), p. 021. DOI: 10.1007/JHEP12(2011)021. arXiv: 1109.3581 [hep-ph].

[156] Ratindranath Akhoury, Ryo Saotome, and George Sterman. *High Energy Scattering in Perturbative Quantum Gravity at Next to Leading Power*. 2013. arXiv: 1308.5204 [hep-th].

[157] Eric Laenen et al. "Next-to-eikonal corrections to soft gluon radiation: a diagrammatic approach". In: *JHEP* 1101 (2011), p. 141. DOI: 10.1007/JHEP01(2011)141. arXiv: 1010.1860 [hep-ph].

[158] A.J. Larkoski, D. Neill, and I.W. Stewart. *Soft Theorems from Effective Field Theory*. 2014. arXiv: 1412.3108 [hep-th].